

THE UNIVERSITY OF CALGARY

**A ROBUSTNESS MODEL
USING THE FOUR-POINT IMPLICIT TECHNIQUE
TO SOLVE THE ST. VENANT EQUATIONS**

by

Catriona Vrkljan

A THESIS

**SUBMITTED TO THE FACULTY OF GRADUATE STUDIES
IN PARTIAL FULFILMENT OF THE REQUIREMENTS FOR THE
DEGREE OF MASTER OF ENGINEERING**

DEPARTMENT OF CIVIL ENGINEERING

CALGARY, ALBERTA

SEPTEMBER, 1996

© Catriona Vrkljan 1996



National Library
of Canada

Acquisitions and
Bibliographic Services

395 Wellington Street
Ottawa ON K1A 0N4
Canada

Bibliothèque nationale
du Canada

Acquisitions et
services bibliographiques

395, rue Wellington
Ottawa ON K1A 0N4
Canada

Your file *Votre référence*

Our file *Notre référence*

The author has granted a non-exclusive licence allowing the National Library of Canada to reproduce, loan, distribute or sell copies of his/her thesis by any means and in any form or format, making this thesis available to interested persons.

The author retains ownership of the copyright in his/her thesis. Neither the thesis nor substantial extracts from it may be printed or otherwise reproduced with the author's permission.

L'auteur a accordé une licence non exclusive permettant à la Bibliothèque nationale du Canada de reproduire, prêter, distribuer ou vendre des copies de sa thèse de quelque manière et sous quelque forme que ce soit pour mettre des exemplaires de cette thèse à la disposition des personnes intéressées.

L'auteur conserve la propriété du droit d'auteur qui protège sa thèse. Ni la thèse ni des extraits substantiels de celle-ci ne doivent être imprimés ou autrement reproduits sans son autorisation.

0-612-20811-7

ABSTRACT

The weighted four-point, implicit, finite difference technique is a full dynamic solution technique representing standard hydraulic engineering practice for simulation of one-dimensional, gradually-varied, unsteady open channel flow. Under certain flow conditions, the technique fails due to numerical instabilities within the solution. Because of the potential for such instability, many engineers rely on approximate solution methods and thus accept inaccurate results. This thesis describes a method in which a full dynamic solution was obtained throughout the simulation, except for those time steps which exhibited severe instability. For these time steps, the momentum equation was reduced to an approximate equation by reducing the contribution of the acceleration terms. A multiplicative coefficient was included for each of the momentum equation terms, and the value of some of the coefficients automatically reduced when instability was detected. With this method, a full dynamic solution was applied even under suddenly varied flow conditions.

ACKNOWLEDGEMENTS

My respect and thanks go to my supervisor, Dr. David Manz, for his encouragement and patience. My heartfelt gratitude and love go to my husband, Dave, for all of his support and for his unwavering belief in me.

TABLE OF CONTENTS

Approval Sheet	ii
Abstract	iii
Acknowledgements	iv
Table of Contents	v
List of Tables	ix
List of Figures	x
List of Symbols	xi
CHAPTER 1. INTRODUCTION	1
1.1 The Need for Simulation	1
1.2 Simulation Procedures	3
1.3 A Robust Simulation Procedure	6
CHAPTER 2. OBJECTIVES	8
CHAPTER 3. LITERATURE REVIEW	9
3.1 Introduction	9
3.2 Saint Venant Equations	10
3.2.1 The Continuity Equation	10
3.2.2 The Momentum Equation	13

3.2.2.1 Forces Acting on the Element	15
3.2.2.2 Momentum Entering Element	18
3.2.2.3 Rate of Change of Momentum	18
3.2.3 Assumptions Made in the Dynamic Equations	19
3.3 Terms in the Momentum Equation	20
3.3.1 Momentum Equation Approximations	24
3.3.2 Application of Approximations	26
3.3.3 Application of Best Available Solution Procedure	27
3.4 Numerical Solution of Full Dynamic Equations	29
3.4.1 Four-Point Implicit Finite Difference Technique	30
3.4.2 Stability and Accuracy of Technique	32
3.4.3 Failure Flow Conditions	35
3.4.4 Solution Robustness with Variation of Δt and θ	36
3.5 Problem Statement	38
CHAPTER 4. ROBUSTNESS MODEL	39
4.1 Introduction	39
4.2 Description of the Four-Point Implicit Model	39
4.3 Robustness Model	43
4.3.1 Program Logic	46
4.3.2 Application of Robustness	50
4.3.3 Selected Criteria	51

4.4 Parameter Selection	52
4.4.1 Channel Characteristics	53
4.4.2 Finite Difference Parameters	53
4.4.3 Stable Flow Condition	61
4.4.4 Contribution of Momentum Equation Terms	61
CHAPTER 5. NUMERICAL EXPERIMENTS	66
5.1 Introduction	66
5.2 Results	66
5.2.1 Unstable Full Dynamic Solution	68
5.2.2 Unstable Robust Solutions	68
5.2.3 Adjustment of Coefficients A_1 and A_2	77
CHAPTER 6. SUMMARY AND CONCLUSION	82
CHAPTER 7. DISCUSSION AND RECOMMENDATIONS	87
LITERATURE CITED	92
APPENDIX A. FOUR POINT FINITE DIFFERENCE TECHNIQUE	95
A.1 Distance Time Grid	95
A.2 Continuity Equation	97

A.3 Momentum Equation	99
A.4 Solution Procedure	100
APPENDIX B. PROGRAM CODE	103

LIST OF TABLES

5.1 Selected Flow Conditions	67
5.2 Applied Parameter Adjustments	67

LIST OF FIGURES

3.1 Channel Element for Derivation of Continuity Equation	12
3.2 Channel Element for Derivation of Momentum Equation	14
4.1 Program Flowchart	47
4.2 Discharge Profiles for Variation of Δx	55
4.3 Discharge Profiles for Variation of Δt	56
4.4 Discharge Profiles for Variation of θ	58
4.5 Discharge Profiles for Variation of A_1 and A_2	59
4.6 Discharge Profiles for Stable Solution	62
4.7 Momentum Equation Terms for Stable Solution	64
5.1 Discharge Profiles for Unstable Flow Condition #1	69
5.2 Discharge Profiles for Unstable Flow Condition #1-a	70
5.3 Discharge Profiles for Unstable Flow Condition #1-b	71
5.4 Discharge Profiles for Unstable Flow Condition #2	73
5.5 Discharge Profiles for Unstable Flow Condition #2-a	74
5.6 Discharge Profiles for Unstable Flow Condition #2-b	75
5.7 Discharge Profiles for Unstable Flow Condition #2-c	76
5.8 Discharge Profiles for Unstable Flow Condition #3	78
5.9 Discharge Profiles for Unstable Flow Condition #3-a	79
5.10 Discharge Profiles for Unstable Flow Condition #3-b	80
A.1 Distance-Time Grid	96

LIST OF SYMBOLS

A	cross-sectional area at centre of channel element
A_1, A_2 etc.	momentum equation term multiplicative coefficients
B	width of water surface of channel
C_n	Courant number
C_w	celerity of kinematic wave
d	total derivative
F	force applied to channel element; function for numerical solution
F_g	gravity force due to weight of fluid in channel element
F_p	hydrostatic pressure force
F_s	shear force
g	acceleration due to gravity
G	function for numerical solution
i	distance grid point index
i	rate of distributed lateral outflow per unit length of channel
j	time grid point index
k	label for k^{th} iteration in solution procedure
L	length of channel
m	point on time-distance grid
N	number of subreaches in a system for numerical solution
n	Manning's coefficient of roughness

P	wetted perimeter of channel
p	rate of distributed lateral inflow per unit length of channel
Q	discharge at centre of channel element
q	net rate of distributed lateral inflow per unit length of channel
q_i	rate of bulk lateral inflow per unit length of channel
q_o	rate of bulk lateral outflow per unit length of channel
R	hydraulic radius at centre of channel
r	residual error calculated in numerical solution
S_o	channel bed slope
S_f	channel friction slope
S_w	wind energy slope
t	time
V	average velocity of flow at centre of channel element
v_i	velocity component, in direction of flow, of bulk lateral inflow
W	weight of fluid in channel element
x	distance along channel
X	distance location along channel
y	depth at centre of channel element
z	depth above a reference datum
Δt	time step (interval)
Δx	distance step (interval)
δ	partial derivative

α	grid function for finite difference technique
θ	finite difference weighting coefficient
τ_0	mean longitudinal shear stress
ρ	density of water in channel element
γ	specific weight of water in channel element
η	depth measurement variable
ϕ	angle of channel bed slope with horizontal

CHAPTER 1. INTRODUCTION

As world resources, both financial and natural, become more scarce, all engineered systems must become more efficient in design and operation. Water conveyance systems for irrigation are no exception and, by their very nature, are often introduced in areas where water itself is in limited supply. In order to use these systems efficiently, the best available technology must be applied for their operation as well as for their design. In his paper, Manz (1994) suggested that maximum use should be made of existing conveyance system infrastructure since replacement or extensive rehabilitation is frequently neither affordable nor necessary, and the required performance improvements can often be achieved by modifying existing management and operational practices. Such modifications are most readily identified through the use of computer simulations of the hydraulic system. Manz (1994) suggested that through the use of appropriate simulation models, existing and proposed conveyance systems could be evaluated in order to improve the quality of delivery, to minimize water and energy losses, to minimize capital and rehabilitation costs, and to minimize management, operational, and maintenance costs.

1.1 The Need for Simulation

In order to operate, and design, an irrigation system efficiently, standard

engineering practice includes the use of computer models to simulate the unsteady flow conditions in the open-channel system. Many different models are used, the most accurate of which provide a solution to the full dynamic equations describing the flow. The advantages of such a full dynamic solution, over an approximate solution technique, include: (1) solution accuracy, (2) calculation of the time to an event, (3) consideration of channel backwater effects, and (4) consideration of wave dispersion and attenuation. Dynamic models require adequate input data including flow conditions and channel characteristics, such as cross-section, bed slope, and channel roughness. For a manmade irrigation canal system, channel characteristics and flow conditions, which are controlled and gradually varied, are usually known and available. Thus, sufficient input data is generally available so that, as Manz (1994) suggested, the accuracy of a dynamic simulation is attainable for irrigation conveyance systems through the use of an appropriate, cost-effective, full dynamic model.

In the past, dynamic simulation models have not been widely used because the numerical solution technique can become unstable under certain flow conditions. If severe numerical instability occurs during the simulation, the solution technique can fail and cause the program to terminate, leaving the user without a useful result. Because of the potential for such failure, approximate methods, which are not subject to such instability, have been widely applied with little concern over the solution inaccuracies introduced by the approximations. In

order to provide an accurate solution for open-channel irrigation systems, a full dynamic solution is required. Manz (1994) suggested that a suitable simulation model should apply the best available technology within a robust format so that application under a wide variety of input conditions would reliably and easily provide the most accurate result reasonably possible. He described such a model as a robust application without undue compromise of the integrity of the various hydraulic, hydrologic, and operational theories or algorithms used in the solution procedure. In his paper, Lai (1986) described a robust procedure as one which provides a result that degrades slowly as the problem deviates farther and farther from the assumptions upon which the procedure is based. In other words, instability, and subsequent program failure, does not suddenly occur when flow conditions are varied. A robust model which avoids severe numerical instabilities is needed so that the best available technology, a full dynamic solution of the open channel flow equations, can be obtained under virtually all flow conditions.

1.2 Simulation Procedures

For simulation of one-dimensional, gradually varied, unsteady, open channel flow in a well defined channel, the best available solution is provided by an accurate numerical solution of the full dynamic St. Venant Equations. These equations have been derived by numerous authors including Henderson (1966). The four-point implicit finite difference technique, described by Amein (1968), is

a full dynamic solution technique which, as reported by Manz (1994), represents standard hydraulic engineering practice and is based on verified theory. This solution technique offers the following advantages over other full dynamic solution methods (Manz, 1991): (1) the solution can be obtained at desired locations along the channel without reducing the solution accuracy by interpolation, (2) realistic control structures, such as radial gates, can be easily programmed, (3) the required input data is the same as channel design data so is generally available, and (4) adjustment of the finite difference parameters (Δx , Δt , θ) provides a stable and robust solution under conditions of varied channel characteristics and flow conditions. The technique has been verified and calibrated, and the accuracy, conservation, convergence and stability investigated by El Maawy (1991). The solution method was found to be satisfactory by the Canadian Society of Civil Engineers Task Committee on River Models (1990) in its program to evaluate river simulation models and, as reported by Fread (1981), is used in the widely accepted US National Weather Service model DWOPER.

Much of the traditional literature, including Henderson (1966) and Chow, Maidment, and Mays (1988), reports that the weighted four-point implicit solution technique is inherently stable for all flow conditions with properly selected finite difference parameters. Fread (1981) reported computational problems with the solution procedure for rapidly rising hydrographs and nonlinear channel cross-

sections. El Maawy (1991) reported numerical instabilities under conditions of rapidly varied flow in combination with certain time intervals. A rapidly varying flow condition can occur briefly in time within a gradually varied flow profile and the resulting numerical instability in the solution procedure can cause a program using the four-point implicit technique to terminate. Manz (1994) discussed that within a simulation, this type of flow condition (a surge or bore) could be caused by rapid adjustment of hydraulic structures which could occur during emergency conditions or improper canal operation. The potential occurrence of such numerical instability has supported the continued use of simulation programs employing less accurate, approximate solution techniques.

In order to simplify the required solution techniques, approximate methods were developed by simplifying the dynamic St. Venant continuity and momentum equations describing open channel flow so that a direct mathematical solution could be obtained. The most common simplifications involved neglecting some or all of the nonlinear terms in the momentum equation. Commonly used approximate techniques include the following: (1) the diffusion wave model, in which the acceleration, or differential velocity, terms are neglected, (2) the kinematic wave model, in which the acceleration and pressure slope, or depth, terms are neglected, and (3) the steady-state model, in which steady-state flow conditions are determined for each time and input condition. The well-accepted US Army Corps of Engineers' river model HEC-RAS (1995), and previously

HEC-2, uses the steady-state technique and well-accepted stormwater models, such as SWMM (Huber, 1988) and OTTHYMO (Wisner, 1989), use a modified kinematic technique for the routing component.

Standard practice for solution under severe flow conditions, such as a brief surge, is currently application of an approximate solution method throughout the simulation period. The simplifications applied in the approximate methods allow the use of a simpler procedure which avoids numerical instabilities; however, the resulting solution is not accurate. Approximate solutions are particularly inaccurate for unsteady flow conditions in which backwater or dispersion effects are significant or for channels in which lateral inflows and outflows (rainfall, seepage, etc.) occur. Although all of these effects are generally significant in an irrigation canal system, approximate methods are still widely used today.

1.3 A Robust Simulation Procedure

Use of a full dynamic solution for open channel simulation models has historically been avoided for the following two reasons: (1) use of a high-speed digital computer is required to solve the numerical procedure, and (2) numerical instability resulting in program failure can occur under certain flow conditions. The first reason is virtually obsolete today as high-speed personal computers are widely available. The potential for severe numerical instability remains the

only hurdle preventing the widespread application of an accurate dynamic solution procedure to problems of unsteady, gradually varied, open channel flow in well defined channels.

An even more robust solution procedure than the weighted four-point implicit finite difference technique is required in order to provide a simulation model which is suitable under virtually all conditions and provides an accurate solution to the dynamic equations. The work presented here represents an important step toward creating such a robust and accurate model. The four-point implicit technique was used to solve the full dynamic St. Venant equations and a procedure developed to suppress severe numerical instabilities, caused by briefly occurring, rapidly varied, flow conditions, which would otherwise have caused the simulation to fail. A modification was made to the solution technique so that, for the brief time period of numerical instability only, the momentum equation used within the solution procedure was reduced from the full dynamic equation toward a simplified equation used in the approximate techniques. In this way, the best available technology was applied at all times during the simulation while the severe unstable condition causing program failure was avoided.

CHAPTER 2. OBJECTIVES

For most flow conditions in a well-defined open channel, the best available technology today is an accurate numerical solution to the full dynamic St. Venant equations. The four-point implicit finite difference technique provides a well-documented, widely accepted, verified, easily applicable solution method for these equations. Although fairly robust, this technique is susceptible to failure, and subsequent program termination, due to numerical instabilities which can occur within the solution due to sudden changes in flow or channel conditions. The objective of this thesis work was to develop an extremely robust model for which these numerical instabilities do not cause program failure.

To suppress the instability causing program failure, the potential of reducing the contributions of some of the terms in the momentum equation, namely the two acceleration terms, was investigated. Multiplicative coefficients were included in the momentum equation, one for each term. The objective was to avoid program failure by reducing the value of the coefficients, and thus the contribution of the associated terms, in the solution. The investigation required identification of criteria which would predict insipient instability and thus could be used to reduce the value of these coefficients automatically within the solution procedure, and thus prevent program failure.

CHAPTER 3. PROBLEM CLARIFICATION

3.1 Introduction

This chapter includes a derivation of the St. Venant equations of open channel flow from the principles of conservation of mass and of conservation of momentum. The assumptions made in these derivations, and necessary for the proper application of these equations, are then summarized. Momentum equation terms, each accounting for a part of the fluid motion and contributing a different effect to the solution, are identified and described. Two approximate solution techniques, the kinematic wave and the diffusion wave, are introduced based on the removal of various terms in the momentum equation. The idea of developing a model which would apply the best available solution technique is then introduced and the basis of using the full dynamic equations whenever possible and moving towards the approximate diffusion technique within the solution procedure by removing the momentum equation acceleration terms is discussed. The approximate solution technique is necessary since numerical instabilities which develop in the full-dynamic solution due to severe flow conditions otherwise caused the solution program to fail. The four-point implicit finite difference solution technique used for this work is described in detail and the stability and accuracy of the technique discussed. A discussion of flow conditions causing instabilities reported in the literature is also included. A

description of a method used previously to increase the robustness of the technique, by adjustment of the parameters Δt and θ within the solution procedure, is included and the potential for further improved robustness by adjustment of the momentum equation coefficients to control solution stability is introduced in the problem statement.

3.2 Saint Venant Equations

The theory describing one-dimensional, gradually-varied, unsteady flow was originally presented by De Saint Venant in 1871. This flow is described by two one-dimensional, partial differential equations which are collectively known as the St. Venant equations and represent the conservation of mass and the conservation of momentum. The complete derivation of these equations has been well documented by Henderson (1966) and Chow (1959), so only a summarized derivation has been presented here.

3.2.1 The Continuity Equation

The principle of conservation of mass states that, within a channel element, the net change in discharge plus the change in storage must be zero. As presented by Robertson and Crowe (1985), the principle of conservation of mass for an incompressible fluid of constant density can be stated as:

$$\left[\begin{array}{l} \text{flow volume entering} \\ \text{a channel element} \end{array} \right] - \left[\begin{array}{l} \text{flow volume exiting} \\ \text{a channel element} \end{array} \right] = \left[\begin{array}{l} \text{rate of change of volume} \\ \text{in that channel element} \end{array} \right]$$

Application of this principle to the channel element shown in Figure 3.1 allowed the following derivation of the continuity equation:

$$\left[\begin{array}{l} \text{flow volume entering} \\ \text{a channel element} \end{array} \right] = \left(A - \frac{\delta A}{\delta x} \frac{\Delta x}{2} \right) \left(V - \frac{\delta V}{\delta x} \frac{\Delta x}{2} \right) + q_i \Delta x + p \Delta x$$

$$\left[\begin{array}{l} \text{flow volume exiting} \\ \text{a channel element} \end{array} \right] = \left(A + \frac{\delta A}{\delta x} \frac{\Delta x}{2} \right) \left(V + \frac{\delta V}{\delta x} \frac{\Delta x}{2} \right) + q_o \Delta x + i \Delta x$$

$$\left[\begin{array}{l} \text{rate of change of} \\ \text{volume stored in} \\ \text{a channel element} \end{array} \right] = \frac{\delta(A\Delta x)}{\delta t} = \frac{\delta A}{\delta t} \Delta x$$

where:

q_i = rate of bulk lateral inflow per unit length (flow direction velocity component)

q_o = rate of bulk lateral outflow per unit length (velocity in direction of flow)

p = rate of distributed lateral inflow per unit length (no velocity component)

i = rate of distributed lateral outflow per unit length (no velocity component)

The continuity equation then becomes:

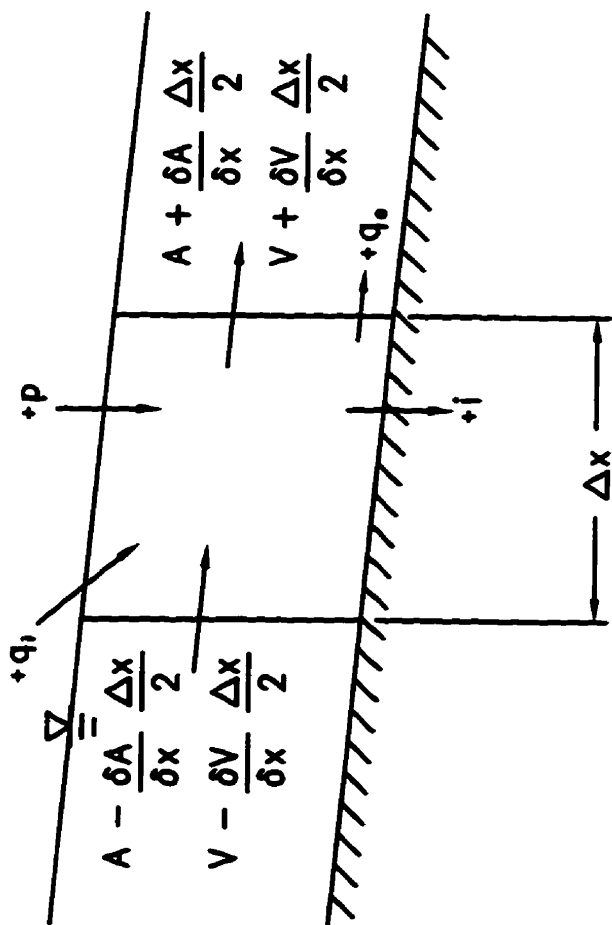
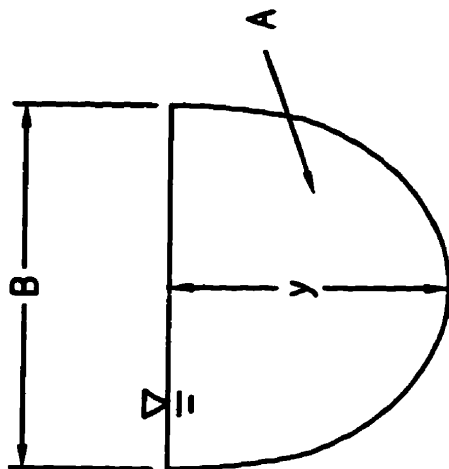


Figure 3.1 Channel Element for Derivation of Continuity Equation

$$A \frac{\delta V}{\delta x} + V \frac{\delta A}{\delta x} + \frac{\delta A}{\delta t} - (q_i + p - q_o - i) = 0 \quad [3.1]$$

For a non-prismatic channel, width B is a function of time (t) and of longitudinal distance (x), so that:

$$\frac{\delta A}{\delta t} = B \frac{\delta y}{\delta t} \quad \text{and} \quad \frac{\delta A}{\delta x} = B \frac{\delta y}{\delta x} + y \frac{\delta B}{\delta x} \quad [3.2]$$

Dividing equation [3.1] through by B and assuming a prismatic channel where width B is not a function of distance (x), the continuity equation used for this thesis work is obtained as:

$$\frac{A}{B} \frac{\delta V}{\delta x} + V \frac{\delta y}{\delta x} + \frac{\delta y}{\delta t} - \frac{1}{B} (q_i + p - q_o - i) = 0 \quad [3.3]$$

3.2.2 The Momentum Equation

The momentum equation is a combination of the momentum principle and Newton's Second Law of Motion, as presented by French (1985), states that:

$$\left[\begin{array}{l} \text{the sum of external} \\ \text{forces applied to a} \\ \text{control volume} \end{array} \right] + \left[\begin{array}{l} \text{net momentum} \\ \text{flux entering the} \\ \text{control volume} \end{array} \right] = \left[\begin{array}{l} \text{rate of change of} \\ \text{momentum in the} \\ \text{control volume} \end{array} \right]$$

Application of this principle to the channel element shown in Figure 3.2, and assumption of a uniform velocity distribution across the channel, allows the following derivation of the momentum equation:

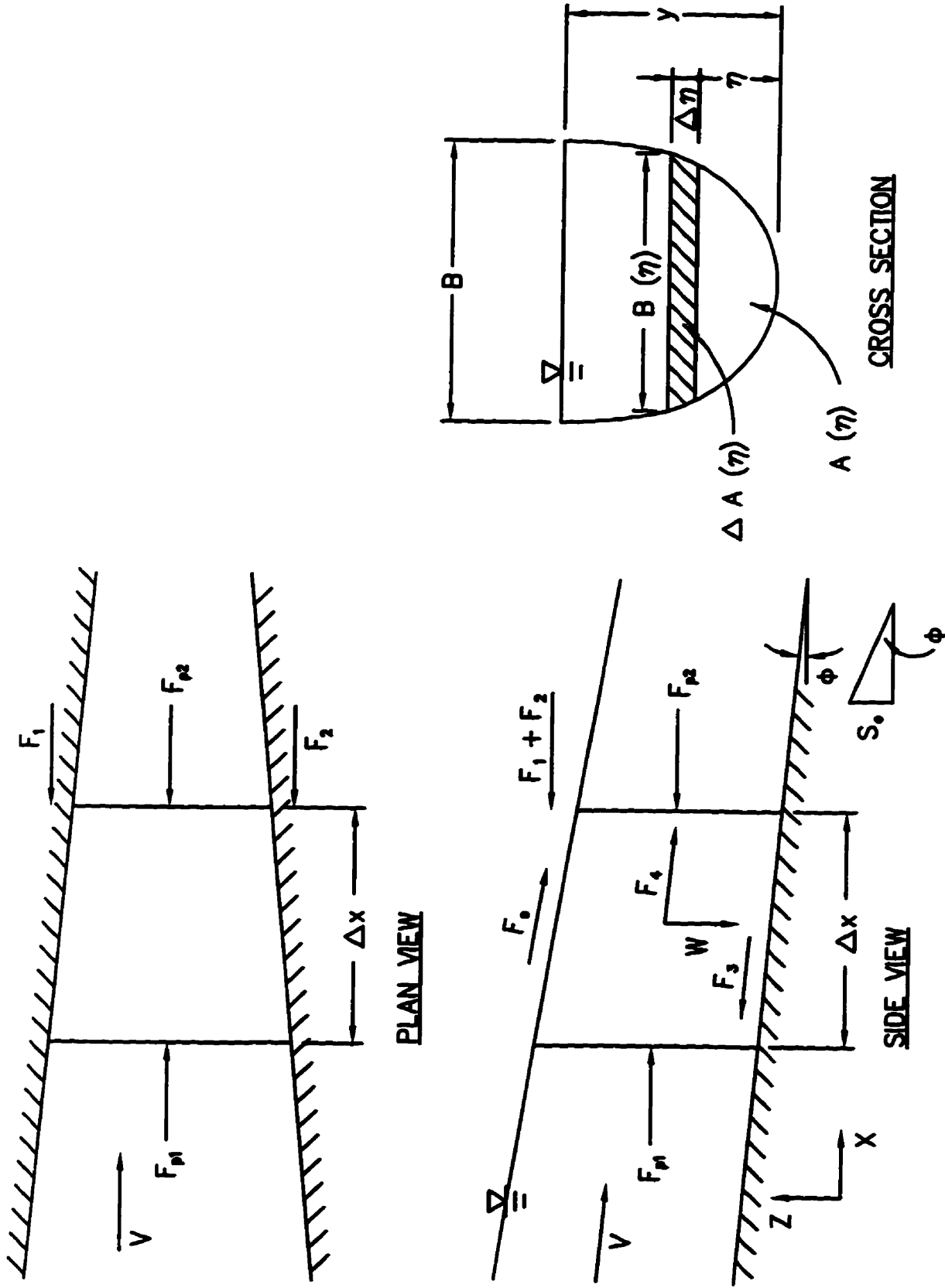


Figure 3.2 Channel Element for Derivation of Momentum Equation

$$[\text{sum of external forces}] = \sum_{\rightarrow} F = F_{p1} - F_{p2} - F_1 - F_2 - F_3 + F_4 + F_5$$

$$[\text{net momentum flux entering a channel element}] = \frac{\delta(\rho QV)}{\delta x} \Delta x$$

$$[\text{rate of change of momentum in a channel element}] = \frac{\delta(\rho VA \Delta x)}{\delta t}$$

The momentum equation then becomes:

$$\sum_{\rightarrow} F + \frac{\delta(\rho QV)}{\delta x} \Delta x = \frac{\delta(\rho VA \Delta x)}{\delta t} \quad [3.4]$$

3.2.2.1 Forces acting on the element

Assuming a hydrostatic pressure distribution, and referring to Figure 3.2, the hydrostatic pressure force is given by the equation:

$$F_p = \int_0^y \gamma(y - \eta) dA = \int_0^y \gamma(y - \eta) B dy \quad [3.5]$$

where: $dA = B dy$, and

B is a function of η .

From Figure 3.2,

$$F_{p2} = F_{p1} + \frac{\delta F_p}{\delta x} \Delta x \quad [3.6]$$

and, since $F_1 + F_2$ represents the change in F_p due to the change in width, B , with channel distance x ,

$$F_1 + F_2 = \int_0^y \Delta x \gamma (y - \eta) \frac{\delta B}{\delta x} d\eta \quad [3.7]$$

Using the derivative product rule,

$$\frac{\delta F_p}{\delta x} = \int_0^y \gamma B \frac{\delta y}{\delta x} d\eta + \int_0^y \gamma (y - \eta) \frac{\delta B}{\delta x} d\eta \quad [3.8]$$

Combining equations [3.6] through [3.8], the following is obtained:

$$F_{p1} - F_{p2} - (F_1 + F_2) = -\Delta x \int_0^y \gamma B \frac{\delta y}{\delta x} d\eta = -\gamma \Delta x \frac{\delta y}{\delta x} A \quad [3.9]$$

since $A = \int_0^y B d\eta$.

Assuming the channel bed is constant (no scour or deposition), the shear force acting on the fluid by the bed is equal to the stress multiplied by the contact area so that:

$$F_3 = \tau_o P \Delta x \quad [3.10]$$

For conditions of uniform flow, the shear force, F_s , resists the weight of the fluid, F_4 , so that:

$$F_s = \tau_o P \Delta x = F_4 = \gamma A \Delta x S_o \quad [3.11]$$

which provides:

$$\tau_o = \gamma R S_o \quad [3.12]$$

Assuming that the resistance equations developed for uniform flow (where $S_o = S_f$) are applicable to this unsteady, non-uniform flow, the shear force acting on the channel element is given by:

$$F_3 = (\gamma R S_o) P \Delta x = \gamma A \Delta x S_o \quad [3.13]$$

where: P = wetted perimeter, and

$R = \frac{A}{P}$, hydraulic radius.

For small angles of ϕ , where $\sin\phi \approx \tan\phi$, the force due to the weight of the fluid in the element is:

$$F_4 = W \sin\phi = \gamma A \Delta x S_o \quad [3.14]$$

The force due to wind shear on the surface of the channel element can be

derived similarly to that done above for the channel bed, with the following result:

$$F_s = \gamma A \Delta x S_w \quad [3.15]$$

3.2.2.2 Momentum Entering the Channel Element

Referring again to Figure 3.2, the net momentum flux entering channel element is the momentum entering minus the momentum exiting:

$$[\text{momentum entering}] = \rho Q V + \rho q_i \Delta x v_i \quad [3.16]$$

$$[\text{momentum exiting}] = \rho Q V + \frac{\delta(\rho Q V)}{\delta x} \Delta x + \rho q_o \Delta x V \quad [3.17]$$

$$[\text{net momentum entering}] = -\frac{\delta(\rho Q V)}{\delta x} \Delta x + \rho q_i \Delta x v_i - \rho q_o \Delta x V \quad [3.18]$$

where, v_i is the velocity component in the direction of flow of bulk lateral inflow.

3.2.2.3 Rate of Change of Momentum

Referring again to Figure 3.2, the rate of change, or accumulation, of momentum

in the channel element is:

$$[\text{momentum accumulation}] = \frac{\delta(\rho VA \Delta x)}{\delta t} \quad [3.19]$$

Combining equations [3.9], [3.13], [3.15], [3.18], and [3.19], the following momentum equation is obtained:

$$\begin{aligned} -\gamma \Delta x \frac{\delta y}{\delta x} A - \gamma A \Delta x S_f + \gamma A \Delta x S_o - \gamma A \Delta x S_w \\ - \frac{\delta(\rho QV)}{\delta x} \Delta x + \rho q_i \Delta x v_i - \rho q_o \Delta x V = \frac{\delta(\rho VA \Delta x)}{\delta t} \end{aligned} \quad [3.20]$$

Dividing by $\rho \Delta x$ and rearranging:

$$\frac{\delta(VA)}{\delta t} + \frac{\delta(V(VA))}{\delta x} + Ag \frac{\delta y}{\delta x} + Vq_o - v_i q_i + Ag(S_f - S_o + S_w) = 0 \quad [3.21]$$

Expanding the first two terms, assuming wind shear is negligible and bulk lateral inflow and outflow are zero, substituting equation [3.1] into [3.21], and rearranging and simplifying, the momentum equation becomes:

$$\frac{\delta V}{\delta t} + V \frac{\delta V}{\delta x} + g \frac{\delta y}{\delta x} + g(S_f - S_o) + \frac{V}{A} q = 0 \quad [3.22]$$

where: $q = p - i$.

3.2.3 Assumptions Made in the Dynamic Equations

Several assumptions were made in the derivation and simplification of the

original St. Venant equations in order to obtain the forms of equations [3.3] and [3.22]. These assumptions are further discussed by Chow et al. (1988) and Weinmann (1977). For the derived equations to be applicable for a particular combination of flow conditions and channel characteristics, the assumptions must be reasonable. The assumptions are summarized as follows:

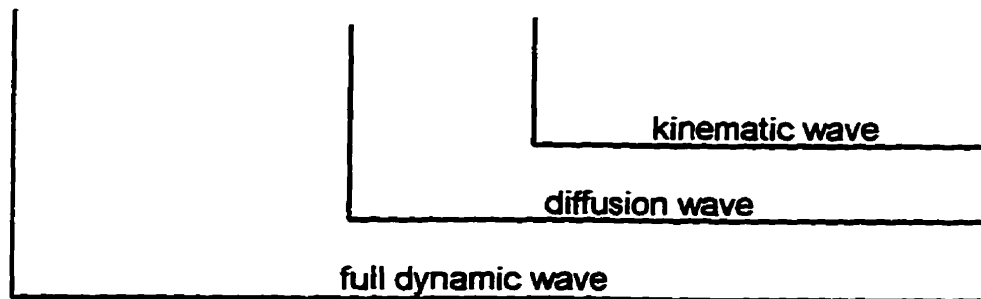
- one-dimensional flow (longitudinal flow variations only);
- horizontal water surface and uniform velocity distribution across the channel;
- incompressible, homogeneous flow;
- gradually varied flow with hydrostatic pressure distribution throughout;
- resistance effects adequately described with resistance coefficients and equations developed for steady uniform turbulent flow;
- longitudinal channel axis approximated as a straight line;
- fixed channel bottom slope (no scour or deposition);
- channel bottom slope small so that $\sin\phi \approx \tan\phi$;
- zero net bulk lateral inflow entering channel;
- total distributed outflow is q_o (zero momentum in direction of flow);
- negligible wind effects; and
- prismatic channel.

3.3 Terms in the Momentum Equation

The momentum equation consists of five terms, referred to as 'term1' through

'term5', each representing a physical process affecting flow momentum, as discussed by Chow et al. (1988) and as indicated in equation [3.23] below. A multiplicative coefficient was introduced for each term to establish the momentum equation used for the robustness model developed for this thesis work as follows:

$$\begin{array}{cccccc}
 A_1 \frac{\delta V}{\delta t} & + & A_2 V \frac{\delta V}{\delta x} & + & A_3 g \frac{\delta y}{\delta x} & + & A_4 g (S_f - S_o) & + & A_5 \frac{V}{A} q & = & 0 & [3.23] \\
 \text{term1} & & \text{term2} & & \text{term3} & & \text{term4} & & \text{term5} & & &
 \end{array}$$



where:

$$\text{term1} = A_1 \frac{\delta V}{\delta t} \quad \text{the local acceleration term,}$$

$$\text{term2} = A_2 V \frac{\delta V}{\delta x} \quad \text{the convective acceleration term,}$$

$$\text{term3} = A_3 g \frac{\delta y}{\delta x} \quad \text{the pressure force term,}$$

$$\text{term4} = A_4 g (S_f - S_o) \quad \text{with } A_4 g S_f \text{ the friction force, or shear, term,}$$

$$\text{and } A_4 g S_o \text{ the gravity force, or bed slope, term, and}$$

$$\text{term5} = A_5 \frac{V}{A} q \quad \text{the net distributed inflow term.}$$

The two acceleration terms, local and convective, are collectively known as the inertial terms and represent the change in momentum due to the change in velocity with time (momentum accumulation) and the change in velocity with channel distance (momentum flux), respectively. The pressure force term represents the change in momentum due to the change in depth, and thus the change in hydrostatic pressure, along the channel. The friction and gravity force terms represent the difference between the forces due to the weight of the fluid and to the shear against the channel bottom and are proportional to the friction and bed slopes of the channel, respectively. The inflow term represents the net distributed inflow for the channel section.

In the following discussion regarding the contributions and significance of the various momentum equation terms, information presented by Weinmann (1977), Henderson (1966), and Chow (1959) has been included. For routing a hydrograph down a steep channel, the friction and gravity slope terms dominate the flow characteristics. For channels of flat bed slope, the pressure term is also important. The acceleration terms are important for steeply rising or falling

hydrographs. When backwater effects from channel transitions or boundary structures are significant, the pressure and acceleration terms are important. These terms are the only terms in the equation that can simulate velocity changes in time or in the upstream direction. The pressure and acceleration terms allow calculation of backwater effects and wave attenuation and subsidence and thus produce the looped discharge rating curve expected for unsteady, gradually varied flow.

Henderson (1966) reported that for a fast-rising flood in a steep natural channel ($S_0 > .002$), the contribution of the pressure term, convective acceleration, and local acceleration terms were about one, two, and three orders of magnitude, respectively, less than the gravity term. Weinmann (1977) suggested that the magnitude of the pressure term was dependent on the steepness of the inflow hydrograph and inversely proportional to channel slope. He also reported that for channels of flat bed slope, the pressure term might be of similar magnitude to the gravity term and the two acceleration terms somewhat smaller than the pressure term. For steeper channels, he reported a pressure gradient term of about an order of magnitude smaller than friction slope and acceleration terms an order of magnitude smaller again. Both Henderson (1966) and Weinmann (1977) reported that for steep slopes, the gravity slope term dominated the flow but the acceleration terms were significant, while for flat bed slopes, the pressure term was important. The pressure and acceleration terms were

reported to be important for fast-rising hydrographs and whenever backwater effects or the time of an event were important to the result.

The relative significance of the two acceleration terms, term1 and term2, has not been discussed in the literature. Although both represent acceleration effects, they are derived separately within the momentum equation (see Section 3.2).

Term1 was derived from the momentum accumulation within the control volume while term2 was derived from the momentum flux through the control section.

Weinmann (1977) and Henderson (1966) only discuss their combined significance and magnitude, without mention of their respective contributions.

3.3.1 Momentum Equation Approximations

Before high-speed digital computers were readily available to solve numerical methods, solution of the full dynamic St. Venant Equations, represented by equations [3.3] and [3.22], presented serious difficulty. In order to simplify the solution procedure required for unsteady flow routing, approximate methods were developed in which certain terms in the momentum equation were neglected in order to linearize the momentum equation. An explicit solution could then be obtained for linear conditions. Justification for the removal of the various terms was based on the assumption that the contribution of the neglected terms was small compared to the remaining terms. The most commonly used

approximate methods are the diffusion wave, in which the two acceleration terms are neglected, and the kinematic wave in which the pressure term is neglected as well as the acceleration terms.

With a kinematic wave solution technique, only the channel and friction slope terms are retained so that uniform flow is calculated. In this case, a straight-line rating curve is predicted which is characteristic of steady-state flow, as discussed by French (1985). Weinmann (1977) summarized that a kinematic wave solution cannot predict backwater effects and can only model the wave crest, can only propagate the crest downstream, reports maximum stage and maximum discharge at the same time, and underestimates the maximum discharge. A diffusion wave technique includes the pressure term and so can represent wave attenuation and subsidence and can provide an approximate looped rating curve.

As mentioned previously, approximate methods are still widely used for open channel unsteady flow modelling applications. These techniques are applied without justification of whether the terms which are neglected are truly negligible. The contribution of these neglected terms is assumed to be unimportant for solution of the problem. The results of the approximate solution are then accepted and used in the remainder of the design process.

For this work, multiplicative coefficients were included for each of the momentum equation terms. Referring to equation [3.23], if coefficients A_1 and A_2 were set to zero, then term1 and term2 would be set to zero and the diffusion wave equation obtained; and, with A_1 , A_2 , and A_3 , set to zero, the kinematic wave equation would be obtained. These coefficients were introduced so that the solution procedure could be varied from solution of the full dynamic momentum equation through the diffusion equation to the kinematic equation.

3.3.2 Application of Approximations

In a kinematic wave procedure, the acceleration and pressure terms are neglected so the solution cannot predict backwater effects nor provide the looped rating curve characteristic of unsteady open channel flow. The diffusion technique includes the pressure term and so can approximate these effects. These two effects are significant to many problems of unsteady, open-channel flow problems where predictions are often required regarding the effect of operating a canal structure or the anticipated time and maximum values of depth and discharge for a flood condition. In an operated canal with numerous gate and weir structures separating reaches of relatively short length, backwater effects would likely be extremely significant. The uniform flow conditions simulated by the kinematic wave equation may never exist in such a canal. Thus, for long, steep channels with slowly-rising hydrographs where gravity and friction

effects dominate, a kinematic, or even a steady-state model, may provide reasonable results. For a channel of intermediate slope with transitions or control structures causing backwater effects, a full dynamic solution is required for an accurate result. In other words, terms are neglected arbitrarily to simplify the solution procedure without consideration of whether the neglected terms are significant. In cases where backwater effects are known to exist, the acceleration terms are neglected even though their effects are known to be important.

Of course, a solution can only be as accurate as the input data available, so where the quality of the input data is sufficiently poor that the model result will be approximate anyway, an approximate solution method may provide acceptable results. Weinmann (1977) concluded that approximate techniques may be warranted for simulation of channels for which some or all of the following conditions are true: (1) accurate channel geometry and flow conditions are not known, (2) channel bottom is very rough, (3) flow conditions vary very slowly, and (4) flow conditions are supercritical. For manmade channels with regular cross-sections and controlled flows, an accurate solution technique is virtually always warranted. In spite of the obvious problems, models based on the kinematic technique are still widely accepted.

3.3.3 Application of Best Available Solution Procedure

The standard open-channel flow model used in industry today is the US Army Corps of Engineers (1995) model HEC-RAS, formerly known as HEC-2.

Although an unsteady component is reportedly to be released in the near future, only the steady flow version is currently available. The QUALHYMO (Rowney, 1991) and SWMM (Huber, 1988) families of stormwater models include several open-channel routing options including kinematic wave and dynamic solution methods. The dynamic solution component to the SWMM model, EXTRAN, is unstable under varying flow conditions, so the approximate method solutions are still generally used.

As described above, the availability of high-speed digital computers makes the main reason for using an approximate solution technique for unsteady flow routing, that a proper full dynamic solution requires use of numerical methods, unjustifiable. The required solution procedures are readily solved using a personal computer and relatively simple programming techniques. Except under extreme flow conditions where a numerical solution technique may become mathematically unstable, the improved accuracy of a full dynamic solution greatly outweighs any difficulty introduced by the requirement for a numerical solution. Because potentially important terms in the momentum equation are assumed negligible and removed, an approximate solution procedure does not provide the best answer. Today, the best available technology is the simultaneous solution of the full dynamic equations.

3.4 Numerical Solution of Full Dynamic Equations

For the system of full dynamic, St. Venant equations, including the continuity equation [3.3] and momentum equation [3.23] described above, there is no known analytical solution. The system can only be solved by use of a numerical solution technique and a digital computer. Numerical methods to solve the complete form of the St. Venant equations were described by Strelkoff (1969), among others. For reasons discussed in Section 1.2, the four-point implicit, finite difference method developed by Amein and Fang (1970) for the solution of the system of equations, together with the boundary conditions, was used for this work. This method has been used extensively by many authors including Weinmann (1977), Fread (1981), and Manz (1994) and reportedly provides an accurate solution to the full dynamic equations. Manz (1994) summarized the advantages of this solution method over other full-dynamic solution techniques as follows: (1) the ability to incorporate distributed lateral inflow or outflow (e.g. precipitation or seepage), (2) no restrictions on the hydraulic and operational characteristics of the modelled hydraulic control structures (eg. radial gates), (3) relatively minor programming effort, (4) use of the same input information required for the design of canals and associated control structures, and (5) is based on verified theory and standard hydraulic engineering practise.

3.4.1 Four-Point Implicit Finite Difference Technique

The four-point implicit solution technique has been widely used in industry and well documented by Weinmann (1977), Fread (1981), and El-Maawy (1991) as an accurate and robust solution technique for unsteady flow routing. The method is useful for practical application since the solution is obtained at specified locations in space and time, the value of Δx need not be constant along the reach, and the stability of the solution can be controlled by variation of the finite difference parameters Δx , Δt , and θ . The robustness of the four-point implicit technique is due to the flexibility of the technique which allows this variation of Δx , Δt , and θ within the solution procedure.

As described by Weinmann (1977), the equation system to be solved consists of two nonlinear, first order, first degree, partial differential hyperbolic equations, the continuity and momentum equations, with x and t as independent variables and y and V as dependent variables. The other terms are constants or functions of the independent or dependent variables. For each time step of increment Δt , the solution involves the determination of depth and velocity at the ends of each channel section, each of some length Δx . The continuity and momentum equations are approximated by finite difference equations, and written at each channel section to be used in the computation. For a reach divided into N channel sections where the values of velocity and depth are to be evaluated, two

finite difference equations are written at each section giving $2(N-1)$ equations for the $2N$ unknowns. Since the system of finite difference equations contains two more unknowns than equations, boundary equations at the upstream and downstream extremes of the channel reach are required to provide two additional equations. Together with the two boundary conditions and a complete initial condition, a system of $2N$ nonlinear algebraic equations is produced. The resulting system of equations is solved simultaneously by an iterative procedure. The coefficient matrix which results from the system of finite difference equations has a banded pentadiagonal structure which allows use of an efficient solution algorithm in order to minimize both required computer storage and computing time. The solution is marched forward in time using the previous solution as the first estimate for the next time.

The Newton Raphson technique was chosen as the iterative procedure for solution of the system since it converges quickly when the first approximation of the solution is reasonable and, as reported by Lai (1986), is efficient and reliable. In the program, a solution was accepted at each finite interval of time, defined by Δt , when successive iterative values of depth and velocity varied by less than the specified tolerance value of 0.001 m. Numerical solution of a steady-state backwater calculation was used as the initial condition required to start the procedure. The downstream boundary was set as a full-width, sharp-crested weir, and the upstream boundary set with an inflow discharge

hydrograph. Within the simulation, one or both of the boundary conditions was adjusted to cause a change in flow conditions. The weir was either raised or lowered and/or the discharge hydrograph either increased or decreased. Using the solution from the previous time step as the initial estimate, the Newton Raphson technique was used to converge to the solution at the new time step.

3.4.2 Stability and Accuracy of the Four Point Implicit Technique

The Amein four-point implicit finite difference technique has been used extensively in open channel models, including the US National Weather Service models DWOPER and DAMBRK as well as Manz' (1994) model ICSS, and thus the stability and accuracy of the solution method have been well investigated by Weinmann (1977), El-Maawy (1991) and others. As discussed by Lai (1986), the stability and convergence of the solution technique affects the accuracy of the result. The stability of the solution technique refers to the difference between the numerical solution and the exact solution of the finite difference equations. Convergence refers to the difference between the theoretical solution of the partial differential equations and the finite difference equations. Accuracy refers to the difference between the actual solution of the problem, which remains unknown, and the computed result. Stability is obtained when small numerical errors, which include truncation errors due to discretization of the differential equations and round-off errors due to the limit of calculation precision, are not

amplified by the computational procedure.

Traditional references such as Chow et al. (1988) and French (1985) reported the stability of the implicit method to be independent of the Courant condition; however, El Maawy (1991) found this to be true only within a range. The Courant condition represents the ratio of $\frac{\Delta t}{\Delta x}$ and is calculated as: $\Delta t \leq \frac{\Delta x}{C_w}$, where C_w is the celerity of the wave and equal to \sqrt{gy} for a kinematic wave (French, 1985). Thus, the Courant number, C_n , is calculated as $\frac{\Delta t}{\Delta x} C_w$ and should be less than or equal to one for the Courant condition to be satisfied.

The implicit finite difference technique has generally been considered unconditionally stable for any ratio of $\frac{\Delta x}{\Delta t}$ when θ is held within the range $0.5 \leq \theta \leq 1$. Fread (1973) reported, however, that instabilities were encountered for certain upstream boundary hydrographs and Δt time steps even for θ values within this range. He reported that the accuracy of the solution was effected by the size of the time step and the characteristics of the discharge hydrograph at the upstream channel boundary. Fread also reported that although a large Δt was desirable in order to reduce computation time, especially for long-duration simulations, when Δt was made large truncation errors caused distortion, dispersion and attenuation of the peak. El Maawy (1991) reported serious instabilities when Δx was significantly larger than would be suggested by the Courant condition, and when θ was close to 0.5 with a steep hydrograph. Both

reported that values of θ less than 0.5 caused severe instabilities. El-Maawy also observed that Δt must be small enough to detail the flow adequately, and that an upper limit to Δt existed to ensure stability as the flow variation became more severe. Both reported that the solution was reliably stable, convergent and accurate when Δt and Δx were selected to satisfy the Courant condition.

Lai (1986) reported that some dispersion always occurred for θ values greater than 0.5, a condition which was more pronounced as Δt was increased and less significant as Δx was decreased. Fread (1973) found that distortion was minimized when θ values were in the lower range, and recommended a value for θ of 0.55 to balance distortion due to large time steps while ensuring theoretical stability. El-Maawy (1991) found that a θ of 0.6 was effective for rapidly varying flow, and a θ of 0.55 effective for more gradual flow variations. Fread (1973) summarized his analysis indicating that stability decreases with increasing values of Δt and decreasing values of θ as well as with steepening inflow hydrographs, and that distortion increases with increasing channel length or Manning roughness n and decreases with increasing initial channel depth or channel bottom slope.

With the four-point implicit technique, the finite difference parameters Δx , Δt , and θ are selected to control convergence, stability, and dispersion of the solution wave. As discussed by Fread (1981), when Δt was reduced within the procedure, the solution became more stable. In reducing Δt , the Courant

number, proportional to $\frac{\Delta t}{\Delta x}$ was reduced. A similar effect could have been obtained with an increased Δx , however, variation of Δx within the procedure can cause reduced solution accuracy since interpolation could be required in order to obtain results at the desired locations along the channel.

3.4.3 Failure Flow Conditions

The previous discussion emphasized that although the four-point implicit technique has been reported to be unconditionally stable for values of θ greater than 0.5, severe instabilities can occur under some flow conditions. Fread (1983) found cases of instability, resulting from steep input hydrographs and changes in cross section, sufficiently severe that adjustment of Δx , Δt , and θ was not sufficient to provide a solution. French (1985) reported that steep inflow hydrographs, and resulting surges, and sudden channel transitions could cause rapidly-varied flow conditions. Solution difficulty would be expected for conditions approaching rapidly varied flow since the St. Venant equations are valid only for gradually-varied flow; however, even gradually-varied flow conditions can result in unstable calculations causing failure. Relatively steep water surface and discharge profiles would be more likely to result in solution failure since the large values of the pressure and acceleration terms could induce instabilities in the numerical solution. A flow profile for which the pressure slope term, $\frac{\delta y}{\delta x}$, is negative, such as for an M2 water surface profile, would be

likely to produce failure for a mild channel slope, since the depth could approach zero within an unstable calculation. For the channel used for this thesis work, with a sharp-crested weir as the downstream control, gradually varied flow conditions would produce an M1 backwater curve with slightly positive $\frac{\delta y}{\delta x}$ term structure. A sudden increase in the inflow hydrograph would produce a surge with a steep M2 profile at its leading edge. An increase in downstream weir depth could exaggerate this effect by initially reducing the downstream discharge against the raised weir and thus increasing the relative surge. For a steep channel, the momentarily decreased discharge over the raised weir could produce a similarly steep S2 profile and negative $\frac{\delta y}{\delta x}$ term. Thus, an unstable condition might be induced in the gradually-varied unsteady flow model by simultaneously introducing a sudden increase in the inflow hydrograph and an increase in the height of the weir.

3.4.4 Solution Robustness with Variation of Δt and θ

In his paper, Fread (1981) described an automatic procedure used in the program DWOPER, contained within the finite difference solution algorithm to increase the robust nature of the four-point implicit method. He reported that rapidly rising hydrographs and non-linear cross-section properties caused computational problems resulting in non-convergence in the Newton-Raphson iteration or in erroneously low computed depths at the leading edge of steep

wave fronts. When either of these conditions were sensed in the program, an automatic procedure consisting of two parts was implemented. First, the time step (Δt) was reduced by a factor of 2 and the computations repeated; if the same problem persisted, Δt was again halved and the computation repeated. This continued until a successful solution was obtained or the time step had been reduced to 1/16 of the original size. If a successful solution was obtained, the computation proceeded to the next time step using the original Δt . If the solution using $\frac{\Delta t}{16}$ was unsuccessful, the θ weighting factor was increased by 0.1 and a time step of $\frac{\Delta t}{2}$ used. Upon achieving a successful solution, θ and Δt were restored to their original values. Unsuccessful solutions were treated by increasing θ and repeating the computation until $\theta = 1$, at which point the automatic procedure terminated and the solution with $\theta = 1$ and $\frac{\Delta t}{2}$ was used to advance forward in time, resetting Δt and θ again to the original values.

The four point implicit finite difference method provides the flexibility to vary the finite difference parameters Δt and θ in the middle of a simulation, as described above. However, the instability described by Fread, due the mathematical errors resulting from steep input hydrographs and changes in cross section, can be sufficiently severe that adjustment of Δt and θ is unsuccessful in allowing a solution. Fread described that if the algorithm used in DWOPER was unsuccessful, the solution obtained with $\frac{\Delta t}{16}$ and $\theta = 1$ was accepted. Fread did not report investigation of conditions for which these parameters did not allow a

solution.

3.5 Problem Statement

For practical application, a solution technique must be reliably robust under virtually all flow conditions. With variation of Δt and θ within a simulation, the four-point implicit finite difference technique is both reliable and robust for many flow conditions and channel characteristics, however numerical instability causing program failure can still occur. For this thesis work, a method to adjust parameters in addition to Δt and θ was developed in order to investigate the potential for an even more robust solution technique. The procedure developed allowed a full dynamic solution to be applied throughout a simulation, except for those time steps exhibiting numerical instability. For those unstable time steps, an approximate technique, in which the contribution from some of the terms in the momentum equation was reduced, was applied so that program termination was avoided. In this way, the best available procedure was used for each time step. In other words, a full dynamic solution was provided for all time steps except those for which the technique was unable to provide any solution; only then was an approximate technique applied.

CHAPTER 4. ROBUSTNESS MODEL

4.1 Introduction

This chapter begins with a description of the four-point implicit finite difference solution technique and the discretized continuity and momentum equations used for this work, including the multiplicative coefficients A_1 through A_5 applied to the various terms in the momentum equation. This method was used to investigate the potential of a 'robustness model' which would eliminate program failure due to numerical instability. The method involved an automatic adjustment of the coefficients, A_1 and A_2 , as well as the traditional parameters of Δt and θ . The criteria used for application of the adjustments, and a logic flowchart of the program, were also included. A description of the channel characteristics, finite difference parameters, and flow conditions selected to test the robustness of the model follow. The chapter concludes with a description of a modelled stable solution and a discussion of the contributions of the various momentum equation terms to that solution.

4.2 Description of the Four-Point Implicit Model

For this thesis work, a single channel reach computer simulation model was programmed to solve the full dynamic St. Venant equations using the four-point,

implicit, finite difference technique described by Weinmann (1977) and Fread (1981). As discussed in Section 1.2, this technique represents standard engineering practise and has been verified and investigated by others. The model included a steady state backwater calculation for the initial condition, an input hydrograph of discharge versus time for the upstream boundary condition, and flow over a sharp-crested weir for the downstream boundary. Lateral inflow and outflow were set to zero since this was intended to be a general investigation of the effects of adjusting the contribution of the momentum equation terms, rather than specific for certain channel and flow conditions. Downstream weir height was variable within the simulation.

The work done by El Maawy (1991), based on the four-point implicit technique, included calibration. His results were used to verify the robustness model developed for this thesis work. The results using the robustness model agreed well (within less than five percent) with El Maawy's calibrated results.

For convenience, the St. Venant equations of one-dimensional, unsteady, gradually varying, open channel flow, equations [3.3] and [3.23] discussed above, were repeated here:

Continuity equation:

$$\frac{A}{B} \frac{\delta V}{\delta x} + V \frac{\delta y}{\delta x} + \frac{\delta y}{\delta t} - \frac{1}{B} (q_i + p - q_o + i) = 0 \quad [3.3]$$

Momentum equation:

$$A_1 \frac{\delta V}{\delta t} + A_2 V \frac{\delta V}{\delta x} + A_3 g \frac{\delta y}{\delta x} + A_4 g (S_f - S_o) + A_5 \frac{V}{A} q = 0 \quad [3.23]$$

After application of the four-point implicit finite-difference technique and simplification, the discretized continuity and momentum equations of the following form were used for programming. A description of the discretization of these equations was included in Appendix A.

Continuity equation:

$$\begin{aligned} & y_{i-1}^{j+1} + y_i^{j+1} + C_1 + \frac{\Delta t}{\Delta x} \theta^2 \left[\left(\frac{A}{B} \right)_{i-1}^{j+1} + \left(\frac{A}{B} \right)_i^{j+1} \right] [V_{i-1}^{j+1} - V_i^{j+1}] \\ & + \frac{\Delta t}{\Delta x} \theta C_2 [V_{i-1}^{j+1} - V_i^{j+1}] + \frac{\Delta t}{\Delta x} \theta C_3 \left[\left(\frac{A}{B} \right)_{i-1}^{j+1} + \left(\frac{A}{B} \right)_i^{j+1} \right] + C_4 \\ & + \frac{\Delta t}{\Delta x} \theta^2 [V_{i-1}^{j+1} + V_i^{j+1}] [y_{i-1}^{j+1} - y_i^{j+1}] + \frac{\Delta t}{\Delta x} \theta C_5 [y_{i-1}^{j+1} - y_i^{j+1}] \\ & + \frac{\Delta t}{\Delta x} \theta C_6 [V_{i-1}^{j+1} + V_i^{j+1}] + C_7 - \Delta t q \theta \left[\left(\frac{1}{B} \right)_{i-1}^{j+1} + \left(\frac{1}{B} \right)_i^{j+1} \right] - C_8 = 0 \end{aligned} \quad [4.1]$$

where:

$$C_1 = -[y_{i-1}^j + y_i^j]$$

$$C_2 = (1 - \theta) \left[\left(\frac{A}{B} \right)_{i-1}^j + \left(\frac{A}{B} \right)_i^j \right]$$

$$C_3 = (1 - \theta)[V_{i+1}^j - V_i^j]$$

$$C_4 = \frac{\Delta t}{\Delta x} C_2 C_3$$

$$C_5 = (1 - \theta)[V_{i+1}^j + V_i^j]$$

$$C_6 = (1 - \theta)[y_{i+1}^j - y_i^j]$$

$$C_7 = \frac{\Delta t}{\Delta x} C_5 C_6$$

$$C_8 = \Delta t q (1 - \theta) \left[\left(\frac{1}{B} \right)_{i+1}^j + \left(\frac{1}{B} \right)_i^j \right]$$

Momentum equation:

$$\begin{aligned} & \frac{A_1 \Delta x}{g \Delta t} [V_{i+1}^{j+1} + V_i^{j+1}] + A_1 C_9 + \frac{A_2}{g} \theta^2 [(V_{i+1}^{j+1})^2 - (V_i^{j+1})^2] \\ & + \frac{A_2}{g} \theta C_{10} [V_{i+1}^{j+1} - V_i^{j+1}] + \frac{A_2}{g} \theta C_{11} [V_{i+1}^{j+1} + V_i^{j+1}] + A_2 C_{12} \\ & + 2A_3 \theta [y_{i+1}^{j+1} - y_i^{j+1}] + A_3 C_{13} + A_4 \theta \Delta x [S_{i+1}^{j+1} + S_i^{j+1}] \\ & + A_4 C_{14} + A_4 C_{15} + \frac{A_5}{g} q \theta \Delta x \left[\left(\frac{V}{A} \right)_{i+1}^{j+1} + \left(\frac{V}{A} \right)_i^{j+1} \right] + A_5 C_{16} = 0 \end{aligned} \quad [4.2]$$

where:

$$C_9 = \frac{1}{g} \frac{\Delta x}{\Delta t} [V_{i+1}^j + V_i^j]$$

$$C_{10} = (1 - \theta)[V_{i-1}^j + V_i^j]$$

$$C_{11} = (1 - \theta)[V_{i-1}^j - V_i^j]$$

$$C_{12} = \frac{(1 - \theta)^2}{g} [(V_{i-1}^j)^2 - (V_i^j)^2]$$

$$C_{13} = 2(1 - \theta)[y_{i-1}^j - y_i^j]$$

$$C_{14} = 2[z_{i-1}^j - z_i^j]$$

$$C_{15} = \Delta x(1 - \theta)[S_{i-1}^j + S_i^j]$$

$$C_{16} = \Delta x q \frac{(1 - \theta)}{g} \left[\left(\frac{V}{A} \right)_{i-1}^j + \left(\frac{V}{A} \right)_i^j \right] \quad \text{and}$$

$$S_i^{j-1} = n^2 |V_i^{j-1}| V_i^{j-1} \left[\frac{P_i^{j-1}}{A_i^{j-1}} \right]^{\frac{4}{3}} \quad (\text{and similarly for } S_{i-1}^{j-1}, S_i^j, \text{ and } S_{i-1}^j).$$

4.3 Robustness Model

As discussed in Section 3.4.2, the four-point implicit technique is very stable for a wide range of input conditions. The technique allows solution stability to be controlled within the procedure through adjustment of the finite difference parameters Δx , Δt , and θ . Fread (1983) described a procedure used in the DWOPER program, as discussed in Section 3.4.4, in which the parameters Δt and θ were adjusted when an incipient instability or program failure was sensed. In that program, when either non-convergence in the Newton-Raphson iteration

or an erroneously low computed depth was detected, an automatic procedure was initiated to first reduce Δt , and then to increase θ in order to increase the stability of the solution. Although effective in increasing solution stability generally, the solution technique described by Fread (1983) was subject to failure under certain flow conditions for which adjustment of Δt and θ was insufficient to prevent program failure.

As discussed in Chapter 2, the objective of this work was to investigate the potential for a very robust version of the four-point implicit technique in which severe instabilities developed in the solution were sufficiently suppressed that program termination was avoided. In addition to adjustment of the finite difference parameters Δt and θ , the momentum term coefficients, A_1 and A_2 (discussed in Section 3.3), were automatically reduced in order to suppress the instability introduced by their respective momentum terms. As the values of the two selected coefficients (A_1 and A_2) were reduced to zero, the contribution from the momentum equation acceleration terms (term1 and term2) was reduced to negligible and the instabilities introduced by these terms eliminated. When the coefficients were set between zero and one, the contribution from the affected terms was reduced so that any numerical instability introduced by these terms was suppressed. With coefficients A_1 and A_2 set to zero, the contribution from the momentum equation acceleration terms was neglected and the solution technique was a diffusion wave approximate technique. If coefficients A_1 , A_2 and

A_3 , were set to zero, the acceleration and pressure terms would be neglected and the solution would become a kinematic wave approximate technique.

The initial intent for this work was to reduce the solution from full dynamic through diffusion, by reducing coefficients A_1 and A_2 towards zero, and then to kinematic by reducing A_3 towards zero as well. The initial condition used for this work was a steady-state backwater calculation behind a weir. The kinematic equation describes uniform flow for which the friction and gravity slopes are balanced. With coefficients A_1 , A_2 and A_3 set to zero, the solution technique would attempt to solve for a zero residual condition where the residual was the difference between the friction and channel bed slope terms (given zero distributed inflow). The calculated residuals would then be the difference between the steady flow initial condition and the uniform flow condition, which would always be non zero. Therefore, reduction of the momentum equation to the kinematic form would be unreasonable with a backwater calculation initial condition.

For this work, coefficient A_3 was not adjusted since, as discussed above, application of a kinematic approximate solution was not reasonable with the selected initial condition. Adjustment of coefficients A_1 and A_2 , and thus reduction of the momentum equation towards the diffusion wave equation, was investigated. The parameter Δx was not adjusted since interpolation, with a

resulting loss of accuracy, would have been required for x-locations between previous channel sections.

4.3.1 Program Logic

A simplified flowchart of the procedure, illustrating the logic applied in the robustness model, is shown in Figure 4.1. The logic follows the four-point implicit finite difference technique except that prior to a solution advancing to the next iteration, for any specific iteration within a specific time step, the solution was checked against a specific criteria and, for a positive outcome, an adjustment was made to a selected parameter (Δt , θ , A_1 and/or A_2). An example of the FORTRAN program code was included in Appendix B.

As illustrated in Figure 4.1, the unsteady flow calculation loop was started following initialization and calculation of the initial condition. The initial condition was a steady flow backwater calculation behind the downstream sharp crested weir. The constants were then calculated based on the depth and velocity values obtained for either the initial condition or for the previous time step. The Newton Raphson iteration loop was started and the values of the residuals, the difference between the function values and the theoretically correct value zero, were calculated and checked against an acceptable minimum value. If all the residuals, for that time step and iteration, were less than the minimum value, the

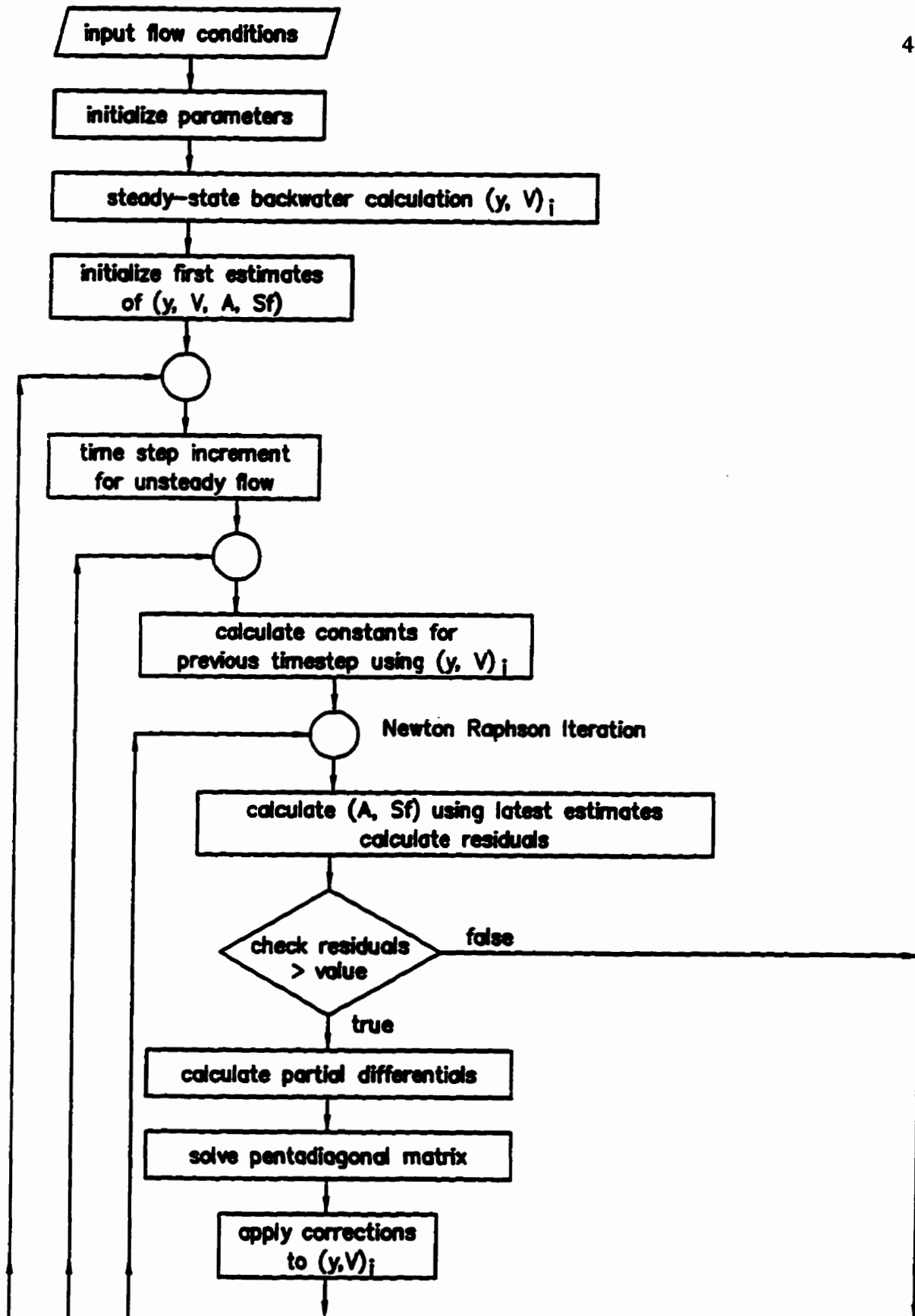


Figure 4.1 Program Flowchart

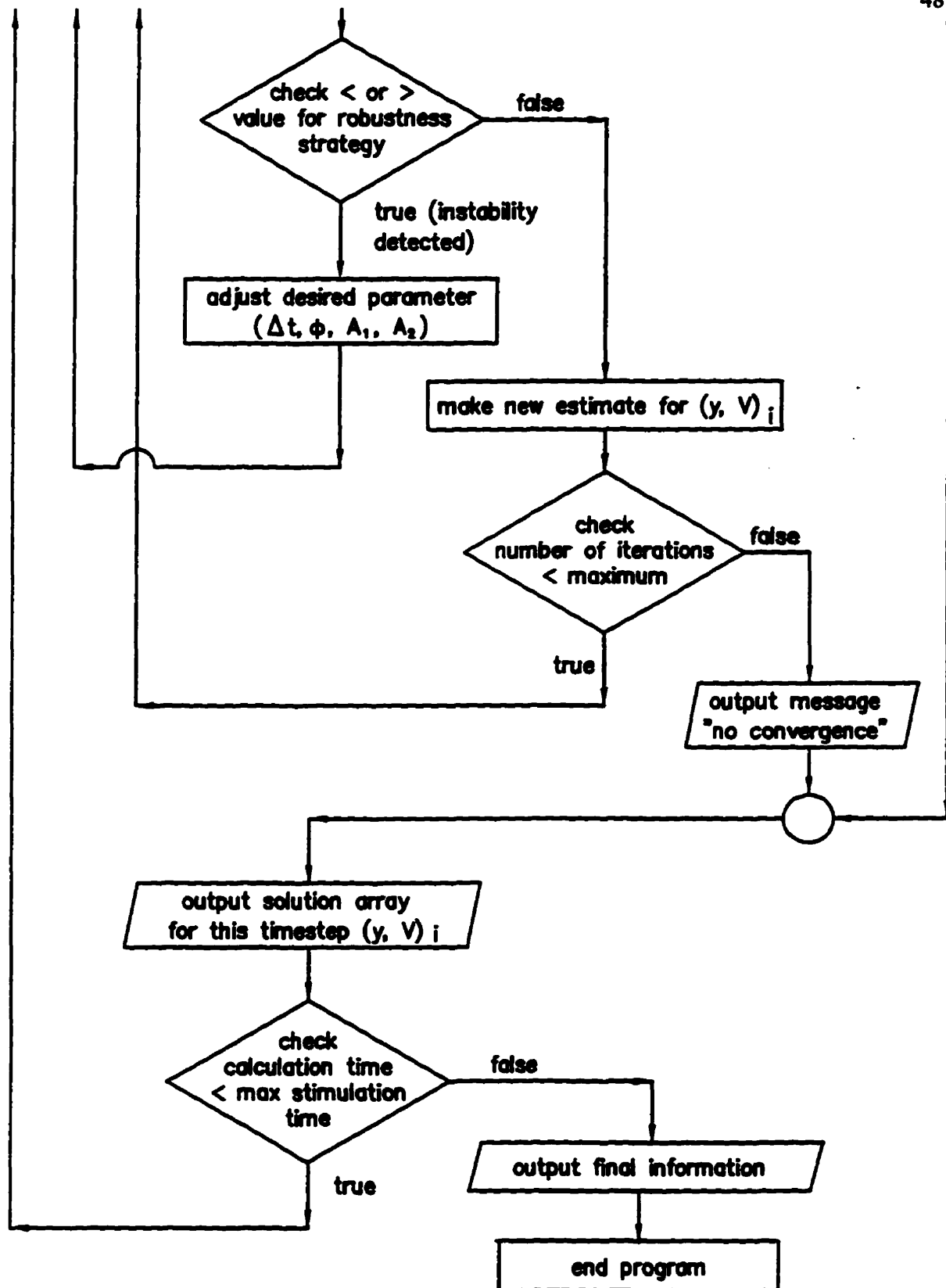


Figure 4.1 Program Flowchart, continued

estimate was accepted as the solution and the unsteady flow loop restarted for the next time step. For each time step, the solution obtained for the previous time step was used as the initial estimate for the next.

If all the residuals were not less than the minimum value, as would occur at a time step for which the input flow condition, or downstream boundary, had been changed, the partial differentials were calculated and a pentadiagonal matrix procedure used to solve the simultaneous equations. The corrections (Δy and ΔV) returned from the matrix solver were then applied to the previous estimate values to provide the new solution at this time step.

This solution was then tested against the selected robustness criterion. The criterion was selected to detect a serious instability in the solution prior to program failure. If the criteria was met, indicating that a serious instability had occurred, an adjustment was made to the desired parameter (Δt , θ , A_1 , or A_2). After the adjustment, the constants were recalculated using the adjusted parameter(s), the Newton iteration loop was re-entered, and the process was repeated. With this procedure, the programmed model provided a full dynamic solution at all time steps except those for which a numerical instability was detected by the selected criterion.

4.3.2 Application of Robustness

In order to detect a numerical instability, and incipient program failure, a procedure was programmed to check whether a selected criterion was met for any time step calculation within the solution procedure, as described above. When the selected criteria was met for the first time within a given time step, Δt was reduced by half and the computation for that time step repeated. As discussed in Section 3.4.2, such a reduction of Δt reduced the Courant number, which shifted the calculation towards the stable condition defined by $C_n = 1$.

If the instability criteria was met again, θ was increased to 0.6, with Δt kept at one-half, and the computation again repeated. If the criteria was met for a third time, θ was adjusted to 0.8. If the criteria was met again, coefficients A_1 and A_2 were gradually reduced from one towards zero. These coefficients were kept equivalent for the initial investigation. Possible adjustments, applied in subsequent calculations when the criteria continued to be met, were to 0.8, 0.5, 0.3, and 0.1. After each adjustment, a solution for the affected time step was again attempted, using $\frac{\Delta t}{2}$ and $\theta = 0.8$. If the criteria was not met, indicating that there were no severe numerical instabilities, the solution was accepted and the parameters reset to their original values for the next time step calculation. A maximum θ value of 0.8 was selected to minimize dispersion of the solution. Experiments showed that the applied adjustments were virtually identical

whether 0.8 or 1.0 was used as the maximum adjusted value for θ ; however, the dispersion effect of the large θ value was noticeably less with a θ value of 0.8.

4.3.3 Selected Criteria

Two criteria were selected to test for numerical instability and incipient program failure and thus to determine the time steps for which a parameter adjustment was made. The two selected criteria were: (1) an erroneous solution for which a channel depth less than zero ($y < 0$) was calculated, and (2) a supercritical flow condition for which Froude number was greater than one ($Fr > 1$). These two criteria were used in separate simulations so that a comparison could be made of the adjustments and affected time steps. These criteria were selected because they were effective in selecting time steps for which numerical instability occurred and they were theoretically reasonable. The depth in the channel should not be less than zero and the channel and boundary conditions were selected for conditions of subcritical flow.

Several other potential criteria were investigated but with disappointing results. Both Reynolds number and Courant number were tested, but neither was found to indicate the time steps exhibiting instability for the tested flow conditions. Actual values of various momentum equation terms were also tested, however no consistent numeric value was found which was applicable to a variety of time

steps. For the tested flow conditions, the same value of momentum equation terms was reported for time steps with and without instability. Rather than an actual value, a relative change in value of one or more of the momentum terms might prove possible as a criteria. Such an investigation was beyond the scope of this work since the terms would be expected to vary with different flow conditions and this work was intended to be a general application of improved robustness rather than specific to the flow and channel conditions tested. Several different values of Froude number (0.5, 2, 3) were also tested, and although parameter adjustments were applied to slightly different time steps in each case, no clear justification was found for one value over another. The criterion of Froude number greater than one was selected since it indicates the theoretical boundary between subcritical and supercritical flow conditions.

4.4 Parameter Selection

The stability and convergence of the model were assessed by varying the finite difference parameters, Δx , Δt , and θ , which affect the stability of the solution. Using the selected channel characteristics, these parameters were varied until the solution appeared stable and convergent. Calculations of Courant number (See Section 3.4.2) were based on the kinematic wave speed. Lateral inflow was set to zero for all conditions evaluated.

4.4.1 Channel Characteristics

Channel characteristics were selected so that a realistic channel was represented in the model. The selected channel was a rectangular, prismatic channel ($B = 3$ m) with a fairly smooth ($n = .007$) and fairly steep ($S_o = .001$) bed so that the unstable conditions necessary to test the robustness program would be relatively easy to create. In order to ensure adequate detail near the downstream weir, Δx was set to 1 m for 20 m from the weir and was not varied in this region.

4.4.2 Finite Difference Parameters

For investigation of the effect of the finite difference parameters Δx , Δt , and θ , the inflow hydrograph was set to a constant $5 \text{ m}^3/\text{s}$ and the downstream weir height changed in height instantaneously from 1.5 m to 1.0 m two minutes into the simulation. Each parameter was then varied while the others were held constant. First, Δx was varied, while holding Δt and θ constant, then Δt was varied with Δx and θ constant, and finally θ was varied between 0.5 and 1.0, with Δx and Δt held constant. The impact of the variation of the momentum coefficients, A_1 and A_2 , affecting the acceleration terms, was then investigated using the previously determined values of Δx , Δt , and θ .

The results of the investigation into the effects of varying the parameters Δx , Δt , θ , and A_1 and A_2 , were illustrated in Figures 4.2 to 4.5. The figures were plotted for a modelled distance approximately half the distance between the upstream and downstream boundaries. The results verified previous work and theory since the most stable and reasonable solution was obtained with Δt and Δx selected to provide $C_n \approx 1.0$, with θ greater than but close to 0.5, and with A_1 and A_2 equal to 1.

The variation of Δx around 70 m, to produce Courant numbers very different from 1.0, caused instability to be introduced into the solution, as illustrated in Figure 4.2. The solution appeared stable and smooth for $\Delta x = 70$ m, corresponding to Courant number between 1.0 and 1.2. When Δx was increased to 100 m ($C_n \approx 0.7$) or reduced to 30 m ($C_n \approx 2.2$), the solution showed instabilities in the form of overshooting at the peak and steps in the previously smooth curve. For the large Δx , the resulting profile was substantially altered in shape suggesting that this increment was too large to properly detail the flow. The instabilities were only apparent for times near the abrupt change in the inflow hydrograph. For later times, the various Δx profiles were similar showing the reflection back from the weir at about 12 minutes.

The effect of variation of Δt , with Δx set at 70 m as determined in the previous step, was illustrated in Figure 4.3. The result was similar to that for Δx with the

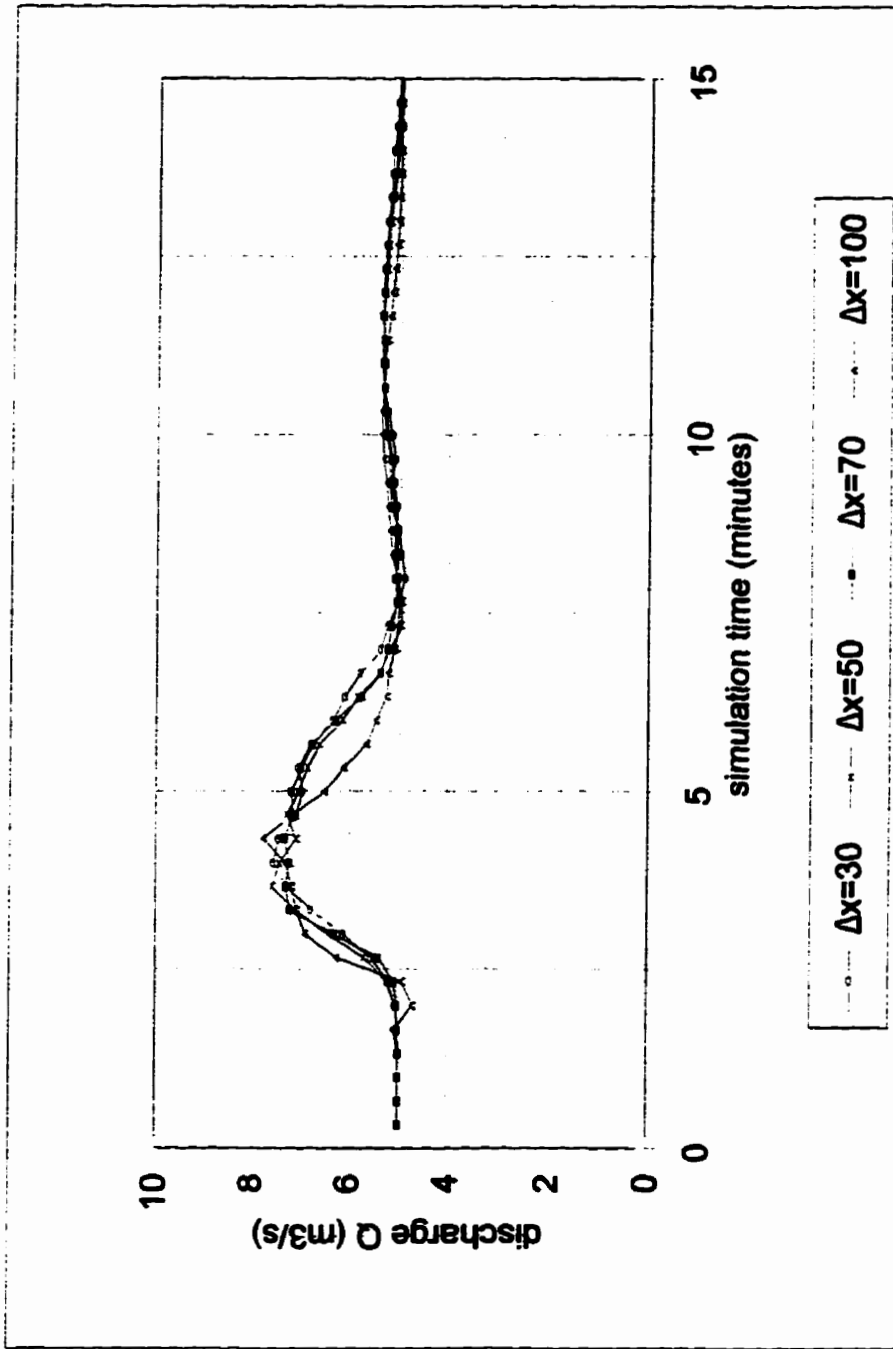


Figure 4.2 Discharge Profiles for Variation of Δx .
 Profiles shown at channel midpoint. $Q = 5 \text{ m}^3/\text{s}$, $P_w = 1.5$ to 1.0 m at 2 min , $\Delta t = 20 \text{ s}$, $\theta = 0.52$, $A_1 = A_2 = 1$.

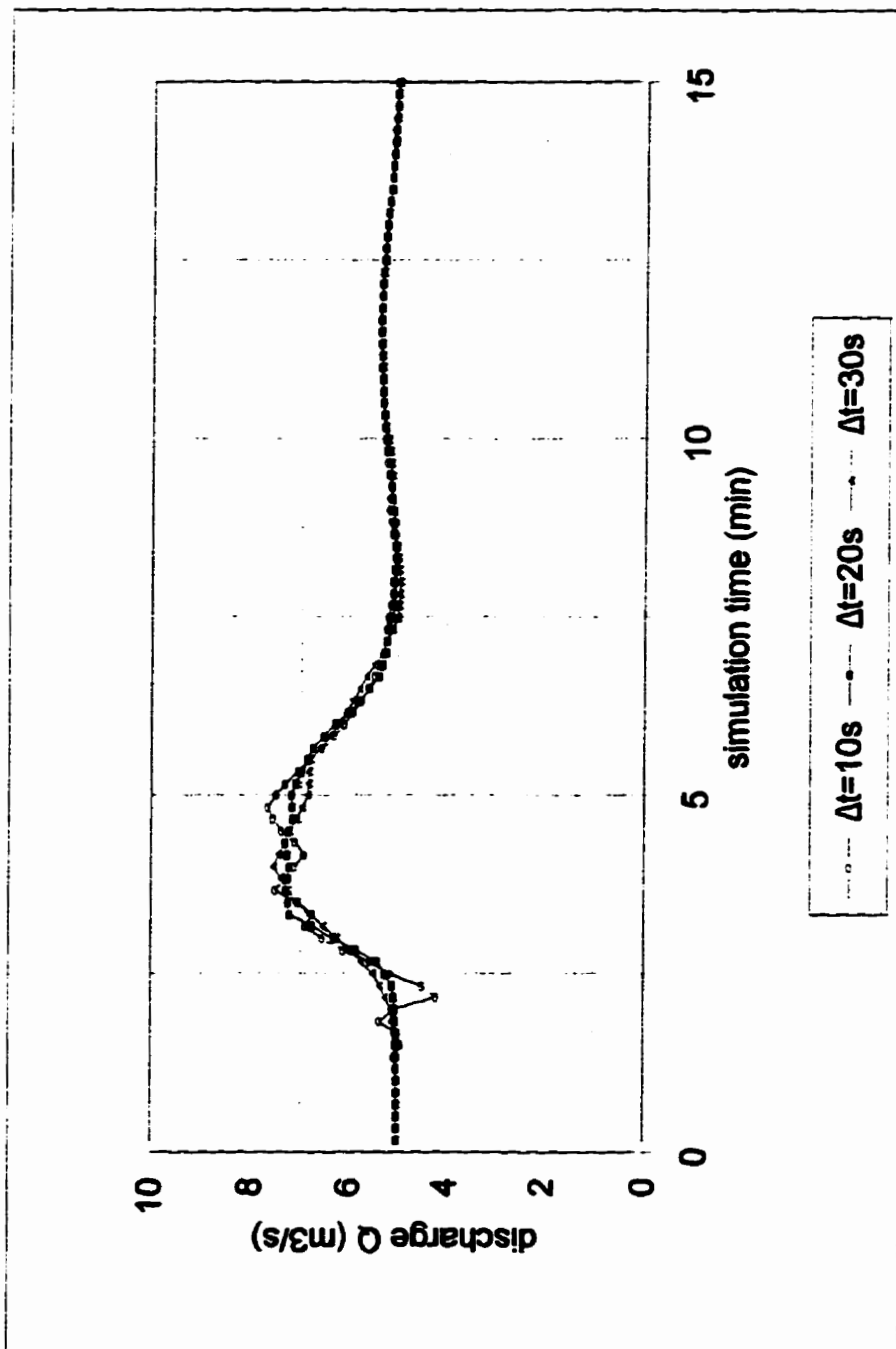


Figure 4.3 Discharge Profiles for Variation of Δt . Profiles shown at channel midpoint. $Q = 5 m^3/s$, $P_w = 1.5$ to $1.0 m$ at $2 min$, $\Delta x = 70m$, $\theta = 0.52$, $A_1 = A_2 = 1$.

most stable solution obtained with $\Delta t = 20$ s ($C_n \approx 1.0$). A reduced Δt of 10 s ($C_n \approx 0.5$) caused instabilities resulting in a distinctly stepped curve, overshooting and searching at the peak, and undershooting as the hydrograph started to rise. A further reduction of Δt caused very large spikes in the solution and finally caused the program to fail. Again, the instabilities were observed near the time of the change in inflow.

The effect of variation of θ , with $\Delta x = 70$ m and $\Delta t = 20$ s as previously determined, was illustrated in Figure 4.4. Stable solutions were obtained for $\theta = 0.55, 0.6, \text{ and } 0.8$. With θ greater than 0.55, dispersion of the wave was apparent with the peak flattening and widening more severely as θ was increased towards 1. With $\theta = 0.5$, the solution showed instability producing a seriously stepped curve. This instability continued for the full duration of the simulation. As suggested by theory, the best solution, stable and without obvious dispersion, was obtained with $\theta = 0.55$. When θ was reduced below 0.5, the program failed.

The effect of varying the momentum coefficients A_1 and A_2 , with the other parameters as previously selected, was illustrated in Figure 4.5. The most accurate solution was expected for $A_1 = A_2 = 1.0$ since the full dynamic equations were solved in that case. The parameters selected above ($\Delta x = 70$ m, $\Delta t = 20$ s, $\theta = 0.55$) provided a smooth curve with $A_1 = A_2 = 1$, which included the

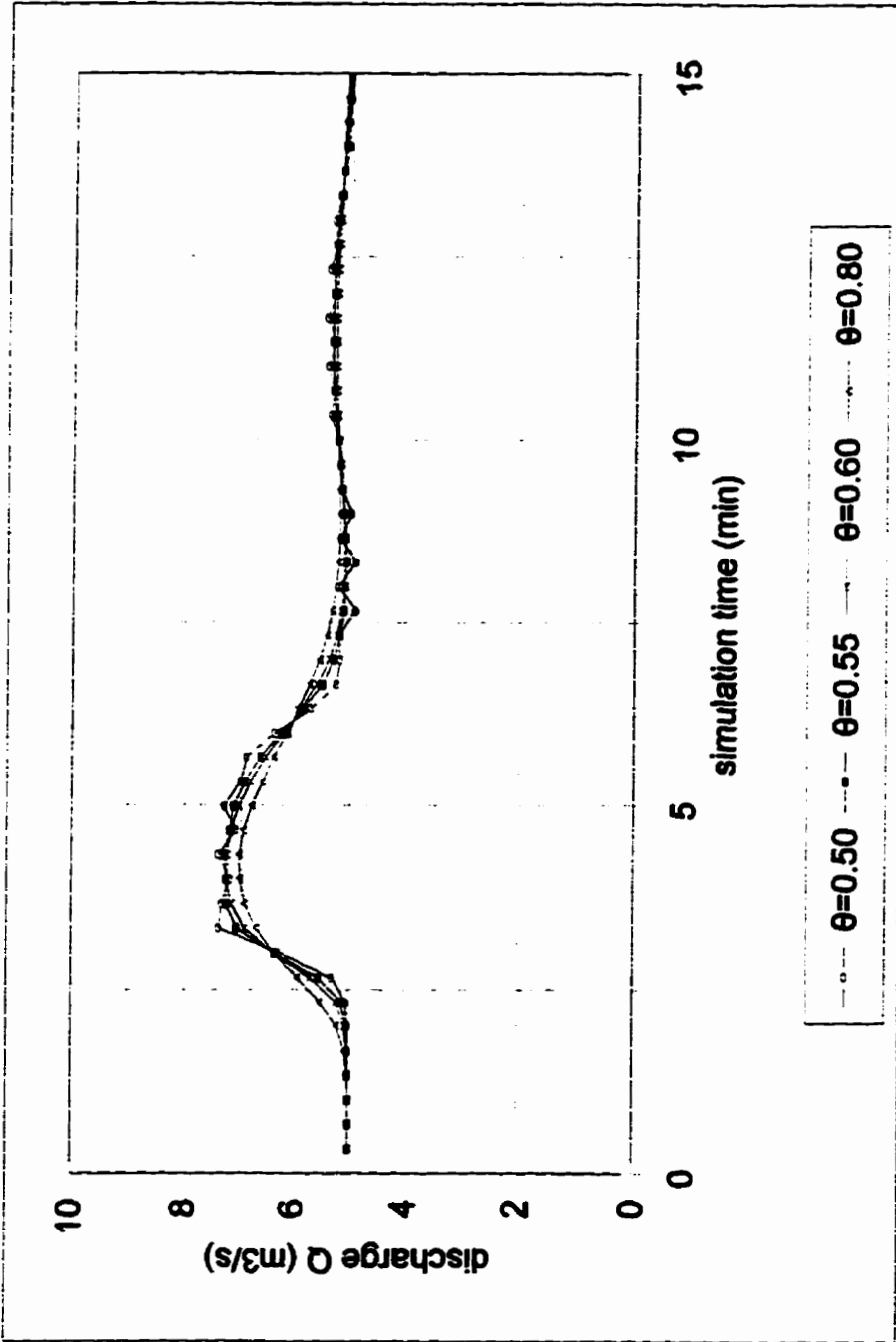


Figure 4.4 Discharge Profiles for Variation of θ . Profiles shown at channel midpoint. $Q = 5 \text{ m}^3/\text{s}$, $P_w = 1.5 \text{ to } 1.0 \text{ m}$ at 2 min, $\Delta x = 70\text{m}$, $\Delta t = 20\text{s}$, $A_1 = A_2 = 1$.

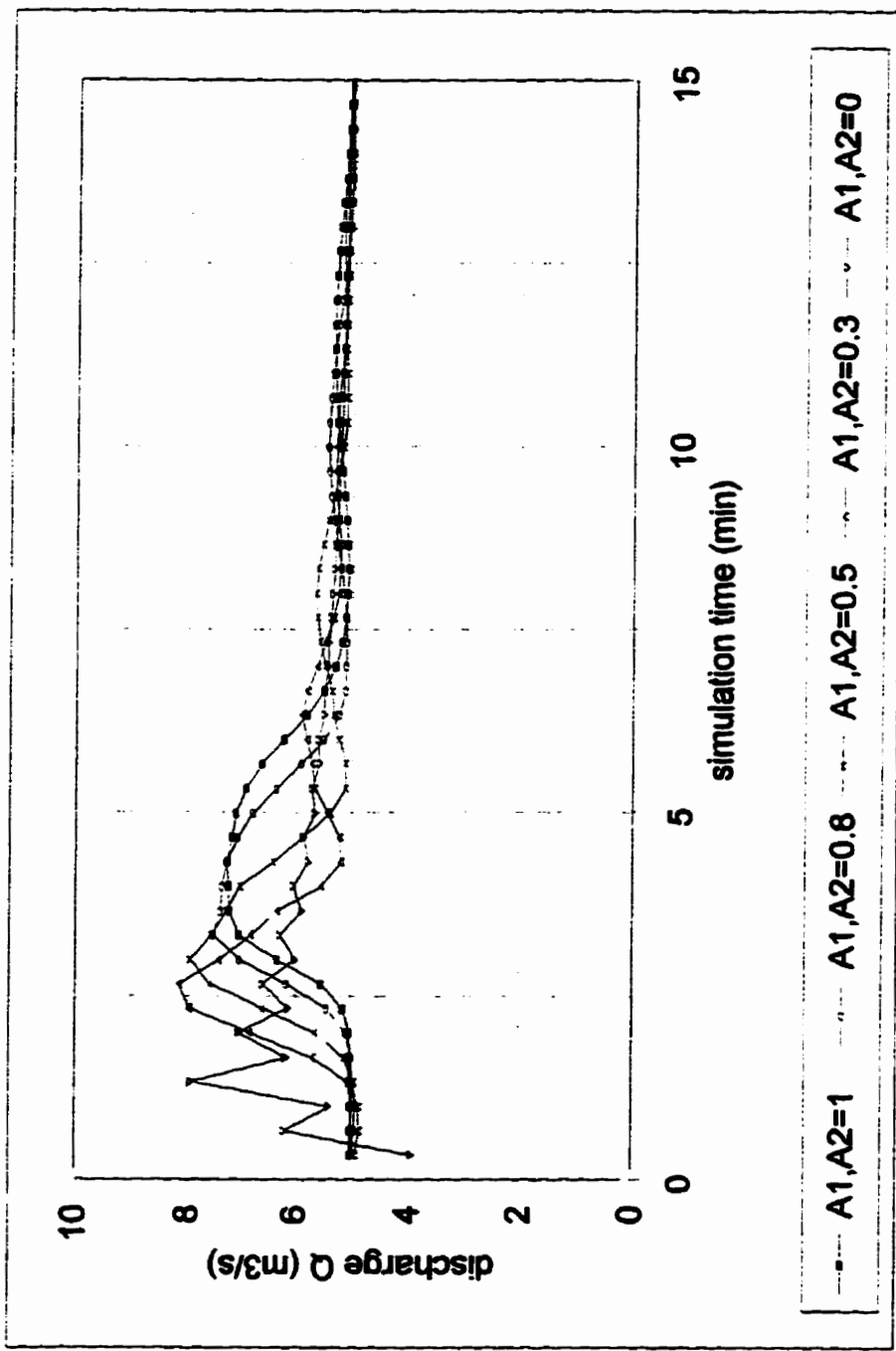


Figure 4.5 Discharge Profiles for Variation of A_1 and A_2 . Profiles shown at channel midpoint. $Q = 5 \text{ m}^3/\text{s}$, $P_w = 1.5$ to 1.0 m at 2 min , $\Delta x = 70 \text{ m}$, $\Delta t = 20 \text{ s}$, $\theta = 0.52$.

reflection effect from the downstream weir at about 12 minutes. With A_1 and A_2 reduced below 1.0, the entire solution was shifted to an earlier time and the peak increased and narrowed. The weir reflection was still evident although increased in amplitude and also shifted to an earlier time. A similar effect was reported by Smith (1980) who found the length of gradually varied flow profile was reduced with an approximate model. As previously discussed, the solution technique used for this work was a full-dynamic method when all coefficients (A_1 to A_5) were set equal to 1, and the approximate diffusion technique when A_1 and A_2 were reduced to zero.

When A_1 and A_2 were reduced to zero, the solution became somewhat unstable and appeared to search between extremes causing a stepped discharge profile. The weir reflection was no longer reported clearly since a diffusion technique solution can only approximate effects in the downstream direction. As discussed in Section 4.3, only coefficients A_1 and A_2 were varied, and these were kept equivalent for this portion of the work.

Results from this investigation suggested that the best solution parameters for this channel and conditions were the following: $\Delta x = 70$ m, $\Delta t = 20$ s, $\theta = 0.55$, and $A_1 = A_2 = 1$. Assuming the celerity of a kinematic wave, these parameters provided a Courant number very close to one for these flow conditions. In order to enhance the potential instability, so that recovery could be tested, the

parameters selected for the rest of this work were as follows: $\Delta x = 50$ m, $\Delta t = 20$ s, and $\theta = 0.52$, which provided a Courant number of slightly more than one under these flow conditions. Within 20 m of the downstream weir, Δx was set at 1 m. The values of Δx were not varied.

4.4.3 Stable Flow Condition

In order to verify that the model was successful, and to provide a comparison for the later unstable solutions, the channel characteristics and finite difference parameters selected above were used to determine a flow condition which provided a stable full dynamic solution. The selected flow condition was a constant inflow hydrograph at 5 m³/s with adjusted weir height from 1.5 m to 1.0 m at 0.5 minutes. The resulting full dynamic solution, plotted at the indicated locations along the channel, was shown in Figure 4.6. The discharge profile indicated a fairly stable solution. Some instability was evident on the rising limbs of the profiles where a sawtooth wave was apparent. Of interest to the discussion of Section 4.4.4 below, the rising limb of the discharge profile occurred at about 3 minutes for the 750 m x-location discharge profile.

4.4.4 Contribution of Momentum Equation Terms

The contributions, and relative significance, of momentum equation term1

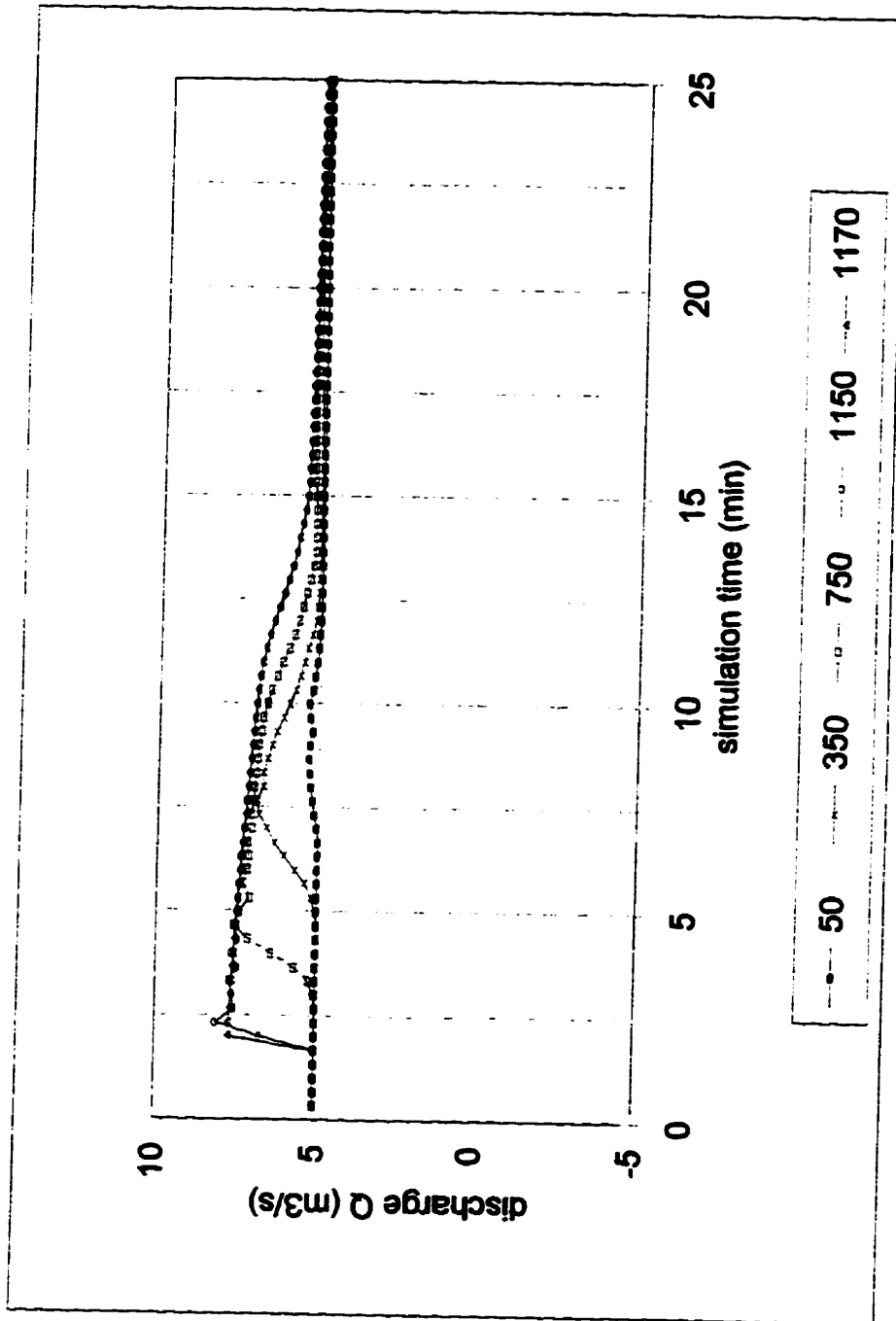


Figure 4.6 Discharge Profiles for Stable Solution. Profiles shown at X-distances indicated. $Q = 5 \text{ m}^3/\text{s}$, $P_w = 1.5$ to 1.0 m at 2.0 min , $\Delta x = 50 \text{ m}$, $\Delta t = 20 \text{ s}$, $\theta = 0.52$, $A_1 = A_2 = 1$.

through term4 for the stable flow condition described above was shown in Figure 4.7. The values plotted for each term were from distance location $X = 750$ m. Term5 was zero for this work since it represented lateral inflow, which was set to zero initially. (The momentum equation terms were defined in Section 3.3.)

Term4, the combined friction and gravity force term, remained fairly constant throughout the simulation at a value of about -0.1. The sign of the term indicates that gravity effects dominate friction effects, since term4 is proportional to $S_f - S_o$, as expected for subcritical flow conditions. For most of the simulation time, term3, the pressure force term, contributed a value of about +0.1, virtually balancing the contribution of term4. The positive value of this term, proportional to $\frac{\delta y}{\delta x}$, indicated that the depth was increasing downstream, as expected towards the weir, except for a moment when the profile reversed. Term1 and term2, the local and convective acceleration terms, respectively, contributed virtually zero for most of the simulation, except near the time at which the change in weir height was applied. A dramatic change in the values of the acceleration terms, term1 and term2, and the pressure term, term3, occurred at about three minutes into the simulation.

The values of term1 and term3 were affected dramatically while the value of term2 was affected to a lesser degree. The changes in term1 and term2 were positive while the change in term3 was negative and the values of these

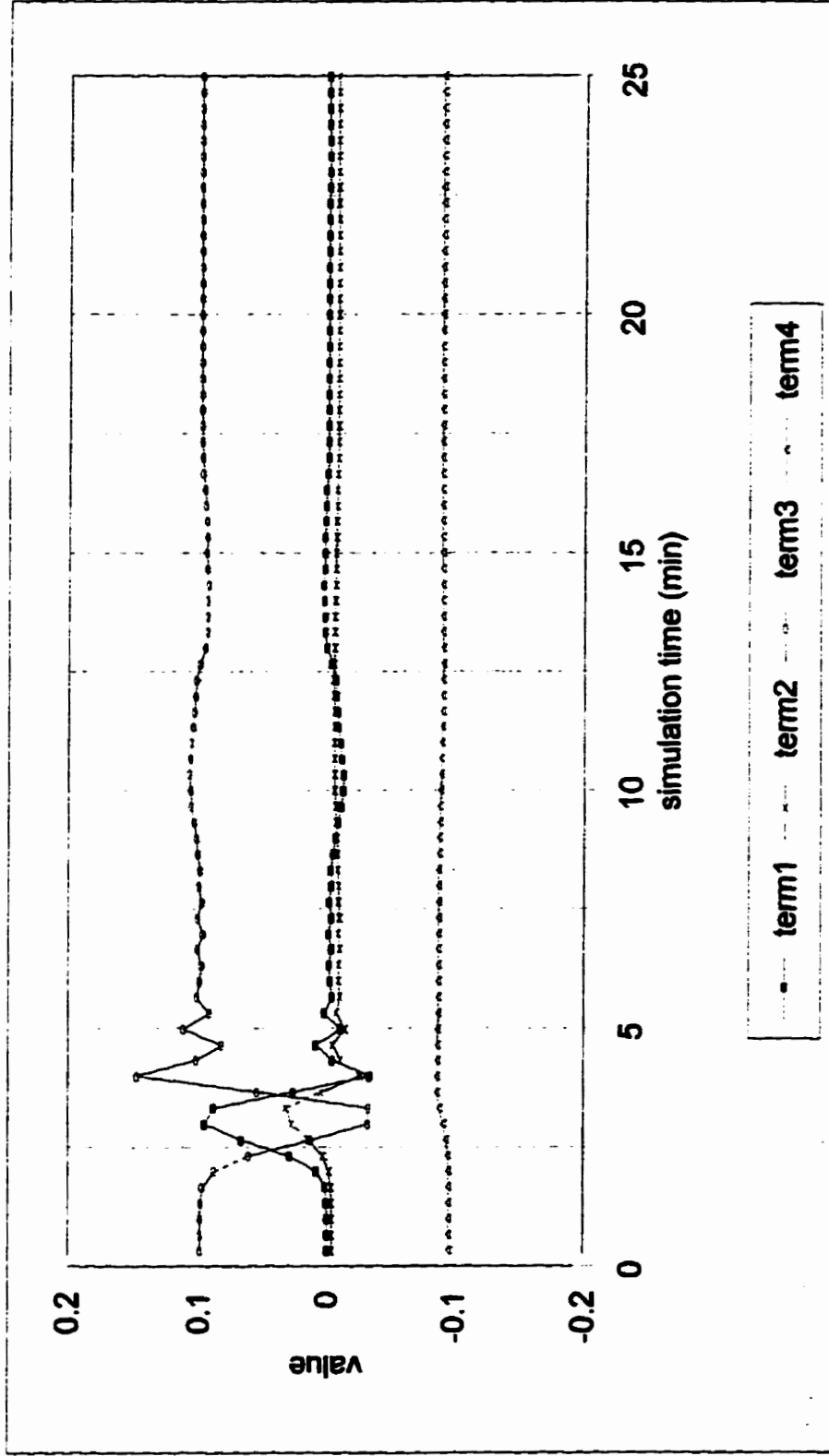


Figure 4.7 Momentum Equation Terms for Stable Solution. Profiles shown at $X = 750$ m. $Q = 5$ m³/s, $P_w = 1.5$ to 1.0 m at 2.0 min, $\Delta x = 50$ m, $\Delta t = 20$ s, $\theta = 0.52$, $A_1 = A_2 = 1$.

changes were such that the sum of the terms remained close to zero. The changes in term3 were balanced by the sum of the changes in term1 and term2. As mentioned in Section 4.4.3 and as shown in Figure 4.6, the rising limb of the discharge profile also occurred at a time of about 3 minutes. The simultaneous occurrence of a dramatic change in discharge profile and in the values of term1 and term2 suggests that numerical instability in the solution can be reduced by reduction of coefficients A_1 through A_5 .

CHAPTER 5. NUMERICAL EXPERIMENTS

5.1 Introduction

Numerical experiments were performed through repeated application of the model. Several unstable flow conditions were selected for which program failure could not be prevented by adjustment of the traditional stability parameters of Δt and θ . Adjustment of coefficients A_1 and A_2 , as well as Δt and θ , was then applied for these flow conditions and program failure prevented. The stable full dynamic solutions discussed in Section 4.4.3 provides a comparison for the unstable solutions obtained here.

5.2 Results

For unstable condition #1, flow conditions were selected for which a full dynamic solution could be obtained with adjustment of Δt and θ . For unstable conditions #2 and #3, flow conditions were chosen for which a full dynamic solution could not be obtained. To obtain a solution for these conditions, adjustment of A_1 and A_2 , as well as Δt and θ , was required. The various flow conditions are summarized in Table 5.1. The automatic procedure programmed into the model caused application of parameter adjustments according to the two selected criteria, $y < 0$ and $Fr > 1$ (as described in Section 4.3). The parameter

Table 5.1 Selected Flow Conditions

flow condition	input Q (m ³ /s)	change at time (min)	weir Pw (m)	change at time (min)	channel L (m)
1	5		1 to 0.5	0.5	1200
2	2 to 5	0.5	0.5 to 1	0.5	600
3	2 to 5	0.5	1.1 to 1.3	0.5	1200

Table 5.2 Applied Parameter Adjustments

flow condition	Figure	initial Cn	criterion applied	solution result	timesteps affected	adjusted parameters		
						Δt	theta	A1=A2
initial parameters:						20	0.52	1.0
1	5.1	1.1-1.3		failure				
1a	5.2	1.1-1.3	y < 0	success	59-60	10		
1b	5.3	1.1-1.3	Fr > 1	success	46-91	10	0.8	
2	5.4	0.9-1.4		failure				
2a	5.5		Fr > 1	failure	3-end	10	0.8	
2b	5.6	0.8-1.5	y < 0	success	15	10	0.8	0.1
2c	5.7	0.9-1.4	Fr > 1	success	3-21	10	0.8	0.5
3	5.8	0.9-1.8		failure				
3a	5.9	1	y < 0	success	26-43	10	0.8	0.5,0.3
3b	5.10	1	Fr > 1	success	3-32	10	0.8	0.5

adjustments applied for solution are summarized in Table 5.2.

5.2.1 Unstable Full Dynamic Solution

Flow conditions for 'unstable condition #1' included a constant inflow hydrograph at $5 \text{ m}^3/\text{s}$ and a sudden decrease in weir height from 1.0 m to 0.5 m at 0.5 minutes. Channel length was 1200 m. The partial profile obtained without adjustment of any parameters, with an insipient instability in the $X = 50 \text{ m}$ profile just before program failure, was shown in Figure 5.1. The complete profile obtained with automatic adjustment of Δt applied according to the criteria $y < 0$, was shown in Figure 5.2. The complete profile obtained with automatic adjustment of Δt and θ applied according to the criteria $Fr > 1$ was included in Figure 5.3. For this flow condition, adjustment of the traditional parameters of Δt and θ was sufficient to prevent program failure so that a full dynamic solution was obtained throughout the simulation.

5.2.2 Unstable Robust Solutions

Flow conditions for 'unstable condition #2' included a sudden increase in the inflow hydrograph from $2 \text{ m}^3/\text{s}$ to $5 \text{ m}^3/\text{s}$ and a sudden increase in weir height from 0.5 m to 1.0 m, both at 0.5 minutes. Channel length was 600 m. The partial profile obtained without adjustment of any parameters, with an insipient

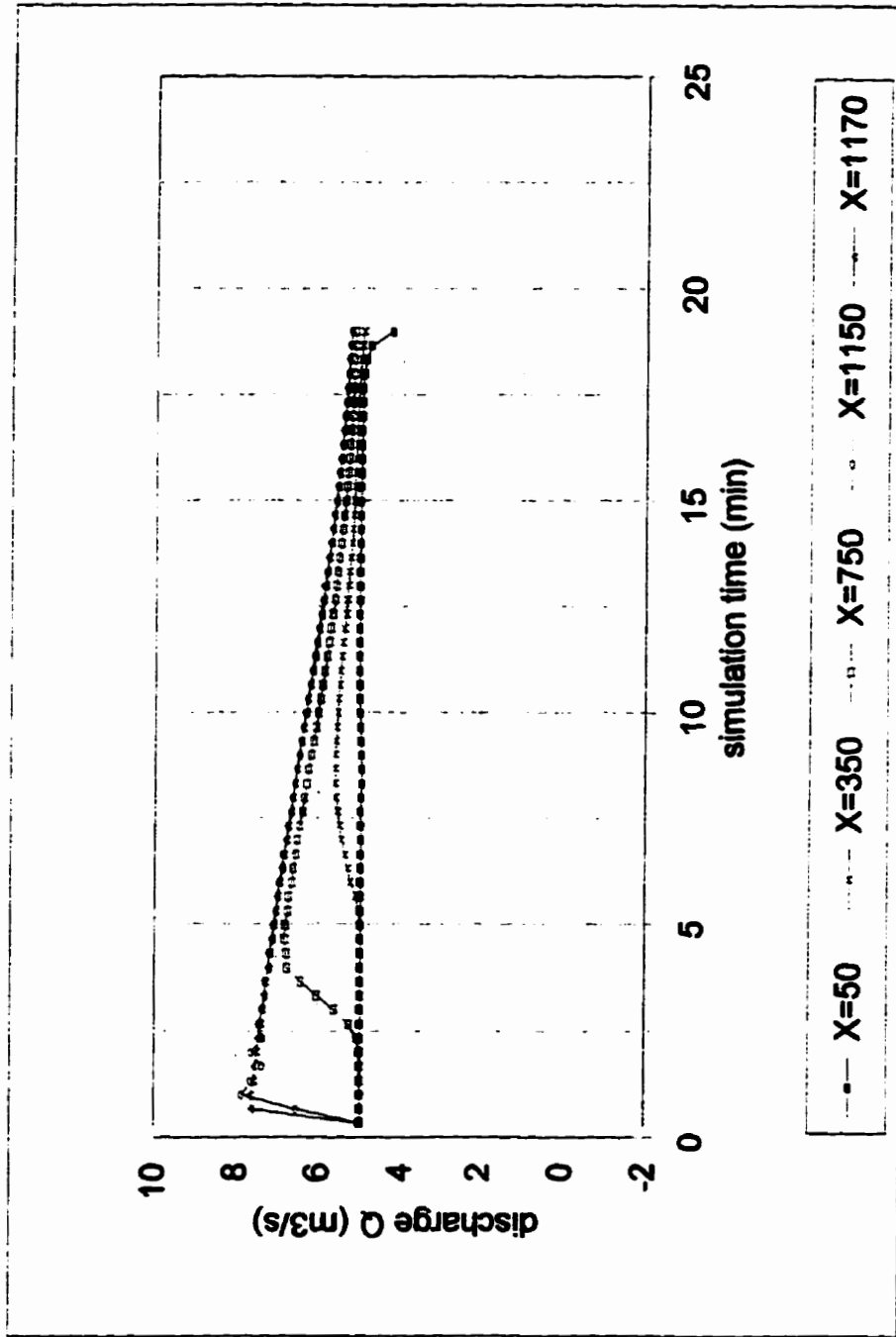


Figure 5.1 Discharge Profiles for Unstable Flow Condition #1. Profiles shown at X-distances indicated. $Q = 5 \text{ m}^3/\text{s}$, $P_w = 1.0$ to 0.5 m at 0.5 min , $\Delta x = 50 \text{ m}$, $\Delta t = 20 \text{ s}$, $\theta = 0.52$, $A_1 = A_2 = 1$.

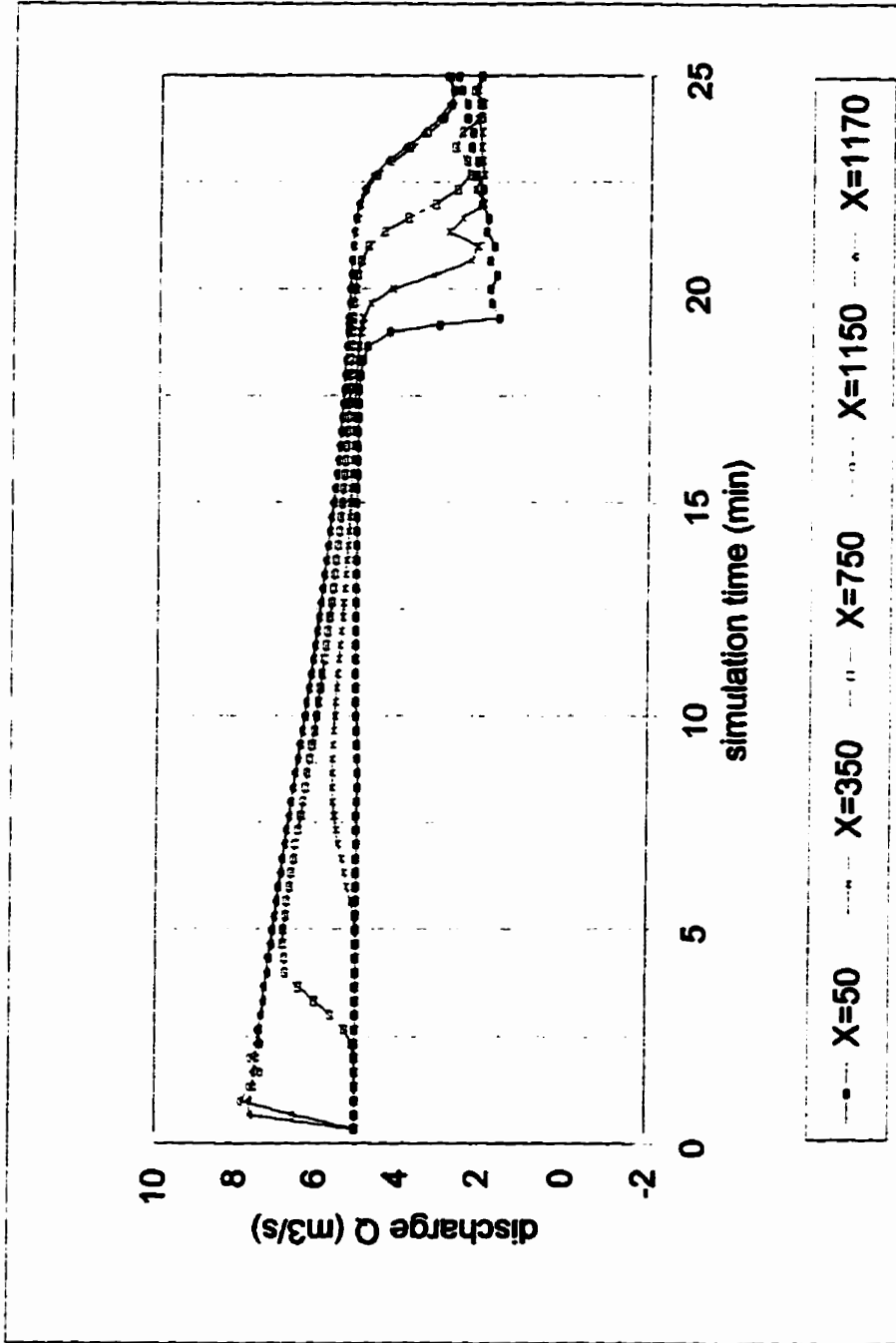


Figure 5.2 Discharge Profiles for Unstable Flow Condition #1-a: Δt adjusted for $y < 0$ criterion. Profiles shown at X-distances indicated. $Q = 5 \text{ m}^3/\text{s}$, $P_w = 1.0$ to 0.5 m at 0.5 min , $\Delta x = 50 \text{ m}$, $\theta = 0.52$, $A_1 = A_2 = 1$.

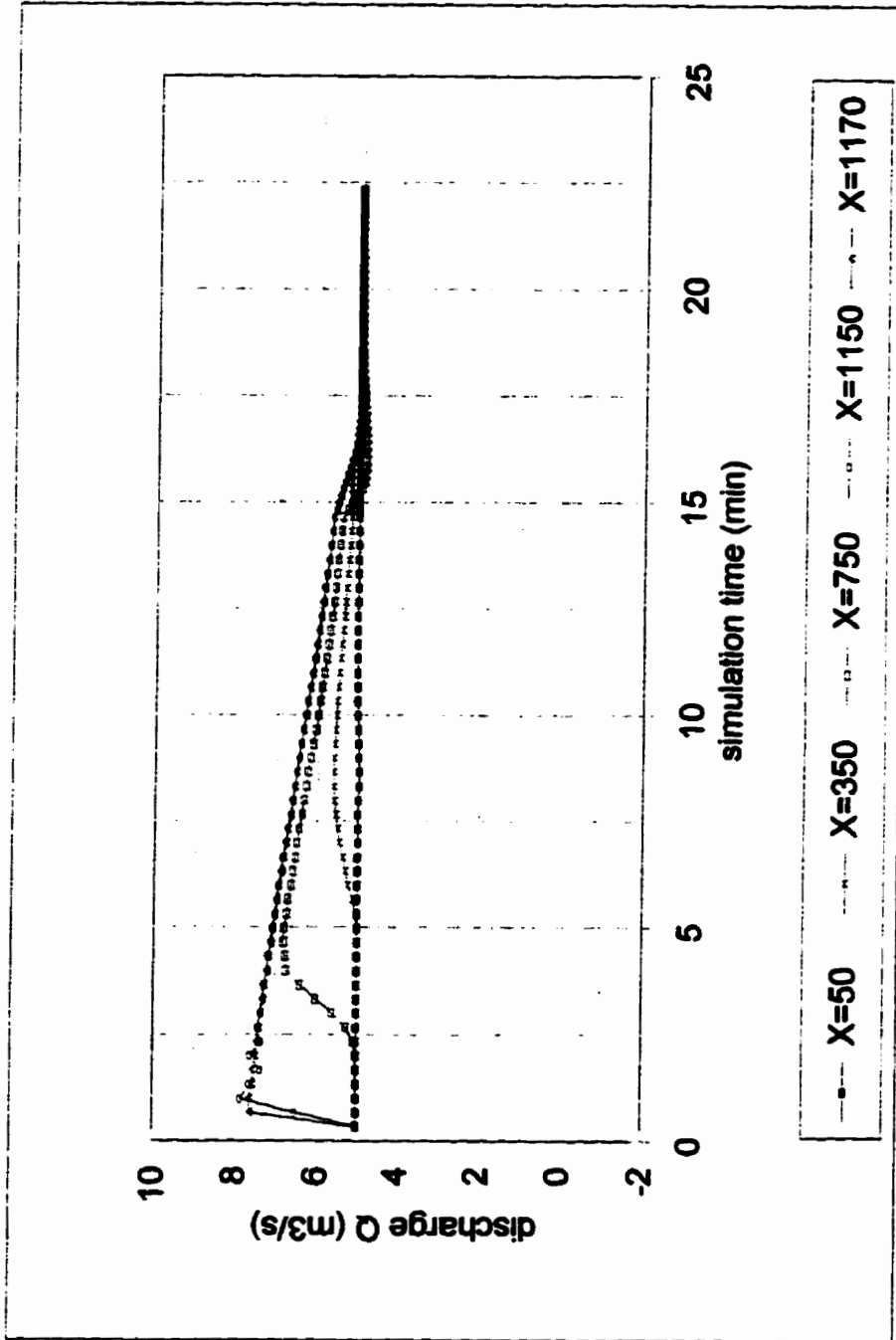


Figure 5.3 Discharge Profiles for Unstable Flow Condition #1-b: Δt and θ adjusted for $Fr > 1$ criterion. Profiles shown at X-distances indicated. $Q = 5 \text{ m}^3/\text{s}$, $P_w = 1.0$ to 0.5 m , $\Delta x = 50 \text{ m}$, $A_1 = A_2 = 1$.

instability in the $X = 50$ m profile just before program failure, was shown in Figure 5.4. The partial profile obtained with adjustment of only the traditional parameters Δt and θ was shown in Figure 5.5. This result suggests that a full dynamic solution under these conditions was not possible due to instability causing program failure. The complete profile obtained with automatic adjustment of A_1 and A_2 , as well as Δt and θ , applied according to the criteria $y < 0$ was shown in Figure 5.6. Although significant instability is still apparent in the solution, a solution was obtained without program failure. The instability was observed to coincide with time steps to which no parameter adjustment was applied. This result suggests that the $y < 0$ criteria did not identify all the time steps for which numerical instability occurred. The complete profile obtained with automatic adjustment of A_1 and A_2 as well as Δt and θ applied according to the criteria $Fr > 1$ was shown in Figure 5.7. Substantially less instability was apparent in this solution suggesting that the adjustments were applied to more appropriate time steps. Again a solution was obtained without program failure. The solution appeared smoothed, suggesting that solution accuracy may have been reduced and that the criteria $Fr > 1$ may have applied the parameter adjustment at too many time steps. With the criteria $Fr > 1$, reduction of A_1 and A_2 to a value of 0.5, as indicated in Table 5.2, was sufficient to suppress the instability and allow program completion. With the criteria $y < 0$, reduction of A_1 and A_2 to a value of 0.1 was required to sufficiently reduce instability. Since the criterion $Fr > 1$ applied adjustments to a broader range on time steps, the

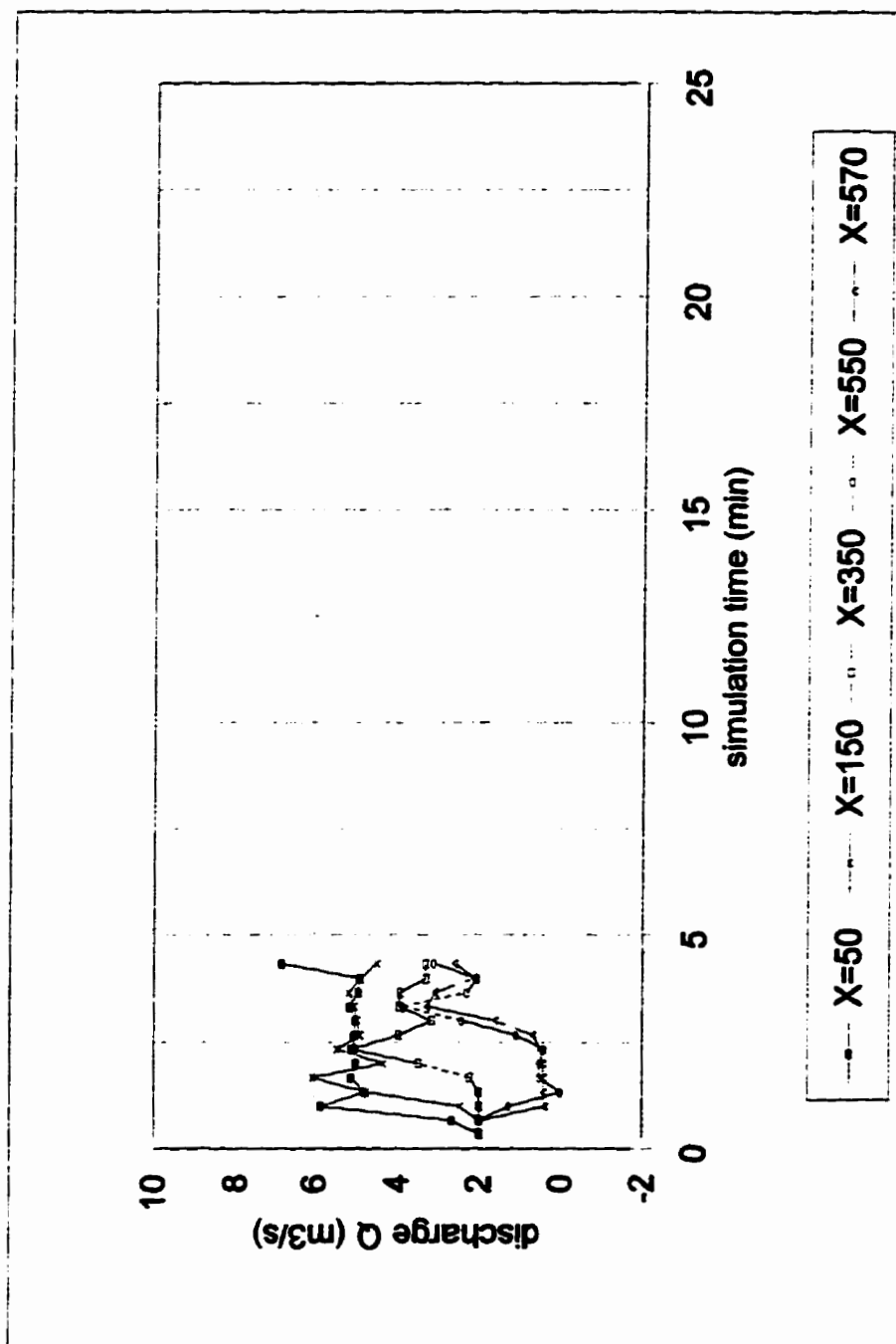


Figure 5.4 Discharge Profiles for Unstable Flow Condition #2. Profiles shown at X-distances indicated. $Q = 2$ to 5 m³/s at 0.5 min, $P_w = 0.5$ to 1.0 m at 0.5 min, $\Delta x = 50$ m, $\Delta t = 20$ s, $\theta = 0.52$, $A_1 = A_2 = 1$.

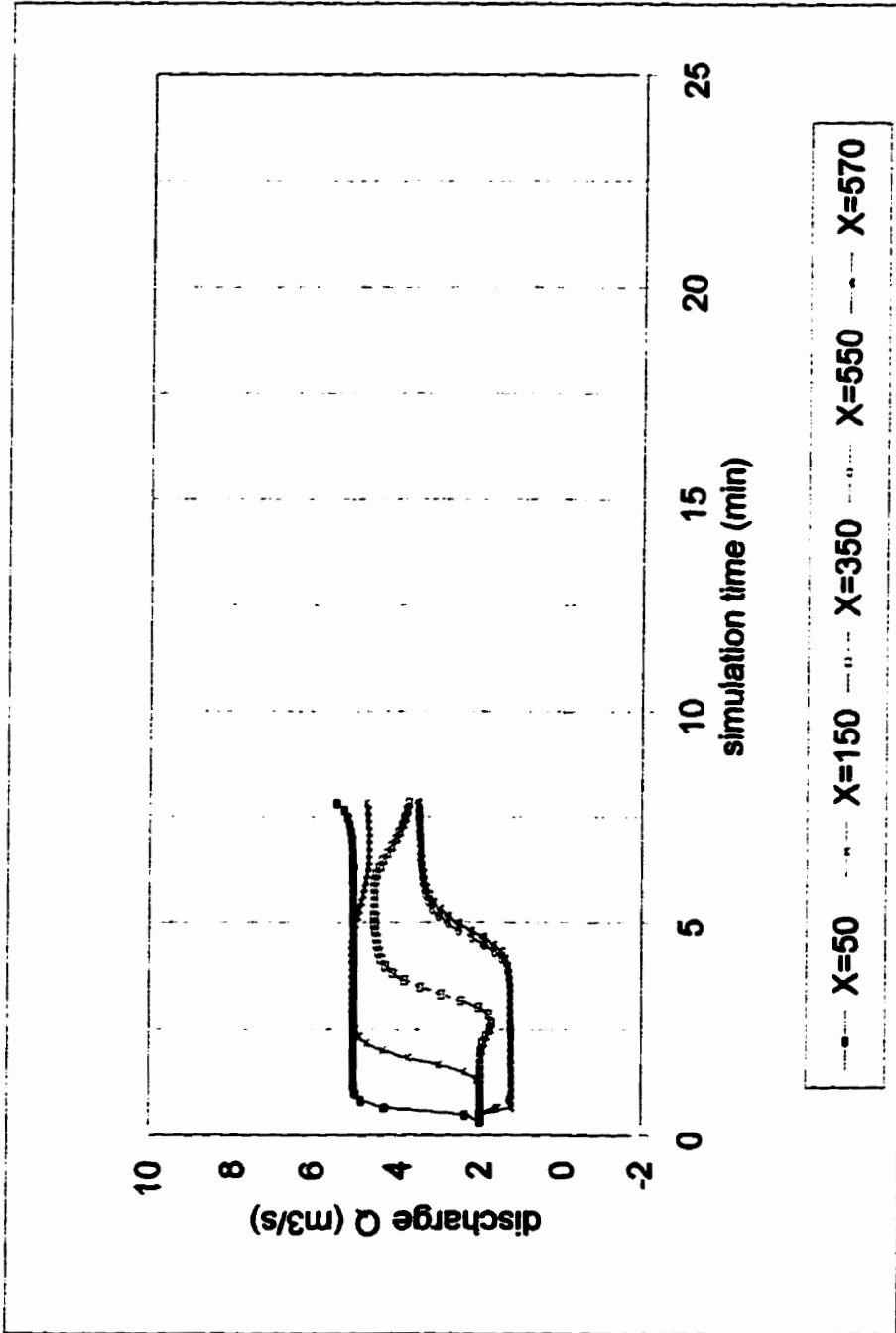


Figure 5.5 Discharge Profiles for Unstable Flow Condition #2-a: Δt and θ adjusted for $Fr > 1$ criterion. Profiles shown at X-distances indicated. $Q = 2$ to $5 \text{ m}^3/\text{s}$ at 0.5 min , $P_w = 0.5$ to 1.0 m at 0.5 min , $\Delta x = 50 \text{ m}$, $A_1 = A_2 = 1$.

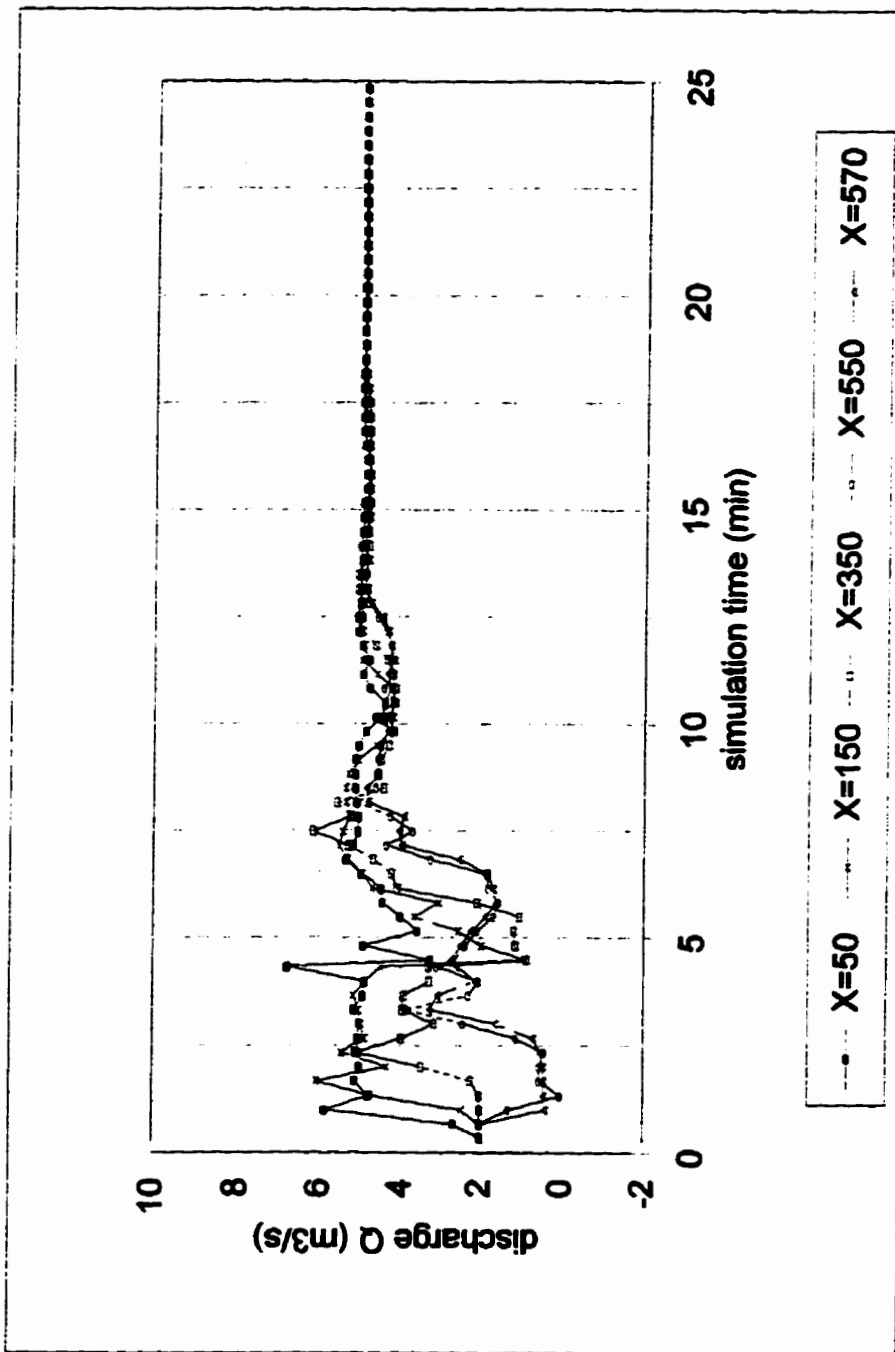


Figure 5.6 Discharge Profiles for Unstable Flow Condition #2-b: Δt , θ , A_1 , and A_2 adjusted for $y < 0$ criterion. Profiles shown at X-distances indicated. $Q = 2$ to $5 \text{ m}^3/\text{s}$ at 0.5 min , $P_w = 0.5$ to 1.0 m at 0.5 min , $\Delta x = 50 \text{ m}$.

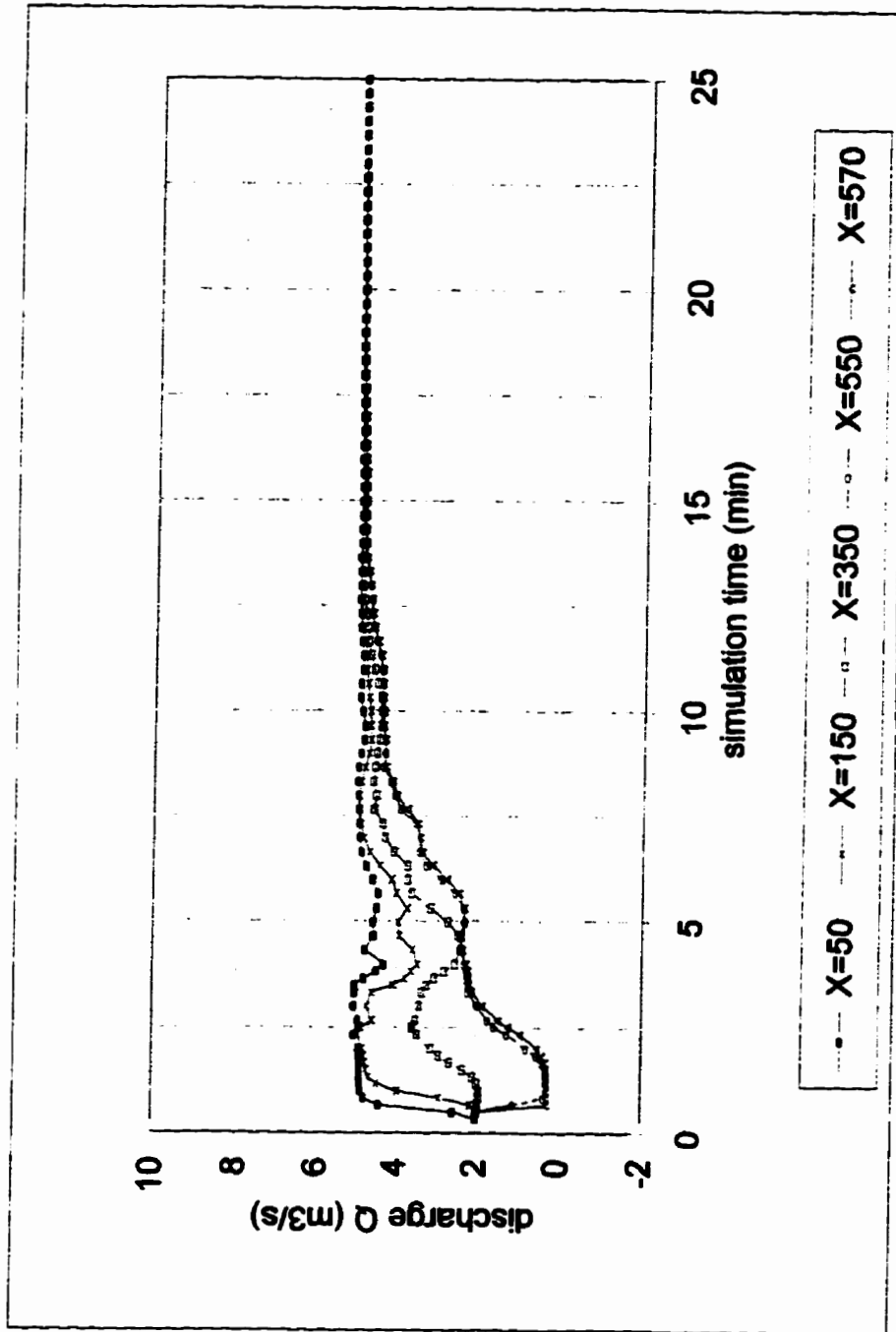


Figure 5.7 Discharge Profiles for Unstable Flow Condition #2-c: Δt , θ , A_1 and A_2 adjusted for $Fr > 1$ criterion. Profiles shown at X-distances indicated. $Q = 2$ to $5 \text{ m}^3/\text{s}$ at 0.5 min, $P_w = 0.5$ to 1.0 m at 0.5 min, $\Delta x = 50\text{m}$.

occurring instability may have been reduced allowing a less severe reduction of A_1 and A_2 . Flow conditions for 'unstable condition #3' involved a sudden increase in inflow hydrograph from $2 \text{ m}^3/\text{s}$ to $5 \text{ m}^3/\text{s}$ and a sudden increase in weir height from 1.1 m to 1.3 m, both at 0.5 minutes. Channel length was 1200 m. The partial profile obtained without adjustment of any parameters, with an insipient instability in various profiles just before program failure, was shown in Figure 5.8. A complete solution was not obtained with adjustment of Δt and θ only. The complete profile obtained with automatic adjustment of A_1 and A_2 as well as Δt and θ applied according to the criteria $y < 0$ was shown in Figure 5.9. Some instability was still apparent in the solution and, again, this instability was observed to coincide with time steps for which no parameter adjustment was applied. The complete profile obtained with automatic adjustment of A_1 and A_2 as well as Δt and θ applied according to the criteria $Fr > 1$ was shown in Figure 5.10. Again, little instability was apparent in the solution suggesting that the adjustments were applied to the appropriate time steps.

5.2.3 Adjustment of Coefficients A_1 and A_2

An investigation of the relative significance of the two acceleration terms, term1 and term2, was completed by allowing adjustment of only one of the respective coefficients, A_1 and A_2 , at a time. The same unstable flow conditions were used as reported above and summarized in Table 5.1. For unstable flow conditions

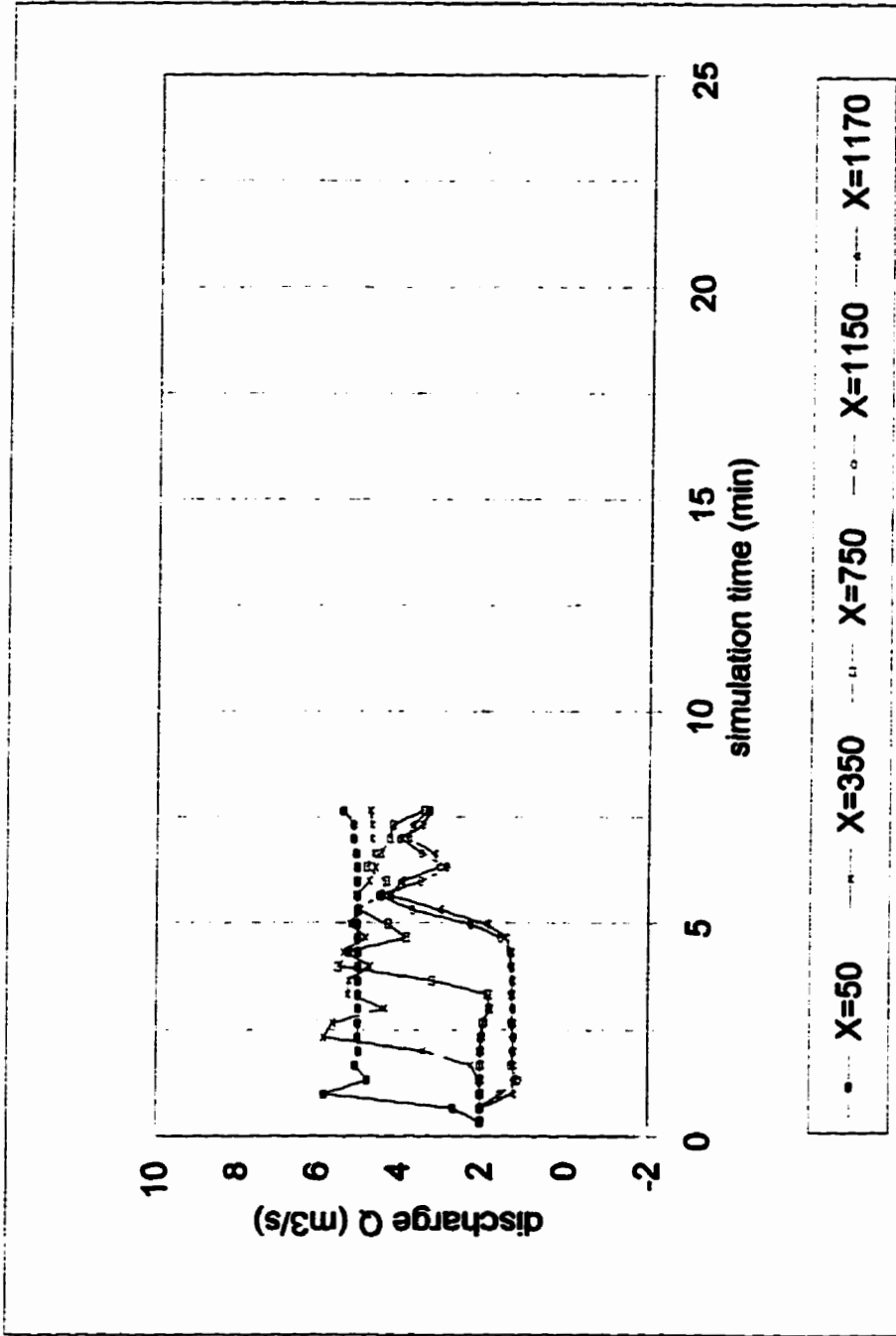


Figure 5.8 Discharge Profiles for Unstable Flow Condition #3. Profiles shown at X-distances indicated.

$Q = 2$ to $5 \text{ m}^3/\text{s}$ at 0.5 min , $P_w = 1.1$ to 1.3 m at 0.5 min , $\Delta x = 50 \text{ m}$, $\Delta t = 20 \text{ s}$, $\theta = 0.52$, $A_1 = A_2 = 1$.

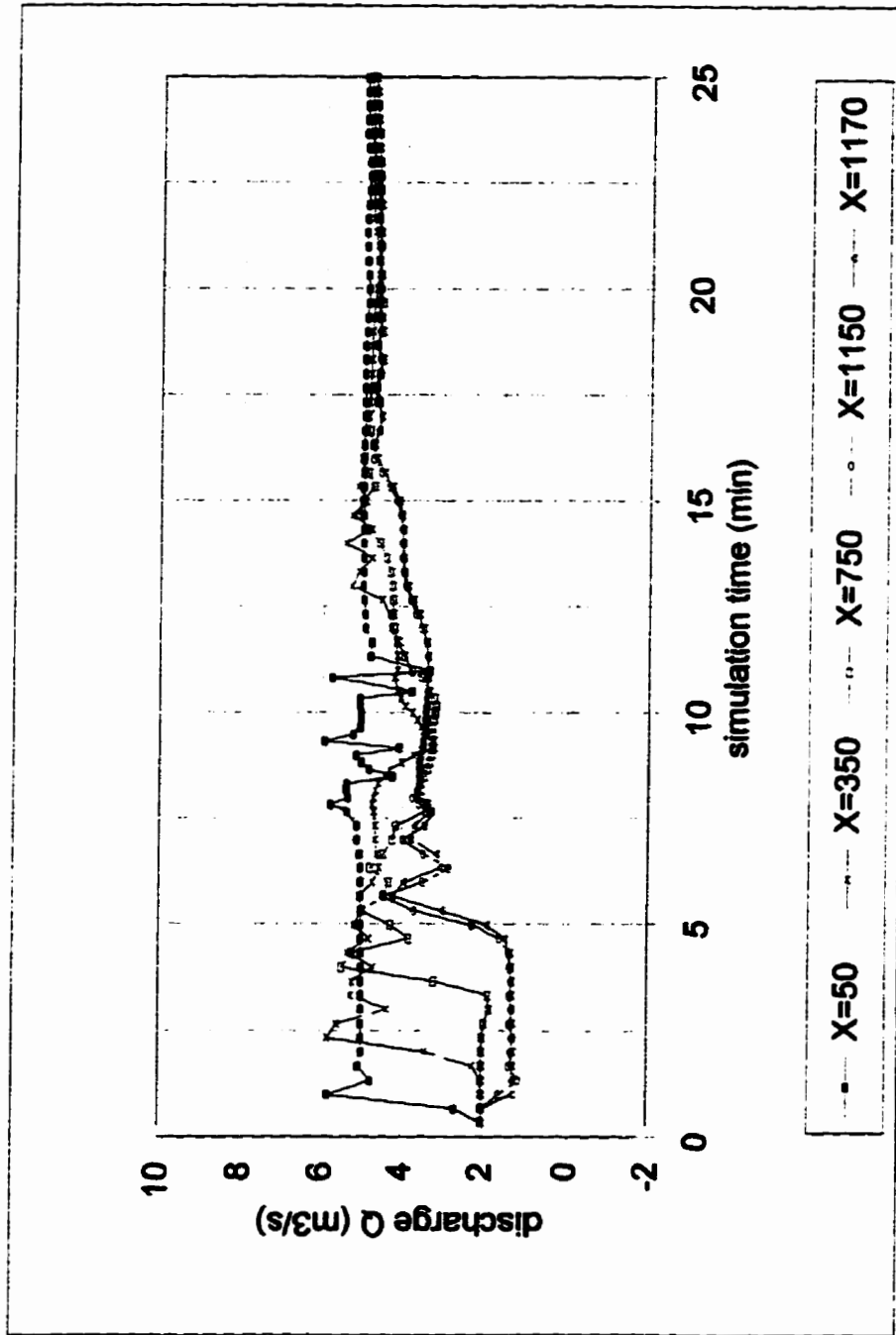


Figure 5.9 Discharge Profiles for Unstable Flow Condition #3-a: Δt , θ , A_1 and A_2 adjusted for $y < 0$ criterion. Profiles shown at X-distances indicated. $Q = 2$ to $5 \text{ m}^3/\text{s}$ at 0.5 min , $P_w = 1.1$ to 1.3 m at 0.5 min , $\Delta x = 50 \text{ m}$.

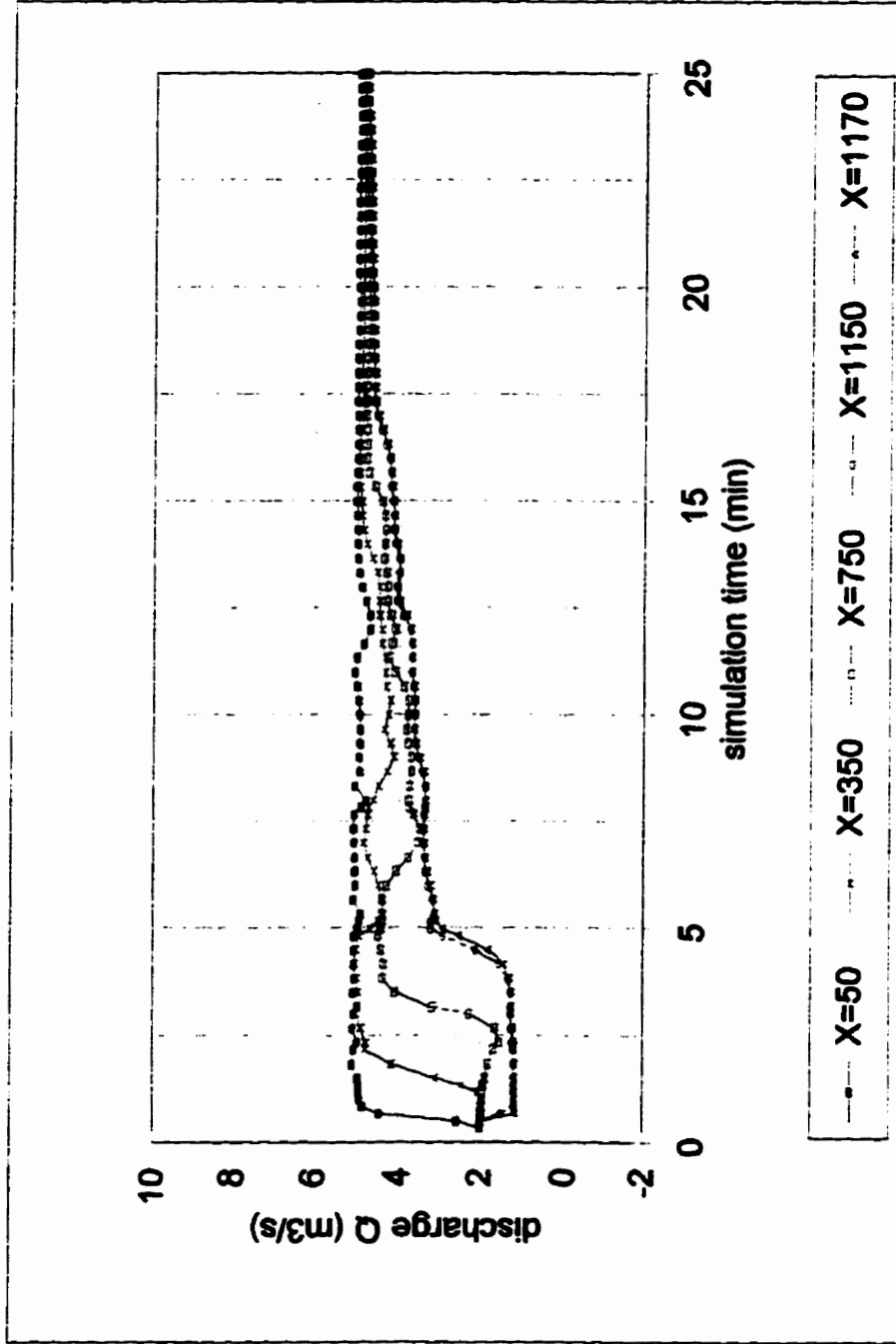


Figure 5.10 Discharge Profiles for Unstable Flow Condition #3-b: Δt , θ , A_1 and A_2 adjusted for $Fr > 1$ criterion. Profiles shown at X-distances indicated. $Q = 2$ to $5 \text{ m}^3/\text{s}$ at 0.5 min, $P_w = 1.1$ to 1.3 m at 0.5 min, $\Delta x = 50 \text{ m}$.

2b, 2c, and 3b, adjustment of coefficient A_1 alone resulted in program failure. For these same flow conditions, adjustment of coefficient A_2 alone was successful. For conditions 2b and 3b, with applied criteria $y < 0$ and $Fr > 1$, respectively, to prevent failure, adjustment of A_2 alone was required for more time steps than required in the solution with both A_1 and A_2 adjusted. For condition 2c with criterion $Fr > 1$, however, adjustment of A_2 alone occurred for fewer time steps than required in the solution with both A_1 and A_2 adjusted. For unstable flow condition 3a, with criteria $y < 0$, the opposite was true. Adjustment of A_2 alone resulted in program failure, while adjustment of A_1 alone provided a solution with fewer adjusted time steps than the solution with adjustment of A_1 and A_2 together.

The results of this investigation were thus inconclusive since the significance of the terms was not consistent. Results indicated that in order to prevent program failure, different acceleration terms required suppression for different flow conditions.

CHAPTER 6. SUMMARY AND CONCLUSION

Using the widely accepted, four-point implicit, finite difference technique to solve the full dynamic, St. Venant equations for gradually-varied, open-channel, unsteady flow, an extremely robust single-reach simulation model was developed. This 'robustness model' was used to investigate a potential method of avoiding program failure by suppressing the severe numerical instabilities developed in the solution procedure under certain flow conditions. An instability criterion was used in the model against which the solution obtained within the numerical technique was automatically checked. This check was performed for each time step, as the calculations progressed. If the criterion indicated instability in the solution, an automatic procedure was commenced in which solution parameters were adjusted to suppress the instability. Robustness was enhanced with this technique so that a solution was successfully obtained under flow conditions which otherwise caused the program to fail.

The additional robustness was created within the four-point technique by assigning a multiplicative coefficient to each of the terms in the momentum equation and then reducing the value of some of these coefficients towards zero. The contribution of the term(s) affected by the coefficient(s) was thus reduced for those time steps for which the selected instability criterion was met. Reduction of coefficients A_1 and A_2 , which were applied to the two acceleration terms in the

momentum equation, was investigated for the tested flow and channel conditions.

As coefficients A_1 and A_2 were reduced from one towards zero, the solution proceeded from the full dynamic towards the diffusion technique. Theoretically, the solution could be taken from the full dynamic through the diffusion to the kinematic, with adjustment of A_3 as well; however, the flow and boundary conditions used for this work were incompatible with the uniform flow modelled by the kinematic equation. In the diffusion technique, the two acceleration terms are neglected while with the kinematic technique, the acceleration and pressure slope terms are neglected. In the robustness model, when A_1 and A_2 are set to zero, the solution procedure uses the diffusion equation; and, if A_1 , A_2 , and A_3 were set to zero, the procedure solves the kinematic equation. In this way, the model provides a solution of the full dynamic equations for all time steps except those selected by the criterion as exhibiting instability. For those time steps meeting the instability criterion, an approximate solution is provided. By applying the parameter adjustments for only those time steps for which the instability criterion is met, a full dynamic solution is obtained for all possible time steps so that the best possible accuracy is maintained throughout the simulation.

As discussed by Fread (1983), the stability of the four-point technique can be enhanced within a simulation by reducing the value of Δt , thus reducing the

Courant number, or by increasing the value of θ . The criterion used by Fread was $y < 0$, and the adjustment was applied automatically when the criterion was met. With adjustment of Δt and θ , a full dynamic solution was provided. Fread reported flow conditions for which these adjustments were insufficient, but he did not report investigation of a method to further increase the stability of the solution. In the work for this thesis, adjustments were applied to Δt and θ initially and then, for time step solutions which continued to meet the instability criterion, the values of the coefficients A_1 and A_2 were gradually reduced. The coefficients were reduced in value between one and zero depending on the persistence of the instability. The tested unstable flow and channel conditions caused the program to fail when only Δt and θ were adjusted, but allowed a successful solution when A_1 and A_2 were also adjusted.

Adjustment of the coefficients was done automatically within the program when the solution obtained for a given time step met the selected instability criterion. Two different criteria were successfully tested to suppress instability which otherwise caused program failure, and several others were investigated. The successfully used criteria were (1) depth less than zero ($y < 0$), and (2) Froude number greater than one ($Fr > 1$). Both criteria were used effectively in preventing program failure which otherwise occurred for the same flow conditions with adjustment of Δt and θ only.

The criterion $Fr > 1$, appeared to cause reduction of the momentum equation coefficients, A_1 and A_2 , to occur more frequently than may have been necessary. Several other values of Froude number were tested, however none was found satisfactory. The criterion $y < 0$, appeared to miss some time steps for which significant instability, although not sufficient to cause program termination, developed in the momentum equation acceleration terms. This result was expected since only negative instability 'spikes' reaching zero depth would be detected leaving positive instabilities unaffected.

In order to improve the stability of the solution technique, some of the accuracy of the full dynamic solution was traded for increased robustness. The method of adjusting the coefficients developed for the robustness model, and the reduction of the solution from the full dynamic towards the diffusion technique, provided the desired additional robustness. The success of the tested procedure in preventing program termination indicates that development of a widely applicable and extremely robust version of the four point implicit finite difference technique is practical. Such a model would allow application of the best available technology, a full dynamic technique, so that an accurate solution could be obtained even under difficult flow conditions. Current standard engineering practice includes application of an approximate model, often a steady-state or kinematic model, for the full duration of a simulation when flow conditions cause solution instability. Through the work for this thesis, a method

to switch from a solution of the full dynamic equations to an approximate method and back again within a simulation run, and to apply the approximate technique for only those time steps exhibiting numerical instability likely to cause program failure, has been identified. This technique could change the entire approach to open channel flow modelling by eliminating the use of approximate method simulations in well-defined channels.

Only full dynamic simulation methods provide sufficiently accurate solutions to problems of open channel design and operation to address the issue of efficiency of use. In a world where water and financial resources are becoming more scarce and more valuable, the efficiency of water conveyance structures is of increasing importance. The potential benefit of widespread use of the accurate solutions provided by application of full dynamic simulation methods is efficient design and operation of conveyance systems and accurate prediction of flood events.

CHAPTER 7. DISCUSSION AND RECOMMENDATIONS

For open channel flow modelling, the use of approximate techniques, which provide a solution to an approximation of the full dynamic equations of open channel flow, is accepted as standard engineering practice. Commonly used approximate models include the diffusion, kinematic, and steady flow techniques. As discussed throughout this thesis, the diffusion and kinematic techniques approximate the momentum equation by neglecting the acceleration terms and the acceleration and pressure slope terms, respectively. Removal of these terms is based on the assumption that their contribution to the solution is negligible. The results of the investigation undertaken for this thesis suggest that the contribution from these terms is significant for the flow and channel conditions modelled in this work. As well, the results suggest that neither the diffusion nor the kinematic technique is reasonable for many applications of open channel flow in well defined channels.

Without the acceleration terms or the pressure slope term, the momentum equation, as used in a kinematic solution procedure, is simply the equation for uniform flow (for zero lateral inflow), as indicated in equation [3.23]. Uniform flow would only occur in a very long consistent channel where gravity and friction forces were balanced. In an operated canal, channel sections are often fairly short and are separated by some type of structure or change in channel cross-

section. Flow conditions in such an operated channel would likely be affected by backwater effects, such as reflections from a channel constriction, so that uniform flow would not occur. A kinematic technique, therefore, would not be appropriate for such channel and flow characteristics.

The diffusion equation neglects the acceleration terms but includes the pressure slope term so that backwater effects can be approximated. However, results from the robustness model developed for this thesis indicated that with the two acceleration term coefficients, A_1 and A_2 , set to zero, numerical instability was introduced into the solution. This result demonstrated that a term other than the acceleration terms was responsible for this instability. The investigation of the acceleration and pressure slope terms indicated that all three terms were affected by instability when a rapid change in input flow conditions occurred in the model, as discussed in Section 4.4.4. By neglecting the acceleration terms (term1 and term2), and the pressure term (term3), the momentum equation was left unbalanced so that the contribution of one term was not reduced by an opposite contribution from another. In the derivation of the momentum equation, the sum of the terms (term1 through term5) was set to zero. Clearly, when some terms are neglected, this assumption can only be true if the values of the neglected terms are near zero. Where rapid changes in input flow conditions occurred, the results of this work indicate that the values of the acceleration terms are not sufficiently near zero to justify neglecting the terms completely. In

addition, the results indicate that the sum of the acceleration and pressure slope terms is necessary to produce a correct solution. These results support the recommendation of Weinmann (1977) that the acceleration terms are important for steeply rising or falling hydrographs. Use of a diffusion equation technique, therefore, must be questioned for simulation of changing flow conditions. The robustness model allowed the use of an accurate, full dynamic solution with application of the less-accurate diffusion technique only at those time steps for which the calculation exhibited numerical instability.

Approximate methods may be useful for flow conditions with little variation in channels of flat bed slope and relatively unknown cross-section. In well-defined channels with varied flow conditions and numerous structures, only a full dynamic solution can provide a correct result. Irrigation systems generally have very regular and known cross-sections and controlled, variable flow conditions. In order for such a system to be efficiently designed and operated, so that construction, operation, and maintenance costs are minimized while available water supply is maximized, an accurate full dynamic simulation model is required. The success of the robustness model developed for this thesis work indicates that an extremely robust model can be developed to provide a solution for the full dynamic equations throughout the simulation except for those time steps which exhibit numerical instability sufficient to otherwise cause program failure. For those time steps, the method provides a solution for an approximate

momentum equation.

Several potential criteria for identifying the time steps affected by severe numerical instability were investigated. Although the two criteria used for this work were successful in preventing program failure, additional criteria could be investigated in order to determine the one(s) that provides the most effective selection of time steps for which to apply the approximation. Application of the coefficient adjustment to too many time steps results in a less accurate solution, while application to too few time steps results in severe instability affecting the solution or causing program failure. In order to develop the best possible criteria, the contribution of the various momentum equation terms, for a variety of flow and channel conditions, needs to be fully understood so that their appropriate contribution can clearly be distinguished from instability.

Through the investigations completed for this thesis work, the following areas were identified for further study:

1. Investigation of other potentially useful criteria for automatic application of coefficient adjustment and determination of the most effective criterion under various flow conditions. Possible criteria could include the magnitude or change in magnitude of the various momentum equation terms.

2. Investigation of the significance of the various momentum equation terms on numerical instability and of the relative magnitude and sign of terms under various flow and channel conditions.

3. Investigation of the effect on solution accuracy of using an approximate technique briefly within the full-dynamic solution. The approximate technique is known to move events earlier in time and to reduce the effects of attenuation and wave reflection, and a quantitative study of these effects on the overall solution would be of value.

4. Investigation of reduction of the other coefficients, A_3 , A_4 , and A_5 , as applicable for various flow and boundary conditions.

LITERATURE CITED

Amein, M. (1968). An implicit method for numerical flood routing. Water Resources Research, 4, 719-726.

Canadian Society for Civil Engineering Task Committee on River Models. (1990). Comparative evaluation of river models. Proceedings of the Annual Conference of the CSCE. Hamilton, Ontario. V, 282-300.

Chow, V. T. (1959). Open-Channel Hydraulics. New York: McGraw-Hill Book Company.

Chow, V. T., Maidment, D. R., & Mays, L. W. (1988). Applied Hydrology. New York: McGraw-Hill Book Company.

El-Maawy, A.A. 1991. Weighted Four-Point Implicit Method of Solution the St. Venant Equations. University of Calgary, Calgary, Alberta.

Fread, D. L. (1973, April). Effects of Time Step Size in Implicit Dynamic Routing. American Water Resources Association, Water Resources Journal, 9(2). 338-351.

Fread, D.L. (1981). Numerical Hydrodynamic Modelling of Rivers for Flood Forecasting by the National Weather Service. Proceedings of the International Conference of Numerical Modelling of River, Channel, and Overland Flow for Water Resources and Environmental Applications. Bratislava, Czechoslovakia.

French, R. H. (1985). Open-Channel Hydraulics. New York: McGraw Hill Book Company.

Henderson F. M. (1966). Open Channel Flow. New York: Macmillan Publishing Company.

Huber W. C. & Dickinson R.E. (1988). SWMM: Storm Water Management Model, Version 4. U.S. Environmental Protection Laboratory. Athens, Georgia.

Lai, C. (1986). Numerical Modelling of Unsteady Open-Channel Flow. Advances in Hydroscience, 14, 161-344.

Manz, D. H. (1994). Modelling Irrigation Conveyance Systems using the ICSS Model. Proceedings of the FAO Expert Consultation on Irrigation Water Delivery Models. Rome, Italy.

Manz, D. H. (1991). [Open Channel Hydraulics]. Unpublished course notes for

Enci 725, University of Calgary, Calgary, Alberta.

Robertson, J. A. & Crowe, C. T. (1985). Engineering Fluid Mechanics. Boston: Houghton Mifflin Company.

Rowney, A.C. & Macrae, C.R. (1991). Qualhymo Users Manual, Release 2.1. The Royal Military College of Canada, Dept. of Civil Engineering, Kingston, Ont.

Smith, A. A. (1980). A Generalized Approach to Kinematic Flood Routing. Journal of Hydrology, 45, Amsterdam: Elsevier Scientific Publishing Company.

Weinmann, P. E. (1977). Comparison of Flood Routing Methods for Natural Rivers. Monash University.

Wisner, P. (1989). Interhymo/Otthymo 89. University of Ottawa, Department of Civil Engineering. Ottawa.

US Army Corps of Engineers Hydrologic Engineering Center. (1995.) HEC-RAS River Analysis System Hydraulic Reference Manual - Draft. Davis, CA.: Author.

APPENDIX A. FOUR-POINT IMPLICIT FINITE DIFFERENCE TECHNIQUE

The St. Venant equations used for this work, derived in Section 3.2, describe one-dimensional, unsteady, gradually varying, open channel flow and are applicable for cases which comply with the assumptions specified in the derivation. The two full dynamic equations, [3.3] and [3.23], were discretized for numerical solution as described below. The four-point implicit finite difference scheme was used to replace the non-linear partial differential St. Venant equations with a set of $2N$ non-linear simultaneous equations. The generalized Newton iterative method was then used to reduce the set of non-linear equations to a set of linear equations for solution.

A.1 Distance Time Grid

At a point m on the distance-time grid shown in Figure A.1, and located entirely within the corner grid points (i, j) , $(i+1, j)$, $(i, j+1)$, and $(i+1, j+1)$ as shown, any variable α is defined as (Manz, 1991):

$$\alpha(m) = \frac{\theta}{2} [\alpha_{i-1}^{j+1} + \alpha_i^{j+1}] + \frac{(1-\theta)}{2} [\alpha_{i-1}^j + \alpha_i^j] \quad [A.1]$$

$$\frac{\delta\alpha(m)}{\delta x} = \frac{\theta}{\Delta x} [\alpha_{i-1}^{j+1} - \alpha_i^{j+1}] + \frac{(1-\theta)}{\Delta x} [\alpha_{i-1}^j - \alpha_i^j] \quad [A.2]$$

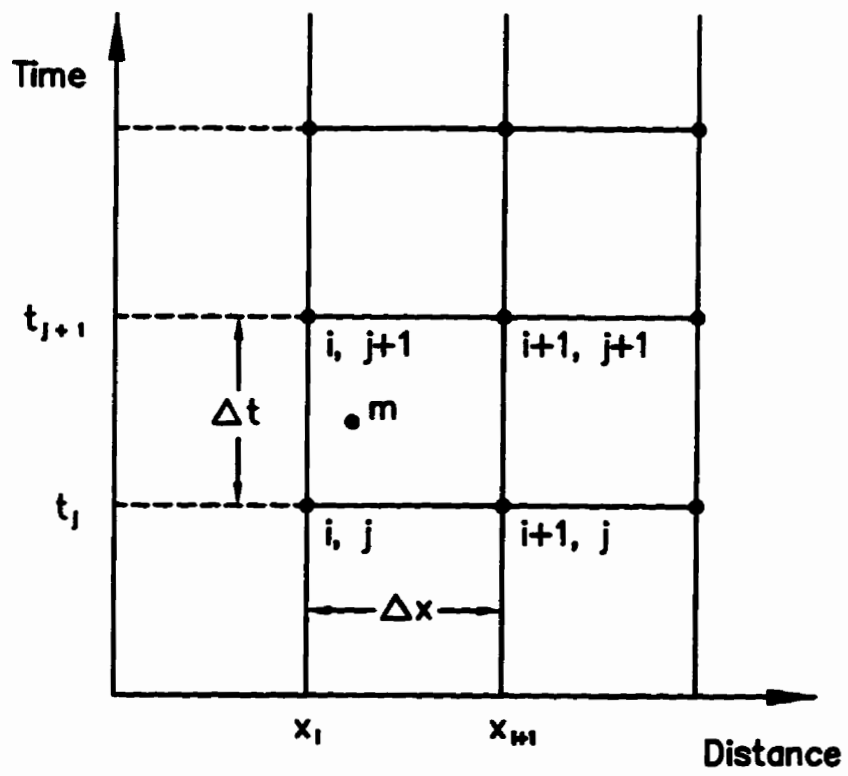


Figure A.1 Distance - Time Grid

$$\frac{\delta\alpha(m)}{\delta t} = \frac{1}{2\Delta t}[\alpha_{i-1}^{j+1} - \alpha_{i-1}^j] + \frac{1}{2\Delta t}[\alpha_i^{j+1} - \alpha_i^j] \quad [\text{A.3}]$$

where, θ is the weighting factor.

The subscripts i and j represent the position along the distance axis and the time value, respectively, so that the velocity at any point and time is represented by V_i^j , for example. At time j , all values are known from the previous time step calculation, so that the unknowns, velocity and depth, occur at time $j+1$. The governing continuity and momentum equations (Equations [3.3] and [3.23]) must be satisfied at the point m . The finite difference operators, specified by equations [A.1], [A.2], and [A.3], were applied to these equations with the results indicated below.

A.2 Continuity Equation

The non-linear partial differential continuity equation used for this work was:

$$\frac{A}{B} \frac{\delta V}{\delta x} + V \frac{\delta y}{\delta x} + \frac{\delta y}{\delta t} - \frac{1}{B} (q_i + p - q_o + i) = 0 \quad [\text{3.3}]$$

Application of the above finite difference scheme to equation [3.3], with simplification, provided the following discretized version of the continuity equation:

$$\begin{aligned}
& y_{i-1}^{j+1} + y_i^{j+1} + C_1 + \frac{\Delta t}{\Delta x} \theta^2 \left[\left(\frac{A}{B} \right)_{i-1}^{j+1} + \left(\frac{A}{B} \right)_i^{j+1} \right] [V_{i-1}^{j+1} - V_i^{j+1}] \\
& + \frac{\Delta t}{\Delta x} \theta C_2 [V_{i-1}^{j+1} - V_i^{j+1}] + \frac{\Delta t}{\Delta x} \theta C_3 \left[\left(\frac{A}{B} \right)_{i-1}^{j+1} + \left(\frac{A}{B} \right)_i^{j+1} \right] + C_4 \\
& + \frac{\Delta t}{\Delta x} \theta^2 [V_{i-1}^{j+1} + V_i^{j+1}] [y_{i-1}^{j+1} - y_i^{j+1}] + \frac{\Delta t}{\Delta x} \theta C_5 [y_{i-1}^{j+1} - y_i^{j+1}] \\
& + \frac{\Delta t}{\Delta x} \theta C_6 [V_{i-1}^{j+1} + V_i^{j+1}] + C_7 - \Delta t q \theta \left[\left(\frac{1}{B} \right)_{i-1}^{j+1} + \left(\frac{1}{B} \right)_i^{j+1} \right] - C_8 = 0
\end{aligned} \tag{4.1}$$

where:

$$C_1 = -[y_{i-1}^j + y_i^j]$$

$$C_2 = (1 - \theta) \left[\left(\frac{A}{B} \right)_{i-1}^j + \left(\frac{A}{B} \right)_i^j \right]$$

$$C_3 = (1 - \theta) [V_{i-1}^j - V_i^j]$$

$$C_4 = \frac{\Delta t}{\Delta x} C_2 C_3$$

$$C_5 = (1 - \theta) [V_{i-1}^j + V_i^j]$$

$$C_6 = (1 - \theta) [y_{i-1}^j - y_i^j]$$

$$C_7 = \frac{\Delta t}{\Delta x} C_5 C_6$$

$$C_8 = \Delta t q (1 - \theta) \left[\left(\frac{1}{B} \right)_{i-1}^j + \left(\frac{1}{B} \right)_i^j \right]$$

A.3 Momentum Equation

The non-linear partial differential momentum equation used for this work was:

$$A_1 \frac{\delta V}{\delta t} + A_2 V \frac{\delta V}{\delta x} + A_3 g \frac{\delta y}{\delta x} + A_4 g (S_f - S_o) + A_5 \frac{V}{A} q = 0 \quad [3.23]$$

This equation included the multiplicative coefficients applied for each of the momentum equation terms and used to investigate the robustness of the solution technique, as discussed in Section 3.3. Application of the above finite difference scheme (Equations [A.1], [A.2], and [A.3]) to equation [3.23], with simplification, provided the following discretized version of the momentum equation:

$$\begin{aligned} & \frac{A_1 \Delta x}{g \Delta t} [V_{i+1}^{j+1} + V_i^{j+1}] + A_1 C_9 + \frac{A_2 \theta^2}{g} [(V_{i+1}^{j+1})^2 - (V_i^{j+1})^2] \\ & + \frac{A_2 \theta C_{10}}{g} [V_{i+1}^{j+1} - V_i^{j+1}] + \frac{A_2 \theta C_{11}}{g} [V_{i+1}^{j+1} + V_i^{j+1}] + A_2 C_{12} \\ & + 2A_3 \theta [y_{i+1}^{j+1} - y_i^{j+1}] + A_3 C_{13} + A_4 \theta \Delta x [S_{f_{i+1}}^{j+1} + S_{f_i}^{j+1}] \\ & + A_4 C_{14} + A_4 C_{15} + \frac{A_5 q \theta \Delta x}{g} \left[\left(\frac{V}{A} \right)_{i+1}^{j+1} + \left(\frac{V}{A} \right)_i^{j+1} \right] + A_5 C_{16} = 0 \end{aligned} \quad [4.2]$$

where:

$$S_{f_i}^{j+1} = n^2 |V_i^{j+1}| V_i^{j+1} \left[\frac{P_i^{j+1}}{A_i^{j+1}} \right]^{\frac{4}{3}} \quad (\text{and similarly for } S_{f_{i+1}}^{j+1}, S_{f_i}^j, \text{ and } S_{f_{i+1}}^j), \text{ and,}$$

$$S_o = \frac{(z_i - z_{i+1})}{\Delta x}, \quad \text{where } z \text{ is the elevation from a reference datum,}$$

and where the following are constants using known (time j) values of the

variables:

$$C_9 = \frac{1}{g} \frac{\Delta x}{\Delta t} [V_{i-1}^j + V_i^j]$$

$$C_{10} = (1 - \theta) [V_{i-1}^j + V_i^j]$$

$$C_{11} = (1 - \theta) [V_{i-1}^j - V_i^j]$$

$$C_{12} = \frac{(1 - \theta)^2}{g} [(V_{i-1}^j)^2 - (V_i^j)^2]$$

$$C_{13} = 2(1 - \theta) [y_{i-1}^j - y_i^j]$$

$$C_{14} = 2 [z_{i-1}^j - z_i^j]$$

$$C_{15} = \Delta x (1 - \theta) [S_{i-1}^j + S_i^j]$$

$$C_{16} = \Delta x q \frac{(1 - \theta)}{g} \left[\left(\frac{V}{A} \right)_{i-1}^j + \left(\frac{V}{A} \right)_i^j \right]$$

A.4 Solution Procedure

There are (N-1) points in space like m , shown in Figure A.1, in the distance-time grid between time j and time $j+1$. The two finite difference equations (Equations [A.4] and [A.5]) were written at each point, and the resulting (N-1) continuity equations and (N-1) momentum equations were represented by $F_i(y_i^{j+1}, V_i^{j+1}, y_{i-1}^{j+1}, V_{i-1}^{j+1})$, and $G_i(y_i^{j+1}, V_i^{j+1}, y_{i-1}^{j+1}, V_{i-1}^{j+1})$, respectively. The two additional equations required to make the set of $2N$ equations for the $2N$ unknowns (y_i and V_i) were obtained from an upstream and a downstream

boundary condition represented by $G_0(y_1, V_1)$ and $F_N(y_N, V_N)$, respectively.

Estimate values were assigned to the unknowns based on the solution to the previous time, and residuals calculated as the value that each equation differs from zero. Where $r_{1,i}^k$ and $r_{2,i}^k$ represented the residuals for the F and G functions, respectively, the set of equations to be solved for the residuals on the k^{th} iteration, and for unknown time $j+1$, were:

$$\begin{aligned}
 G_0(y_1^k, V_1^k) &= r_{2,0}^k \\
 F_1(y_1^k, V_1^k, y_2^k, V_2^k) &= r_{1,1}^k \\
 G_1(y_1^k, V_1^k, y_2^k, V_2^k) &= r_{2,1}^k \\
 &\text{etc.} \\
 F_i(y_i^k, V_i^k, y_{i+1}^k, V_{i+1}^k) &= r_{1,i}^k \\
 G_i(y_i^k, V_i^k, y_{i+1}^k, V_{i+1}^k) &= r_{2,i}^k \\
 &\text{etc.} \\
 F_N(y_N^k, V_N^k) &= r_{1,N}^k
 \end{aligned}
 \tag{A.4}$$

According to the Newton iteration scheme, a new estimate for the unknowns was calculated as:

$$\begin{aligned}
 y_i^{k+1} &= y_i^k + dy_i \quad \text{and,} \\
 V_i^{k+1} &= V_i^k + dV_i
 \end{aligned}
 \tag{A.5}$$

For each time step, the residuals were calculated and checked against the limit. If all the residuals are less than the limit, the solution (y_i, V_i) was accepted. If any of the residuals was larger than the limit, the partial derivatives of the F_i and G_i equations were calculated and defined as a matrix [A]. The residuals calculated were defined as matrix [B]. A sparse pentadiagonal matrix solution technique was used to solve the matrix equation $[A][X] = [B]$ for the solution matrix [X] which then represented the values of dy_i and dV_i to be used for the next estimate of y_i and V_i . The matrix equation was defined as:

$$\begin{aligned}
 \frac{\delta G_0}{\delta y_1} dy_1 + \frac{\delta G_0}{\delta V_1} dV_1 &= -r_{2,0} \\
 \frac{\delta F_1}{\delta y_1} dy_1 + \frac{\delta F_1}{\delta V_1} dV_1 + \frac{\delta F_1}{\delta y_2} dy_2 + \frac{\delta F_1}{\delta V_2} dV_2 &= -r_{1,1} \\
 \frac{\delta G_1}{\delta y_1} dy_1 + \frac{\delta G_1}{\delta V_1} dV_1 + \frac{\delta G_1}{\delta y_2} dy_2 + \frac{\delta G_1}{\delta V_2} dV_2 &= -r_{2,1} \\
 &\text{etc.} \\
 \frac{\delta F_i}{\delta y_i} dy_i + \frac{\delta F_i}{\delta V_i} dV_i + \frac{\delta F_i}{\delta y_{i+1}} dy_{i+1} + \frac{\delta F_i}{\delta V_{i+1}} dV_{i+1} &= -r_{1,i} \\
 \frac{\delta G_i}{\delta y_i} dy_i + \frac{\delta G_i}{\delta V_i} dV_i + \frac{\delta G_i}{\delta y_{i+1}} dy_{i+1} + \frac{\delta G_i}{\delta V_{i+1}} dV_{i+1} &= -r_{2,i} \\
 &\text{etc.} \\
 \frac{\delta F_N}{\delta y_N} dy_N + \frac{\delta F_N}{\delta V_N} dV_N &= -r_{1,N}
 \end{aligned} \tag{A.6}$$

The new estimates were then calculated according to equation [A.7], and the iterative process is repeated until the values of the residuals was less than the set limit, or a maximum number of iterations was exceeded.

APPENDIX B. PROGRAM CODE

The following FORTRAN code was used for the robustness model:

```

*      Robustness model for thesis - June 1996 - C. Vrkljan
*
DOUBLE PRECISION QP, QI, SO, MANN, DELT, SIMTIM, RGO, RFM
DOUBLE PRECISION TIME, LTOT, DELXW, DELX2, SUM, SIML, TIMCHK
DOUBLE PRECISION TIM(11), QIN(10), QUPS(100), DELX(100)
DOUBLE PRECISION Z(100), XST(100), YANS(100,100), VANS(100,100)
DOUBLE PRECISION YNEW(100), YOLD(100), VNEW(100), VOLD(100)
DOUBLE PRECISION DELXUN(100), V(100), QQ(100), XANS(100)
DOUBLE PRECISION G,Q,PW,B,YW,QW,DQW, CE, CW, MATRXB(100)
DOUBLE PRECISION AAL,P1,SF,FY1,FP1,XLAST,UDELX, FR, RE
DOUBLE PRECISION AA,PP,YY, QNEW(10), MATRXA(100,100), QANS(100)
DOUBLE PRECISION Y(100),FY(50),FP(50),A(100),P(100), DELTJ(100)
DOUBLE PRECISION AOLD(100),POLD(100),SFOLD(100),ANEW(100)
DOUBLE PRECISION PNEW(100),SFNEW(100),VALUE,THA,A1,A2,A3,A4,A5
DOUBLE PRECISION C1(100),C2(100),C3(100),C4(100),C5(100)
DOUBLE PRECISION C6(100),C7(100),C8(100),C9(100),C10(100)
DOUBLE PRECISION C11(100),C12(100),C13(100),C14(100),C15(100)
DOUBLE PRECISION C16(100),RF(100),RG(100),FMTF(200),MATRXX(100)
DOUBLE PRECISION DIFY(100),DIFV(100),DIGY(100),DIGV(100)
DOUBLE PRECISION FMTA(200),FMTE(200),FMTD(200),FMTC(200)
DOUBLE PRECISION FWIN(10),TIMP(10),PWJ(100)
DOUBLE PRECISION TERM1,TERM3,INTHA,INA1,INA2,INA3
INTEGER NQ,NP,MJ,M,E,EOLD,UNUS,J,H,N,K,I1,COUNT,CRIT
OPEN (31, FILE='INPUT2.DAT')
OPEN (35, FILE='FLOWIN2.DAT')
OPEN (21, FILE='UNST.OUT')
OPEN (27, FILE='TEMPLOT.TXT')
OPEN (28, FILE='TERMS.TXT')
*
*      input *****
*
READ (31,*) QI,QP,B,SO,MANN,LTOT
READ (31,*) DELXW,DELX2,INTHA,INA1,INA2,INA3,DELT,A4,A5
DELTJ(1) = DELT
*
*      initialize
*
TIM(1) = 0.0D0
G = 9.807D0
*      upstream flow-time and variable weir height
READ (35,*) NQ, SIMTIM
DO 100 I = 1, NQ
  READ (35,*) QIN(I), TIM(I)
100 CONTINUE
READ (35,*) NP
DO 101 I = 1, NP
  READ (35,*) FWIN(I), TIMP(I)
101 CONTINUE

```

```

*      number of time calcs ***
MJ = (SIMTIM * 60.0) / DELT + 1
*      Q - time series ***
DO 110 J = 1, MJ
  TIME = DELT * (J - 1.)
  DO 112 I = 1, NQ
    IF ( I .EQ. NQ ) THEN
      QUPS(J) = QIN(NQ)
      GO TO 115
    ENDIF
    TIMCHK = TIM(I+1) * 60.0
    IF ( TIME .LT. TIMCHK ) THEN
      QUPS(J) = QIN(I)
      GO TO 115
    ENDIF
112   CONTINUE
115   UNUS = 1
  DO 113 I = 1, NP
    IF ( I .EQ. NP ) THEN
      FWJ(J) = PWIN(NP)
      GO TO 116
    ENDIF
    TIMCHK = TIMP(I+1) * 60.0
    IF ( TIME .LT. TIMCHK ) THEN
      FWJ(J) = PWIN(I)
      GO TO 116
    ENDIF
113   CONTINUE
116   UNUS = 1
110   CONTINUE
*
*      initialize for steady flow calcs *****
*
  PW = PWIN(1)
  SUM = 0.0DO
  M = (LTOT - 20.) / DELX2 + 21
  WRITE (21,*) 'M = ', M
  DO 120 I = 1, M-1
    IF ( I .LT. 21 ) THEN
      DELX(I) = DELXW
    ELSE
      DELX(I) = DELX2
    ENDIF
    SIML = SUM + DELX(I)
    SUM = SIML
120   CONTINUE
*
*      verify input
  IF ( SO .GT. 0.1 ) THEN
    PRINT *, 'WARNING Channel slope is large. So = ', SO
    WRITE (21,*) 'WARNING Channel slope is large.'
  ENDIF
  IF ( MANN .GT. 1 ) THEN
    PRINT *, 'WARNING Mannings roughness is large. n = ', MANN
  ENDIF
*
*      boundary condition : sharp-crested weir
*      negligible viscous and surface tension effects

```

```

Q = QUPS(1) + ( QP - QI ) * SIML
YW = 0.0D0
CALL WEIR ( G, Q, PW, B, YW)
AA1 = B * YW
P1 = B + 2.0D0*YW
SF = Q**2.0D0 *MANN**2
$ * P1**(4.0D0/3.0D0) / (AA1**(10.0D0/3.0D0))
*
PRINT *, 'depth at weir YW = ', YW
PRINT *, 'depth PW = ', PW
*
* calculate Froude number
FR = ( Q**2 / (G * B**2 * YW**3) )**0.5
IF ( FR .GT. 1.0 ) THEN
  PRINT *, 'Steady flow is supercritical'
  WRITE (21,*) 'Steady flow is supercritical'
  GO TO 9999
ENDIF
IF ( FR .EQ. 1.0 ) THEN
  PRINT *, 'Flow is critical'
  WRITE (21,*) 'Flow is critical'
ENDIF
IF ( FR .LT. 1.0 ) THEN
  PRINT *
  PRINT *, 'Fr =', FR
  PRINT *, 'Flow is subcritical at weir'
  PRINT *
  WRITE (21,*) 'Flow is Subcritical at weir'
ENDIF
*
* steady flow calculations *****
* Newton's Iterative Method
* Y = y - f(y)/f'(y)
*
Z(1) = 0.0D0
Y(1) = YW
XST(1) = 0.0D0
QQ(1) = Q
YY = YW
XLAST = 0.0D0
DO 140 I = 2, M
  UDELX = DELX(I-1)
  XST(I) = XLAST + UDELX
  QQ(I) = Q + (QP-QI) * XST(I)
  Z(I) = Z(1) + SO * XST(I)
  A(I-1) = B * Y(I-1)
  P(I-1) = B + 2.0D0*Y(I-1)
  AA = A(I-1)
  PP = P(I-1)
  XLAST = XST(I)
*
FY1 = ((QP-QI)*UDELX/2.0D0*G) * ((QQ(I-1)+QQ(I))/(AA**2))
$ + ((MANN**2)*UDELX/2.0D0)
$ * ((PP**(4.0D0/3.0D0))/(AA**(10.0D0/3.0D0))
$ * ((QQ(I-1)**2) + (QQ(I)**2))) + Z(I-1) - Z(I)
FP1 = (-1.0D0) + B/(2.0D0*G*(AA**3))
$ * (QQ(I-1)**2 + QQ(I)**2)
$ - (QP-QI)/G*UDELX*B/(AA**3) * QQ(I)

```

```

$   + (MANN**2)*UDELX*(QQ(I)**2)
$   * (4.000 * (PP**(1.000/3.000))
$   / (3.000 * (AA**(10.000/3.000)))
$   - 5.000 * ( PP**(4.000/3.000) ) * B
$   / (3.000 * (AA**(13.000/3.000))) )
Y(I) = Y(I-1) - FY1 / FP1
*
  DO 150 J = 2, 50
    A(I) = B * Y(I)
    P(I) = B + 2.000 * Y(I)
  *
  FY(J) = Y(I-1) - Y(I) - 1.000/(2.000*G)
$     * ( QQ(I-1)**2/A(I-1)**3
$     + QQ(I)**2/A(I)**3) * ( A(I-1) - A(I) )
$     + (QP-QI) * UDELX/(2.000*G) * ( QQ(I-1)/A(I-1)**2
$     + QQ(I)/A(I)**2)
$     + (MANN**2.000*UDELX/2.000)
$     * ( QQ(I-1)**2 * (P(I-1)**4
$     / A(I-1)**10) ** (1.000/3.000)
$     + QQ(I)**2 * (P(I)**4 / A(I)**10)
$     ** (1.000/3.000) ) + Z(I-1) - Z(I)
  *
  FP(J) = (-1.000) + B/(2.000*G)
$     * ( QQ(I-1)**2/A(I-1)**3
$     + 3.000*QQ(I)**2*A(I-1) / A(I)**4
$     - 2.000*QQ(I)**2 / A(I)**3 )
$     - (QP-QI)*UDELX*B/G * QQ(I)/A(I)**3
$     + MANN**2*UDELX*QQ(I)**2
$     * ( (4.000*P(I)/(3.000*A(I)**10))
$     ** (1.000/3.000) - (5.000*P(I)**4 * B
$     / (3.000*A(I)**13) ) ** (1.000/3.000) )
  *
  YY = Y(I) - FY(J) / FP(J)
  IF ( ABS ( YY - Y(I) ) .LT. 0.0005 ) GO TO 160
  IF (YY .LT. 0.000) THEN
    PRINT *, 'Y less than zero in steady calc at I = ', J
    WRITE (21,*) 'Y less than zero in steady calc at I = ', J
  ENDIF
  FR = ( Q**2 / (G * B**2 * YY**3) )**0.5
  IF (FR .GT. 1.000) THEN
    WRITE (21,*) 'Steady flow is supercritical at I = ', J
    PRINT *, 'Steady flow is supercritical at I = ', J
    GO TO 9999
  ENDIF
  Y(I) = YY
150  CONTINUE
    PRINT *, 'Steady flow calculations did not converge!'
    GO TO 9999
160  UNUS = 1
140  CONTINUE
  *
    A(M) = B * Y(M)
    DO 170 I = 1, M
      V(I) = QQ(I) / A(I)
170  CONTINUE
  *
  PRINT *, 'Steady Flow calculations completed'
  PRINT *, ' '

```

```

*
*   initialize for unsteady flow calcs *****
*
*   turn solution around
  EOLD = 0
  DO 200 I = M, 1, -1
    E = EOLD + 1
  *
    XANS(E) = XST(I)
    YANS(E,1) = Y(I)
    YNEW(E) = Y(I)
    YOLD(E) = YNEW(E)
    VANS(E,1) = V(I)
    VNEW(E) = V(I)
    VOLD(E) = VNEW(E)
  *
    IF ( I .GT. 1 ) THEN
  *
      DELXUN(E) = DELX(I-1)
  *
    ENDIF
    EOLD = E
  200 CONTINUE
  *
  *   set unsteady delta-x and distance
  DO 201 E = 1, M-21
    DELXUN(E) = DELX2
  201 CONTINUE
  DO 202 E = M-20, M-1
    DELXUN(E) = DELXW
  202 CONTINUE
  XANS(1) = 0.000
  XANS(2) = DELX2
  DO 203 E = 2, M
    XANS(E) = XANS(E-1) + DELXUN(E-1)
  203 CONTINUE
  *
  *   set elevation Z
  Z(1) = SIML * SO
  Z(M) = 0.000
  DO 210 I = 2, M-1
    Z(I) = Z(I-1) - SO * DELXUN(I-1)
  210 CONTINUE
  *
  VALUE = .001
  WRITE (28,*) ' J K I term1 term2 term3 term4'
  *
  *   WRITE (28,*) ' J K I YANS(I) QANS(I) TERM1 FR RE'
  WRITE (28,*) ' '
  WRITE (27,*) ' XANS(I) I J YANS(I,J) QANS(I) DELTJ
$ THETA A1'
  WRITE (27,*) ' '
  *
  *   unsteady flow iteration *****
  *
  DO 500 J = 2, MJ
  WRITE (21,*) 'start of j-loop J= ', J
  *
  DELTJ(J) = DELT
  DELTJ(J-1) = DELT
  THA = INTHA
  COUNT = 0
  A1 = INA1
  A2 = INA2

```

```

A3 = INA3
K = 0
*
  PRINT *, 'J = ', J
  QNEW(1) = QUPS(J)
  DO 310 I = 1, M
    AOLD(I) = B * YOLD(I)
    POLD(I) = B + 2.0D0 * YOLD(I)
    SFOLD(I) = (VOLD(I)**2) * MANN**2
$
    * ( (POLD(I)/AOLD(I))**(4.0D0/3.0D0) )
    SFOLD(I) = ABS(VOLD(I)) * (VOLD(I)) * MANN**2.0D0
$
    * ( (POLD(I)/AOLD(I))**(4.0D0/3.0D0) )
310    CONTINUE
  CRIT = 0
315    UNUS=1
*
  constants
  DO 320 H = 1, M-1
    C1(H) = (-1.0D0)*(YOLD(H+1) + YOLD(H))
    C2(H) = (1.0D0-THA)/B * (AOLD(H+1) + AOLD(H))
    C3(H) = (1.0D0-THA) * (VOLD(H+1) - VOLD(H))
    C4(H) = DELTJ(J-1)/DELXUN(H) * C2(H) * C3(H)
    C5(H) = (1.0D0-THA) * (VOLD(H+1) + VOLD(H))
    C6(H) = (1.0D0-THA) * (YOLD(H+1) - YOLD(H))
    C7(H) = DELTJ(J-1)/DELXUN(H) * C5(H) * C6(H)
    C8(H) = DELTJ(J-1) * (QP-QI) * (1.0D0-THA) * 2.0D0/B
    C9(H) = (-1.0D0/G)*DELXUN(H)/DELTJ(J-1)
$
    * (VOLD(H+1)+VOLD(H))
    C10(H) = (1.0D0-THA) * (VOLD(H+1) + VOLD(H))
    C11(H) = (1.0D0-THA) * (VOLD(H+1) - VOLD(H))
$
    C12(H) = ((1.0D0-THA)**2) / G*( (VOLD(H+1)**2)
    - (VOLD(H)**2) )
    C13(H) = 2.0D0*(1.0D0-THA) * (YOLD(H+1) - YOLD(H))
    C14(H) = 2.0D0*(Z(H+1) - Z(H))
    C15(H) = DELXUN(H)*(1.0D0-THA) * (SFOLD(H+1)+SFOLD(H))
    C16(H) = DELXUN(H)/G * (QP-QI)*(1.0D0-THA)
$
    * ( (VOLD(H+1)/AOLD(H+1)) + (VOLD(H)/AOLD(H)) )
320    CONTINUE
*
  Newton Iterative Method *****
*
330  PRINT *, 'K = ', K
  K = K + 1
  DO 335 I = 1, M
    ANEW(I) = B * YNEW(I)
    PNEW(I) = B + 2.0D0 * YNEW(I)
    SFNEW(I) = ABS(VNEW(I)) * (VNEW(I)) * MANN**2.0D0
$
    * ( (PNEW(I)/ANEW(I))**(4.0D0/3.0D0) )
335    CONTINUE
*
  calculate residuals
  DO 340 H = 1, M-1
    RG(H) = A1/G *DELXUN(H)/DELTJ(J) * (VNEW(H+1)+VNEW(H))
$
    + A1*C9(H) + A2/G*(THA**2) * ((VNEW(H+1)**2)
$
    - (VNEW(H)**2))
$
    + A2/G*THA*C11(H) * (VNEW(H+1) + VNEW(H))
$
    RG(H) = RG(H)
$
    + A2/G*THA*C10(H) * (VNEW(H+1) - VNEW(H))

```

```

$      + A2*C12(H) + 2.0D0*A3*THA*(YNEW(H+1) - YNEW(H))
$      + A3*C13(H) + A4*THA*DELXUN(H) *(SFNEW(H+1)
$      + SENEW(H) + A4*C14(H) + A4*C15(H)
$      + A5/G*(QP-QI)*THA*DELXUN(H) *( (VNEW(H+1)
$      / ANEW(H+1)) + (VNEW(H)/ANEW(H)) ) + A5*C16(H)
MATRXB(2*H+1) = (-1.0D0)*RG(H)
*
RF(H) = YNEW(H+1) + YNEW(H) + C1(H)
$ +DEL TJ(J)/DELXUN(H)*(THA**2)/B *(ANEW(H+1)
$ +ANEW(H))*(VNEW(H+1)-VNEW(H))+ DEL TJ(J)/DELXUN(H)
$ *THA*C2(H)*(VNEW(H+1)-VNEW(H))+ DEL TJ(J)/DELXUN(H)
$ *THA*C3(H)/B*(ANEW(H+1)+ANEW(H))+C4(H)+C7(H)-C8(H)
$ +DEL TJ(J)/DELXUN(H)*(THA**2)*(VNEW(H+1)+VNEW(H))
$ *(YNEW(H+1)-YNEW(H))+ DEL TJ(J)/DELXUN(H)*THA*C5(H)
$ *(YNEW(H+1)-YNEW(H))+ DEL TJ(J)/DELXUN(H)*THA*C6(H)
$ *(VNEW(H+1)+VNEW(H))- 2.0D0*DEL TJ(J)*(QP-QI)*THA/B
MATRXB(2*H) = (-1.0D0)*RF(H)
*
340 CONTINUE
*
*      set boundary values
HW = YNEW(M) - PWJ(J)
CE = .6020D0 + .0750D0 * HW/PWJ(J)
CW = 2.0D0/3.0D0 *CE * ((2.0D0*G)**0.50D0)
IF ( YNEW(M) .LT. PWJ(J) ) THEN
  QW = 0.0D0
  GO TO 341
ENDIF
341 QW = CW *B * (HW**1.50D0)
UNUS = 1
RGO = QUPS(J) - VNEW(1)*ANEW(1)
RFM = VNEW(M)*ANEW(M) - QW
MATRXB(1) = (-1.0D0)*RGO
MATRXB(2*M) = (-1.0D0)*RFM
*
*      check residuals
DO 350 I = 1, 2*M
  IF ( ABS(MATRXB(I)) .GT. VALUE) GO TO 325
350 CONTINUE
GO TO 499
325 UNUS = 1
*
*      calculate partials
*
WRITE (21,*) 'start partials K= ', K
DO 360 H = 1, 2*M
  DO 361 I = 1, 2*M
    MATRXA(H,I) = 0.0D0
361 CONTINUE
360 CONTINUE
DO 370 H = 1, M-1
  DIGY(H) = (-2.0D0)*A3*THA
$      + 4.0D0/3.0D0*A4*THA*DELXUN(H)
$      *SENEW(H) *(2.0D0/PNEW(H) -B/ANEW(H))
$      - A5*(QP-QI)*THA*DELXUN(H)*B/G
$      *( VNEW(H)/(ANEW(H)**2) )
MATRXA(2*H+1,2*H-1) = DIGY(H)
DIGY(H+1) = 2.0D0*A3*THA + 4.0D0/3.0D0*A4*THA*DELXUN(H)

```

```

$          *SNEW(H+1) *(2.0D0/PNEW(H+1) -B/ANEW(H+1))
$          - A5*(QP-QI)*THA*DELXUN(H)*B/G
$          *( VNEW(H+1)/(ANEW(H+1)**2) )
MATRXA(2*H+1,2*H+1) = DIGY(H+1)
DIGV(H)      = A1/G*DELXUN(H)/DELTJ(J)
$            - 2.0D0*A2*(THA**2)/G * VNEW(H)
$            - A2/G*THA*C10(H) + A2/G*THA*C11(H)
$            + 2.0D0*A4*THA*DELXUN(H) *SNEW(H)/VNEW(H)
$            + A5/G*(QP-QI)*THA*DELXUN(H)/ANEW(H)
MATRXA(2*H+1,2*H) = DIGV(H)
DIGV(H+1)    = A1/G*DELXUN(H)/DELTJ(J)
$            + 2.0D0*A2/G*(THA**2) * VNEW(H+1)
$            + A2/G*THA*C10(H) + A2/G*THA*C11(H)
DIGV(H+1)    = DIGV(H+1)
$            + 2.0D0*A4*THA*DELXUN(H)*SNEW(H+1)/VNEW(H+1)
$            + A5/G*(QP-QI)*THA*DELXUN(H)/ANEW(H+1)
MATRXA(2*H+1,2*H+2) = DIGV(H+1)
*
DIFY(H)      = 1.-2.*DELTJ(J)/DELXUN(H)*(THA**2)*VNEW(H)
$            + DELTJ(J)/DELXUN(H)*THA*C3(H)
$            - DELTJ(J)/DELXUN(H)*THA*C5(H)
MATRXA(2*H,2*H-1) = DIFY(H)
DIFY(H+1)    = 1.0D0+2.0D0*DELTJ(J)/DELXUN(H)
$            * (THA**2)*VNEW(H+1)
$            + DELTJ(J)/DELXUN(H)*THA*C3(H)
$            + DELTJ(J)/DELXUN(H)*THA*C5(H)
MATRXA(2*H,2*H+1) = DIFY(H+1)
DIFV(H)      = (-1.0D0)*DELTJ(J)/DELXUN(H)*(THA**2)/B
$            *( ANEW(H+1)+ANEW(H) )
$            - DELTJ(J)/DELXUN(H)*THA*C2(H)
DIFV(H)      = DIFV(H)
$            + DELTJ(J)/DELXUN(H)*(THA**2) *( YNEW(H+1)
$            -YNEW(H) ) + DELTJ(J)/DELXUN(H)*THA*C6(H)
MATRXA(2*H,2*H) = DIFV(H)
DIFV(H+1)    = DELTJ(J)/DELXUN(H)*(THA**2)/B*(ANEW(H+1)
$            +ANEW(H) )
$            + DELTJ(J)/DELXUN(H)*THA*C2(H)
DIFV(H+1)    = DIFV(H+1)
$            + DELTJ(J)/DELXUN(H)*(THA**2)*(YNEW(H+1)
$            -YNEW(H) ) + DELTJ(J)/DELXUN(H)*THA*C6(H)
MATRXA(2*H,2*H+2) = DIFV(H+1)
370  CONTINUE
WRITE (21,*) 'end DIG&FY calcs K = ',K,' J= ',J
*
*      check depth is above weir crest
IF ( YNEW(M) .LT. PWJ(J) ) THEN
  DQW = 0.0D0
  GO TO 371
ENDIF
DQW = CW*B*3.0D0/2.0D0*( (YNEW(M)-PWJ(J)) **0.50D0)
371  MATRXA(2*M,2*M-1) = VNEW(M)*B - DQW
MATRXA(2*M,2*M) = B * YNEW(M)
MATRXA(1,1) = (-B) * VNEW(1)
MATRXA(1,2) = (-B) * YNEW(1)
.
*      matrix solution for Y & V adjustments *****
*
N = 2*M

```

```

DO 400 I = 1, N-2
  FMTE(I) = MATRXA(I+2,I)
  FMTF(I) = MATRXA(I,I+2)
400  CONTINUE
DO 410 I = 1, N-1
  FMIA(I) = MATRXA(I+1,I)
  FMTC(I) = MATRXA(I,I+1)
410  CONTINUE
DO 420 I = 1, N
  FMTD(I) = MATRXA(I,I)
420  CONTINUE
*
*   PENTA routine
DO 402 I = 2, N-1
  XMULT=FMIA(I-1) / FMTD(I-1)
  FMTD(I)=FMTD(I) - XMULT*FMTC(I-1)
  FMTC(I)=FMTC(I) - XMULT*FMTF(I-1)
  MATRXB(I)=MATRXB(I) - XMULT*MATRXB(I-1)
  XMULT=FMTE(I-1) / FMTD(I-1)
  FMIA(I)=FMIA(I) - XMULT*FMTC(I-1)
  FMTD(I+1)=FMTD(I+1) - XMULT*FMTF(I-1)
  MATRXB(I+1)=MATRXB(I+1) - XMULT*MATRXB(I-1)
402  CONTINUE
  XMULT = FMIA(N-1) / FMTD(N-1)
  FMTD(N) = FMTD(N) - XMULT*FMTC(N-1)
  MATRXX(N) = (MATRXB(N)-XMULT*MATRXB(N-1))/FMTD(N)
  MATRXX(N-1)=(MATRXB(N-1)-FMTC(N-1)*MATRXX(N))
$    / FMTD(N-1)
DO 403 I = N-2, 1, -1
  MATRXX(I) = (MATRXB(I)-FMTF(I)*MATRXX(I+2)
$    - FMTC(I)*MATRXX(I+1)) / FMTD(I)
403  CONTINUE
*
*   Criterion Check *****
*
WRITE (21,*) 'test new estimate J = ',J,' I = ',I,' K = ',K
DO 404 I = 1, M
  Y(I) = YNEW(I) + MATRXX(2*I-1)
  V(I) = VNEW(I) + MATRXX(2*I)
  IF ( Y(I) .LT. 0.005DO ) THEN
    WRITE (21,*) 'y is < 5mm J = ',J,' K = ',K,' I = ',I
    PRINT *, 'y is < 5mm J = ',J,' K = ',K,' I = ',I
    GO TO 491
  ENDIF
404  CONTINUE
GO TO 495
491  CRIT = CRIT + 1
WRITE (21,*) 'Ytest(I) < 0.005 at J = ',J,' K = ',K
WRITE (21,*) 'CRIT = ',CRIT
IF (CRIT .EQ. 1) GO TO 701
IF (CRIT .EQ. 2) GO TO 702
IF (CRIT .EQ. 3) GO TO 703
IF (CRIT .EQ. 4) GO TO 704
IF (CRIT .EQ. 5) GO TO 705
IF (CRIT .EQ. 6) GO TO 706
IF (CRIT .GT. 6) GO TO 495
701  DELTJ(J) = DELTJ(J) / 2.0DO
DELTJ(J-1) = DELTJ(J)

```

```

WRITE (21,*) 'set delt = ',DELTA(J),' J = ',J,' K = ',K
GO TO 315
702   THA = 0.60D0
WRITE (21,*) 'set tha = ',THA,' J = ',J,' K = ',K
GO TO 315
703   THA = 0.80D0
WRITE (21,*) 'set tha = ',THA,' J = ',J,' K = ',K
GO TO 315
704   A1 = 0.5D0
A2 = A1
WRITE (21,*) 'set A1 A2 = ',A1,' J = ',J,' K = ',K
GO TO 315
705   A1 = 0.3D0
A2 = A1
WRITE (21,*) 'set A1 A2 = ',A1,' J = ',J,' K = ',K
GO TO 315
706   A1 = 0.1D0
A2 = A1
WRITE (21,*) 'set A1 A2 = ',A1,' J = ',J,' K = ',K
GO TO 315
*
*   Criterion Check ends *****
495   UNUS = 1
*
*   make new estimate
WRITE (21,*) 'make new estimate J = ',J,' I = ',I,' K = ',K
DO 450 I = 1, M
  YNEW(I) = YNEW(I) + MATRXX(2*I-1)
  VNEW(I) = VNEW(I) + MATRXX(2*I)
  IF ( YNEW(I) .LT. 0.0D0 ) THEN
    WRITE (21,*) 'y is zero inside new estimate loop'
    WRITE (21,*) 'at J = ',J,' K = ',K,' I = ',I
  ENDIF
450  CONTINUE
*
  IF ( K .LT. 30 ) GO TO 330
498  PRINT *, ' no convergence at j = ',J
  PRINT *, ' reached iteration #k = ', K
  WRITE (21,*) ' '
  WRITE (21,*) ' no convergence at j = ',J
  WRITE (21,*) ' '
499  UNUS = 1
*
  DO 501 I = 1, M
    YANS(I,J) = YNEW(I)
    VANS(I,J) = VNEW(I)
    YOLD(I) = YNEW(I)
    VOLD(I) = VNEW(I)
    QANS(I) = VANS(I,J) * YANS(I,J) * B
501  CONTINUE
  WRITE (21,*) 'YW = ',YNEW(M),' I = M = ',M,' J = ',J
*
*   ****output for plotting
*
*   plot at approximate end and mid-points
I1=2
WRITE (27,931) XANS(I1),I1,J,YANS(I1,J),QANS(I1),DELTA(J),THA,A1
I1=(M-20)/3

```

```

WRITE (27,931) XANS (I1), I1, J, YANS (I1, J), QANS (I1), DELTJ (J), THA, A1
I1=(M-20)*2/3
WRITE (27,931) XANS (I1), I1, J, YANS (I1, J), QANS (I1), DELTJ (J), THA, A1
I1=M-20
WRITE (27,931) XANS (I1), I1, J, YANS (I1, J), QANS (I1), DELTJ (J), THA, A1
I1=M
WRITE (27,931) XANS (I1), I1, J, YANS (I1, J), QANS (I1), DELTJ (J), THA, A1
*
*      ****check terms
DO 399 H = 1, 5
  I1=2
  IF (H .EQ. 2) I1=(M-20)/3
  IF (H .EQ. 3) I1=(M-20)*2/3
  IF (H .EQ. 4) I1=M-20
  IF (H .EQ. 5) I1=M-1
  TERM1 = A1/G*DELXUN(I1)/DELTJ(J) * (VNEW(I1+1)+VNEW(I1))
$      + A1*C9(I1)
$  TERM2 = A2/G*(THA**2.0D0) * ((VNEW(I1+1)**2)
$      - (VNEW(I1)**2)) + A2*C12(I1)
  TERM2 = TERM2
$      + A2/G*THA*C11(I1) * (VNEW(I1+1) + VNEW(I1))
$      + A2/G*THA*C10(I1) * (VNEW(I1+1) - VNEW(I1))
  TERM3 = 2.0D0*A3*THA*(YNEW(I1+1)-YNEW(I1))+A3*C13(I1)
  TERM4 = A4*THA*DELXUN(I1)*(SFNEW(I1+1)+SFNEW(I1))
$      + A4*C14(I1) + A4*C15(I1)
  FR = VNEW(I1) / ( (G * YNEW(I1))**0.5D0 )
  RE = VNEW(I1) * YNEW(I1) / 0.0000169D0
  WRITE (28,932) J, K, I1, TERM1, TERM2, TERM3, TERM4
399  CONTINUE
*
500  CONTINUE
*      j loop end *****
*
WRITE (27,*) ' '
WRITE (27,*) 'input hydrograph'
WRITE (27,*) 'time (s)    Q (m3/s)    PW'
DO 801 J = 2, MJ
  WRITE (27,905) DELTJ(J), QUPS(J-1), PWJ(J)
801  CONTINUE
*
901  FORMAT (' ',2I4.0,6E12.4)
902  FORMAT (' ',I6.0,E12.4)
903  FORMAT (' ',I4.0,2E12.4)
904  FORMAT (' ',5E12.4)
905  FORMAT (' ',3E12.4)
906  FORMAT (' ',4E12.4)
907  FORMAT (' ',I4.0,4E12.4)
908  FORMAT (' ',4E13.6)
909  FORMAT (' ',3I4.0,2E12.4)
912  FORMAT (' ',2I4.0)
911  FORMAT (' ',I4.0,4E15.4)
930  FORMAT (' ',I4.0,2E16.8)
931  FORMAT (' ',E12.4,2I3.0,5E12.4)
932  FORMAT (' ',3I3.0,4E12.4)
9999  END
*
SUBROUTINE WEIR (G, Q, PW, B, YW)
*      iterative solution for depth over rect. s.c. weir

```

```
DOUBLE PRECISION G, Q, PW, B, YW, C, CE, C1
C = 0.6D0 * 2.0D0/3.0D0 * ((2.0D0*G)**0.50D0)
DO 300 K = 1, 9
  H = (Q / (C * B))**(2.0D0/3.0D0)
  CE = 0.6020D0 + 0.0750D0 * H / PW
  C1 = CE * 2.0D0/3.0D0 * ((2.*G)**0.50D0)
  IF ( ABS (C - C1) .LT. 0.00050D0) GO TO 305
  C = C1
300  CONTINUE
  IF ( ABS (C - C1) .GT. 0.0005) THEN
    PRINT *, 'Ce did not converge'
    WRITE (21,*) 'Ce did not converge'
  ENDIF
305  C = C1
  H = ( Q / (C*B) )**(2.0D0/3.0D0)
  YW = H + PW
  RETURN
END
```